NUREG/IA-0132
CAMP001

International Agreement Report

Improvements to the RELAP5/MOD3 Reflood Model and Uncertainty Quantification of Reflood Peak Clad Temperature

Prepared by
Bub Dong Chung, Young Jin Lee, Chan Eok Park, Sang Yong Lee, KAERI
Young Seok Bang, Kwang Won Seul, Hho Jung Kim, KINS

Korea Atomic Energy Research Institute
P.O. Box 105
Yusung, Taejon
305-600 Korea

Korea Institute of Nuclear Safety
P.O. Box 16, Daeduck Danji
Taejon, 305-600 Korea

Office of Nuclear Regulatory Research
U.S. Nuclear Regulatory Commission
Washington, DC 20555-0001

October 1996

Prepared as part of
The Agreement on Research Participation and Technical Exchange
under the International Thermal-Hydraulic Code Assessment
and Maintenance Program (CAMP)

Published by
U.S. Nuclear Regulatory Commission

AVAILABILITY NOTICE

Availability of Reference Materials Cited in NRC Publications

Most documents cited in NRC publications will be available from one of the following sources:

1. The NRC Public Document Room, 2120 L Street, NW., Lower Level, Washington, DC 20555-0001

2. The Superintendent of Documents, U.S. Government Printing Office, P. O. Box 37082, Washington, DC 20402-9328

3. The National Technical Information Service, Springfield, VA 22161-0002

Although the listing that follows represents the majority of documents cited in NRC publications, it is not intended to be exhaustive.

Referenced documents available for inspection and copying for a fee from the NRC Public Document Room include NRC correspondence and internal NRC memoranda; NRC bulletins, circulars, information notices, inspection and investigation notices; licensee event reports; vendor reports and correspondence; Commission papers; and applicant and licensee documents and correspondence.

The following documents in the NUREG series are available for purchase from the Government Printing Office: formal NRC staff and contractor reports, NRC-sponsored conference proceedings, international agreement reports, grantee reports, and NRC booklets and brochures. Also available are regulatory guides, NRC regulations in the *Code of Federal Regulations*, and *Nuclear Regulatory Commission Issuances*.

Documents available from the National Technical Information Service include NUREG-series reports and technical reports prepared by other Federal agencies and reports prepared by the Atomic Energy Commission, forerunner agency to the Nuclear Regulatory Commission.

Documents available from public and special technical libraries include all open literature items, such as books, journal articles, and transactions. *Federal Register* notices, Federal and State legislation, and congressional reports can usually be obtained from these libraries.

Documents such as theses, dissertations, foreign reports and translations, and non-NRC conference proceedings are available for purchase from the organization sponsoring the publication cited.

Single copies of NRC draft reports are available free, to the extent of supply, upon written request to the Office of Administration, Distribution and Mail Services Section, U.S. Nuclear Regulatory Commission, Washington, DC 20555-0001.

Copies of industry codes and standards used in a substantive manner in the NRC regulatory process are maintained at the NRC Library, Two White Flint North, 11545 Rockville Pike, Rockville, MD 20852-2738, for use by the public. Codes and standards are usually copyrighted and may be purchased from the originating organization or, if they are American National Standards, from the American National Standards Institute, 1430 Broadway, New York, NY 10018-3308.

NUREG/IA-0132
CAMP001

International Agreement Report

Improvements to the RELAP5/MOD3 Reflood Model and Uncertainty Quantification of Reflood Peak Clad Temperature

Prepared by
Bub Dong Chung, Young Jin Lee, Chan Eok Park, Sang Yong Lee, KAERI
Young Seok Bang, Kwang Won Seul, Hho Jung Kim, KINS

Korea Atomic Energy Research Institute
P.O. Box 105
Yusung, Taejon
305-600 Korea

Korea Institute of Nuclear Safety
P.O. Box 16, Daeduck Danji
Taejon, 305-600 Korea

Office of Nuclear Regulatory Research
U.S. Nuclear Regulatory Commission
Washington, DC 20555-0001

October 1996

Prepared as part of
The Agreement on Research Participation and Technical Exchange
under the International Thermal-Hydraulic Code Assessment
and Maintenance Program (CAMP)

Published by
U.S. Nuclear Regulatory Commission

Abstract

Assessment of the original RELAP5/MOD3.1 code against the FLECHT SEASET series of experiments has identified some weaknesses of the reflood model, such as the lack of a quenching temperature model, the shortcoming of the Chen transition boiling model, and the incorrect prediction of droplet size and interfacial heat transfer. Also, high temperature spikes during the reflood calculation resulted in high steam flow oscillation and liquid carryover. An effort had been made to improve the code with respect to the above weakness, and the necessary model for the wall heat transfer package and the numerical scheme had been modified. Some important FLECHT-SEASET experiments were assessed using the improved version and standard version. The result from the improved RELAP5/MOD3.1 shows the weaknesses of RELAP5/MOD3.1 were much improved when compared to the standard MOD3.1 code. The prediction of void profile and cladding temperature agreed better with test data, especially for the gravity feed test. The scatter diagram of peak cladding temperatures (PCTs) is made from the comparison of all the calculated PCTs and the corresponding experimental values. The deviation between experimental and calculated PCTs were calculated for 2793 data points. The deviations are shown to be normally distributed, and used to quantify statistically the PCT uncertainty of the code. The upper limit of PCT uncertainty at 95% confidence level is evaluated to be about 99K.

List of Contents

List of Tables

List of Figures

Summary

In the past decade, the benefit of best-estimate methodology rather than artificial conservative approach for the LOCA analysis have become obvious to the industry and regulatory body. In August 1988, the Nuclear Regulatory Commission (NRC) approved the final version of a revised rule on the acceptance of emergency core cooling systems (ECCS). The revised rule contains that an alternate ECCS performance analysis, based on best estimate methodology, may be used to provide more realistic estimates of plant safety margins. According to the preliminary studies, the new methodology of best-estimate analysis is expected to substantial LOCA margin gains over the traditional conservative analysis. Its overall benefit could be translated into reduced costs of million of dollars per year to utility.

This research aims to develop reliable, advanced system thermal-hydraulic computer code and to quantify the uncertainties of code to introduce the best-estimate methodology. One of the best estimate code, RELAP5, has been developed jointly by the NRC and a consortium consisting of several countries and organizations that are members of the International Code Assessment and Application Program (ICAP). The code is being continually updated and recently the RELAP5/MOD3.1 Version has been released after a beta-testing of RELAP5/MOD3 version 7j. Although the emphasis of the RELAP5/MOD3 development was on large-break LOCAs, several deficiencies in its reflood model were identified during the independent assessments of the code as part of RELAP5/MOD3-KAERI Version development.

Some improvements to the RELAP5/MOD3 reflood model have been made. These improvements were made to correct deficiencies in the reflood model identified by the assessment of the RELAP5/MOD3 code against FLECHT-SEASET experiments. The improvements consist of modification of reflood wall heat transfer package and adjusting the droplet size in dispersed flow regime. The time smoothing of wall vaporization and level tracking of transition flow are also added to eliminate the pressure spikes and level oscillation during reflood process. Assessment of the improved model against FLECHT-SEASET experimental data and application of LBLOCA analysis for plant shows that the deficiencies have been corrected. The associated uncertainty is statistically quantified using the FLECHT-SEASET data. The selected test runs include a gravity feed test and several forced feed tests with wide range of the parameters such as flooding rate, system pressure,

initial clad temperature, rod bundle power. The results show that the code under-predicts the peak cladding temperature by 7.56 K on average. The upper limit of the associated uncertainty at 95% confidence level is evaluated to be about 99 K, including the bias due to the under-prediction.

Nomenclatures

cp.	specific heat capacity
d	droplet diameter
g	gravitational constant
Gr.	Grashof number
h	specific enthalpy, heat transfer coefficient
k	thermal conductivity
q"	heat flux
Re	Reynolds number
T	temperature
V	phasic velocity
We	Weber number

Greek

α	void fraction
ρ	phasic density
σ	surface tension
μ	phasic viscosity
Γ	volumetric vaporization rate
τ	time constant

Subscripts

avg	average value
CHF	value at critical heat flux
f	liquid phase
FB	film boiling
fg	saturated phasic difference
g	vapor phase, saturated liquid phase
K	spatial noding index, downstream volume
l	liquid phase
L	spatial noding index, upstream volume
level	value at a level
max	maximum value
MIN	value at minimum stable film boiling
TRAN	transition boiling
v	vapor phase
w	value at wall

1. Introduction

The postulated loss-of-coolant accident (LOCA) of a pressurized water reactor has been the subject of intensive experimental and analytical studies in light water reactor. Many efforts are devoted to the investigation of thermodynamic behavior of reactor core and effectiveness of emergency core cooling system during reflood phase of LOCA.

The series of RELAP code began with RELAPSE, which was released in 1966. Subsequent versions of this code are RELAP2[1], RELAP3[2], and RELAP4[3]. All of these codes were based on the homogeneous equilibrium model (HEM) for describing the two-phase flow process. In 1976, the development of a nonhomogeneous, nonequilibrium model was undertaken for RELAP4. It soon became apparent that a total rewrite of the code was required to efficiently accomplish this goal. The result of this effort was the beginning of the RELAP5 project.

The principal new feature of the RELAP5 series [4,5] is the use of a two-fluid, nonequilibrium, nonhomogeneous, hydrodynamic model for transient simulation of the two-phase system behavior. The MOD3 version of RELAP5 has been developed jointly by the NRC and a consortium consisting of several countries and organizations that are members of the International Code Assessment and Application Program (ICAP). The mission of the RELAP5/MOD3 development program was to develop a code version suitable for the analysis of all transients and postulated accidents in PWR systems, including both large- and small-break loss-of-coolant accidents (LOCAs) as well as the full range of operational transients. The code is being continually updated and recently the MOD3.1 version of RELAP5 [6] has been developed jointly by the NRC and a consortium of International Code Assessment and Application Program (ICAP). Although the emphasis of the RELAP5/MOD3.1 development was on large-break LOCAs, several deficiencies in reflood model were identified during the assessment of FLECHT-SEASET series of experiments [7]. The deficiencies are categorized as 1) High pressure spikes and oscillation during reflood 2) Delayed quenching 3) Incorrect void profile and vapor cooling in dispersed flow.

Parallel to the development of best-estimate code, the Nuclear Regulatory Commission (NRC) approved the final version of a revised rule on the acceptance of emergency core cooling systems (ECCS)[8]. The revised rule contains that an alternate ECCS performance analysis, based on best estimate methodology, may be used to provide more realistic

estimates of plant safety margins. However the licensee must quantify the uncertainty of the estimates and includes that uncertainty when comparing the calculated results with acceptance limits. To support the revised ECCS rule, the NRC research formed a small group of experts, called the Technical Program Group(TPG). The TPG developed a method called the Code Scaling, Applicability, and Uncertainty (CSAU) evaluation methodology [9-15] and demonstrated for Westinghouse four-loop pressurized water reactor with 17x17 fuel using TRAC-PF1/MOD1 code.

The purpose of this study is to present a reflood model and its implementation in RELAP5/MOD3.1. A great deal of effort has been made to solve to the above deficiencies, and the necessary model improvement and code modification has been carried out. The modified reflood model was assessed using FLECHT-SEASET test and it's uncertainty was also quantified.

2. Reflood Model Improvements

The model modification and development activity were focused on solving the RELAP5/MOD3.1 model deficiencies. Followings are suggested to be the primary cause for the fore-mentioned code deficiencies.

a) Unsuitable CHF correlation for low pressure and low flow.
   Discontinuity in the wall heat transfer logic
b) Lack of quenching temperature model
c) Lack of droplet field model in dispersed flow

A great deal of effort has been made to improve the code with respect to the above causes, and the necessary model improvement and code modification has been carried out.

Unlike RELAP5/MOD2, RELAP5/MOD3.1 uses the same heat transfer coefficient logic for all wall surfaces. To avoid discontinuities, reflood surfaces are treated as regular surfaces, thus there is no reflood specific model. Structures flagged as reflood structures differ only in that axial conduction is considered. A boiling curve is used in RELAP5/MOD3.1 to govern the selection of heat transfer correlation's. In particular, the heat transfer regimes modeled are classified as pre-CHF and post-CHF regimes. Condensation heat transfer is also modeled, and the effects of noncondensable gases are modeled. The heat transfer package in RELAP5/MOD3.1 uses heat transfer correlation's that are based on fully developed flow, where entrance length effects are not considered except for the calculation of CHF. The approach of using these correlation's in a transient code such as RELAP is often refereed to as the quasi-steady approach.

The following list gives the modes by which heat is transferred between heat structure surfaces and the fluid in contact with the heat structure.

mode 0 ; Convection to noncondensable-water mixture
mode 1 ; Single-phase liquid convection at critical and super critical pressure
mode 2 ; Single-phase liquid convection at subcritical pressure
mode 3 ; Subcooled nucleate boiling

mode 4 ; Saturated nucleate boiling
mode 5 ; Subcooled transition film boiling
mode 6 ; Saturated transition film boiling
mode 7 ; Subcooled film boiling
mode 8 ; Saturated film boiling
mode 9 ; Single-phase vapor convection
mode 10 ; Condensation when void equals one
mode 11 ; Condensation when void is less than one

If the noncondensable quality is greater than 0.0001, then 20 is added to the node number. If the heat structures are flagged as reflood structure, 40 is added thus the mode number can be 40 to 51. Figure 1 is a schematic diagram showing the logic built into the code to select the appropriate heat transfer mode.

In the modified version, the above wall heat transfer packages were updated when reflood begins. Time smoothing of wall vaporization and level tracking of transition flow are also added to eliminate pressure spikes and level oscillation during reflood process. More detailed model descriptions are provided in the following section.

2.1 Wall Heat Transfer Package

The heat transfer package consists of a library of heat transfer correlation's and selection logic algorithm similar to RELAP5/MOD3.1. For the normal heat structures, the correlation and logic algorithms are exactly the same as those installed in RELAP5/MOD3.1. However when the heat structures are flagged as reflood structure, some modification of correlation's and logic algorithm are performed as shown in Figure 2. The modified correlation's used in each heat transfer regimes are detailed below.

2.1.1 Critical Heat Flux and Transition Boiling

In RELAP5, the transition boiling correlation is based on Chen transition boiling model [16] which is applicable to a dispersed flow regime. The model depends on the Critical Heat Flux (CHF) value and used to determine whether the film boiling occurs. Thus

CHF correlation is important in determining the flow regime. The Groeneveld Look up table [17] was used to determine the CHF. Unfortunately, the value in the table was found to change suddenly with respect to flow and quality at low pressure and low flow condition. It may result in numerical instabilities or oscillation. Modified wall heat transfer package is based on the heat transfer logic developed on the basis of wall temperature. The reflood heat transfer package is similar to RELAP5/MOD2 [5] and based on the comparative study of post-CHF wall heat transfer package of RELAP5 codes which was done at Paul Scherrer Institute (PSI), Switzerland [18].

The intersection of the nucleate boiling and transition boiling heat transfer regimes occurs at the CHF point. To provide for a continuous transition between regimes, the CHF point (q''_{CHF}, T_{CHF}) must be specified. The modified Zuber pool boiling CHF correlation [5, 9] is chosen as a reasonable approximation of the maximum heat flux at the quench front:

$$\dot{q}_{CHF} = \frac{\pi(1-\alpha_g)}{24} h_{fg} \rho_g^{0.5} [g\sigma(\rho_f - \rho_g)]^{0.25} \tag{1}$$

To define the boiling curve, it is necessary to know the surface temperature at which CHF occurs. An iterative procedure [5] is used to find the wall temperature at which the heat flux from Chen nucleate boiling correlation is equal to the critical heat flux. Thus,

$$\dot{q}_{CHEN}(T_{CHF}) = \dot{q}_{CHF} \tag{2}$$

The transition boiling regime is bounded by the CHF point (below which the wall is continuously wetted and nucleate boiling exits) and the minimum stable film boiling point (above which the liquid cannot wet the wall and film boiling exits). The minimum stable film boiling temperature is called sometimes rewetting or quenching temperature. There are several correlation's, i.e., Dix & Anderson [20] , Murao [21], Berenson [22] and Henry [23] correlation. Good agreement between several FLECHT-SEASET data [24] and predicted rewetting temperature was obtained when a formulation of Henry correlation was used [25]. Thus Henry correlation is incorporated in modified RELAP version to determine the minimum stable film boiling temperature and has following form :

$$T_{MIN} = T_{MIN,B} + 0.42(T_{MIN,B} - T_l)\{[\frac{(k\rho C_p)_l}{(k\rho C_p)_w}]^{0.5} \frac{h_{fg}}{C_{pw}(T_{MIN,B} - T_f)}\}^{0.6} \quad (3)$$

$$T_{MIN,B} = T_f + 0.127\frac{\rho_v h_{fg}}{k_v}[\frac{g(\rho_f - \rho_g)}{(\rho_f + \rho_g)}]^{2/3}[\frac{\sigma}{g(\rho_f - \rho_g)}]^{1/2}[\frac{\mu_v}{g(\rho_f - \rho_g)}]^{1/3}$$

At present, there is no consensus on a correlation to use for the transition boiling regime. Modified version employs a simple interpolation scheme for heat transfer between CHF temperature and minimum film boiling temperature.

$$\dot{q}_{TRAN} = \dot{q}_{CHF} + (1-\delta^2)\dot{q}_{FB} \quad (4)$$

where δ *is defined as* $(T_w - T_{MIN})/(T_{CHF} - T_{MIN})$

The above mentioned heat flux should be partitioned to the liquid and the vapor phase for two fluid model. Assuming that the heat transfer coefficient of vapor side does not change much, the energy partition of transition region can be estimated as follows.

$$h_g = h_{g,CHF} + (1-\delta)h_{g,FB}$$
$$\dot{q}_g = h_g(T_w - T_g) \quad (5)$$
$$\dot{q}_f = \dot{q}_{TRAN} - \dot{q}_g$$

2.1.2 Film Boiling

Film boiling is described by heat transfer mechanisms that occur during several flow patterns, namely inverted annular flow, slug flow and dispersed flow. The wall-to-fluid heat transfer mechanisms are conduction across a vapor film blanket next to a heated wall, convection to flowing vapor and between the vapor and droplets, and radiation across the film to a continuous liquid blanket or dispersed mixture of liquid droplets and vapor.

The single phase vapor correlation's become the model basis of the convection heat transfer in film boiling mode. However the presence of the droplet in steam flow provides a source of turbulence additional to that generated by wall shear, and this will enhance the steam convective heat transfer as deduced from steam-only experiments [26]. Several investigators have looked at the effect of turbulence intensity on convective heat transfer in

two-phase dispersed flows. Drucker et al. [27] proposed that the droplets will enhance turbulence in the flow ; hence, heat transfer. The ratio of the two-phase-to-the-single-phase heat transfer coefficient ϕ can be written for entrained flow as

$$\varphi = \frac{h_{TP}}{h_{SP}} = 1 + 3.25\{\frac{(1-\alpha_g)Gr}{\mathrm{Re}^2}\}^{0.5} \tag{6}$$

where $(1-\alpha_g)$ represents the liquid fraction and Grashof number, Gr, and flow Reynolds number, Re, based on steam properties and defined by

$$Gr = \frac{g(\rho_f - \rho_g)\rho_g D_H^{\ 3}}{\mu_g^{\ 2}} \tag{7}$$

and

$$\mathrm{Re} = \frac{\rho_g V_g D_H}{\mu_g} \tag{8}$$

The above two phase enhancement effects are included in the convection term (Dittus Boelter Correlation) of the film boiling mode. Similar enhancement effects are included in other codes, COBRA-TF [28] and Westinghouse BART [29]. The correlation's in RELAP5/MOD3 conduction (modified Bromley Correlation) and radiation model are deemed sufficiently accurate and are not changed.

2.2 Wall Vaporization Smoothing Model

In RELAP5/MOD3, there are two interphase mass transfer terms. One is a wall vaporization due to wall heat transfer and the other is a mass transfer arising from bulk exchange between the liquid and vapor spaces. The latter is treated as a partially implicit term, although the interfacial heat transfer coefficient is estimated explicitly. However the first term, wall vaporization, is treated as an explicit term in the mass and energy equation.

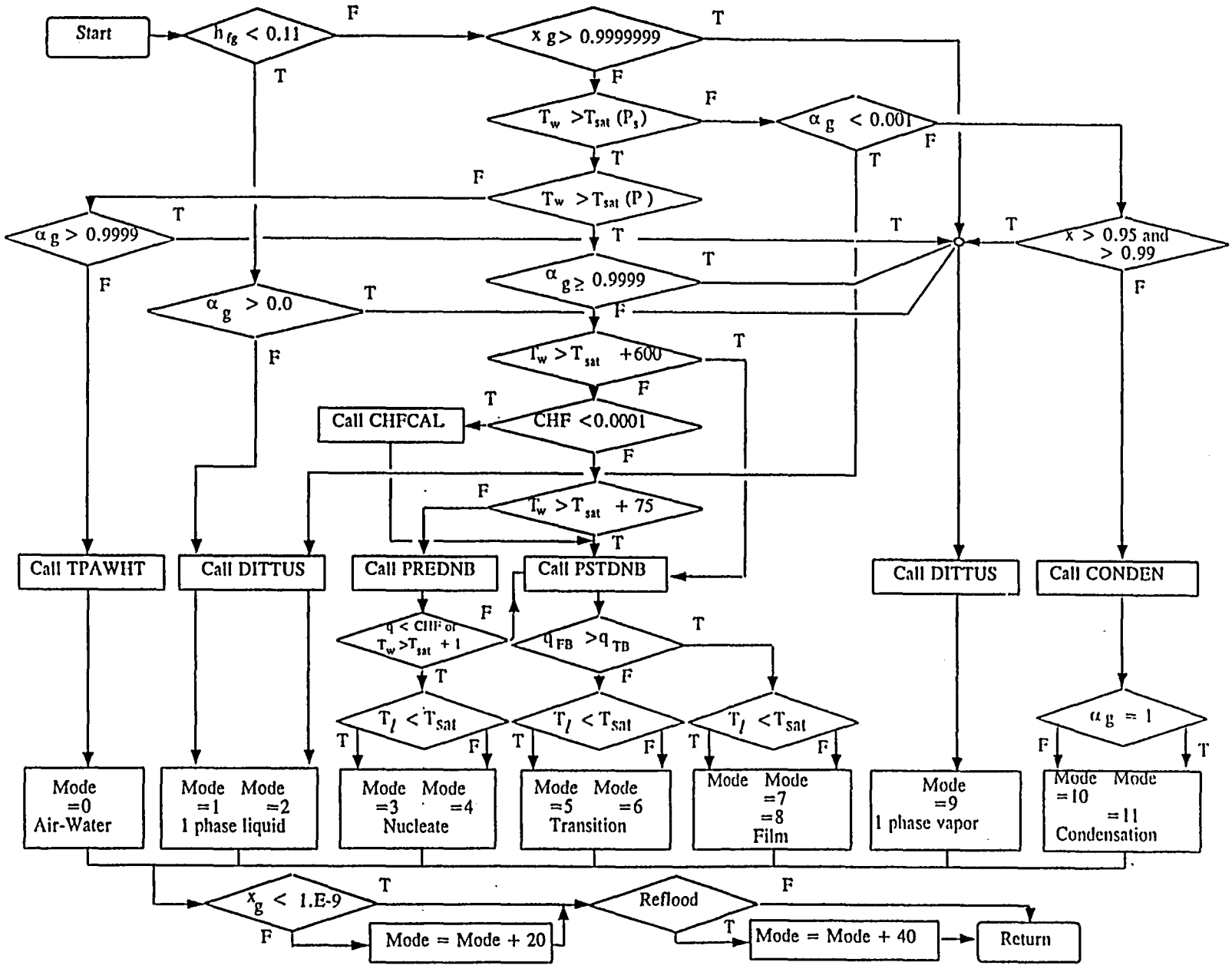

Fig. 1 Schematic of wall heat transfer logic

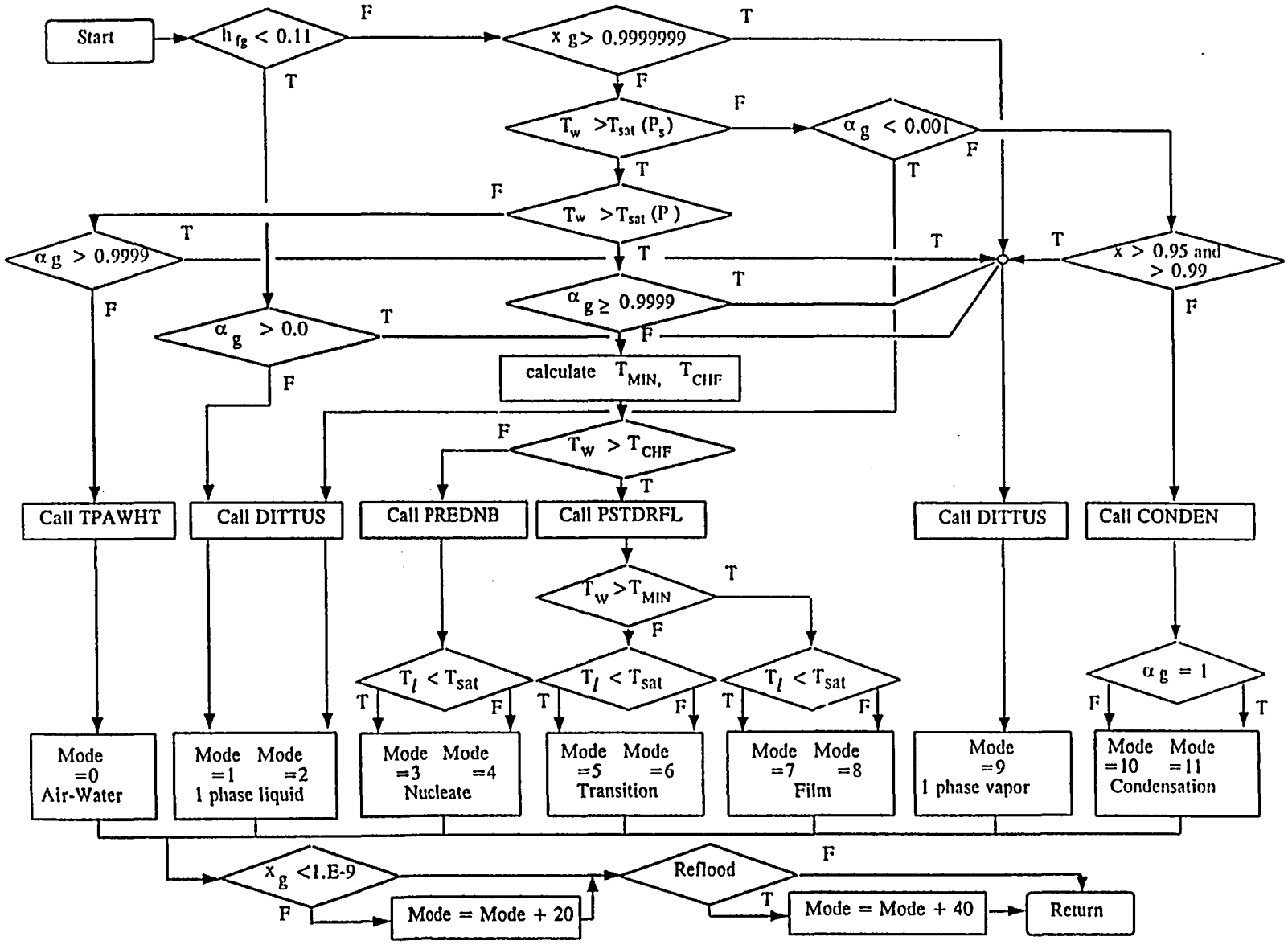

Fig. 2 Schematic of reflood wall heat transfer logic

This scheme was found to cause numerical oscillation. It is well known that a numerical underrelaxation can prevent this kind of oscillations.

Thus time smoothing of wall vaporization is implemented to a modified version as follows.

$$\Gamma_{w,n+1} = \eta\Gamma_{w,n} + (1-\eta)\Gamma_{w,n+1} \tag{9}$$

The underrelaxation factor is of the form, $\eta = e^{-\Delta t/\tau}$, in order to obtain time-step insensitive smoothing. For reflood case $\tau = 0.1$ sec was selected because time constant for major transient phenomena is considered as longer than 0.1 second.

2.3 Water Level Tracking Model for Transition Flow

Such codes as RELAP5 code which use Eulerian coordinate system for the solution of the finite difference equation, cannot track the two phase mixture level unless systems were modeled with very fine nodalization. Although a fine mesh nodalization of reflood heat structure is provided to account for the axial conduction, the lack of level tracking results in incorrect heat transfer coefficient for a fine mesh heat structure in a given coarse mesh hydro-cell. This impact is more severe for the developing flow.

To circumvent this, a level tracking model is newly implemented in modified version for the calculation of the heat transfer coefficient of fine mesh heat structure. The variation of hydraulic parameters in a hydro-cell can be estimated with proper assumptions. One of the major parameters which govern the wall heat transfer is a void fraction. It is assumed that the void fraction in a hydro-cell has a step change between upper and lower void fraction of hydro-cell, while other parameters remain constant. The model is coded as a following equation.

$$\begin{aligned} \alpha_g(z) = \alpha_K \quad & if\ 0 < z < z_{level} \\ \alpha_L \quad & if\ z_{level} < z < 1 \end{aligned} \tag{10}$$

,where α_K means the void fraction of downstream volume, α_L is void fraction of upstream

volume, and α_g is void fraction of given hydro-cell. The water level z_{level} is defined as $(\alpha_g-\alpha_L)/(\alpha_K-\alpha_L)$. The above scheme is activated when $\alpha_K < 0.1$ and $0.1 < \alpha_g < 0.9$, and only one of the cells related to a reflood structure is applicable.

2.4 Droplet Model for Dispersed Flow Regime

In RELAP5/MOD3, the bubbly and mist flow regimes are both considered as dispersed flow. The dispersed bubbles or droplets can be assumed to be spherical particles with a size distribution following the Nukiyama-Tanasawa form [30]. The average diameter d_0 is obtained by assuming that $d_0=(1/2)d_{max}$. The maximum diameter, dmax, is related to the critical Weber number, $We = d_{max}\, \rho_c\, (v_g-v_f)^2/\sigma$. The values for We are taken presently as 10.0 for bubbles and 3.0 for droplet. For reflood case, the value 12 was taken for droplet and average droplet size was restricted between 2.5 mm and hydraulic diameter (10 mm for typical PWR).

However estimated droplet size was too large comparing with the FLECHT-SEASET experiment and COBRA-TF estimations [31]. It results in too much liquid accumulation at the downstream of the quench front and incorrect vapor cooling, according to the PSI evaluation of reflooding model [32]. In the modified version, there is no change in correlation's for interfacial drag and heat transfer, but the average droplet size for reflood case is restricted between 0.2 mm and 2.0 mm according to FLECHT experiment result. All interfacial surface area for mist flow regime were estimated based on the above droplet diameter. Similar restriction on droplet size for dispersed film boiling was proposed by PSI [33]

3. Model Verification

Runs 31504,31805,31302 and 31701 from the experiments of the 161-rod FLECHT-SEASET facility were simulated to assess the reflood model of RELAP5/MOD3/KAERI at various reflood rates and also the run 33338 was simulated for the gravity driven reflood. The electrically heated rod configuration of FLECHT was typical of the full-length Westinghouse 17x17 rod bundle. The rod had a cosine axial power profile. This report includes the input deck model for FLECHT forced feed and gravity feed reflood. The assessments of improved model for RELAP5/MOD3/KAERI were performed and the results were compared with the results obtained using the original RELAP5/MOD3.1. The overall performance of the code predictability was evaluated with respect to the peak cladding temperature and the quenching time.

The objective of FLECHT-SEASET program is to provide experimental heat transfer and two phase flow data in simulated PWR geometry for postulated conditions of reflooding, core boil off, and natural circulation. A series of forced flow and gravity feed bundle reflooding tests and steam cooling tests were conducted on a heater rod bundle whose dimensions are typical of the current PWR fuel rod array. The actual array configuration and dimensions of test heater rods are shown in Figure 3.

The test parameters cover a spectrum of conditions that encompass both the best-estimate and current licensing calculations. These tests examined the effect of initial clad temperature, variable stepped flooding rates, rod peak power, constant low flooding rates, coolant subcooling, and system pressure. Table 1 shows the ranges of test parameters. Detailed descriptions of 161-rod FLECHT-SEASET are described in Reference 1. Of the 161-rod tests, 4 forced feed reflood (31302, 31504, 31701, 31805) and 1 gravity feed reflood (33338) cases, as shown in Table 2, were selected for the developmental assessment.

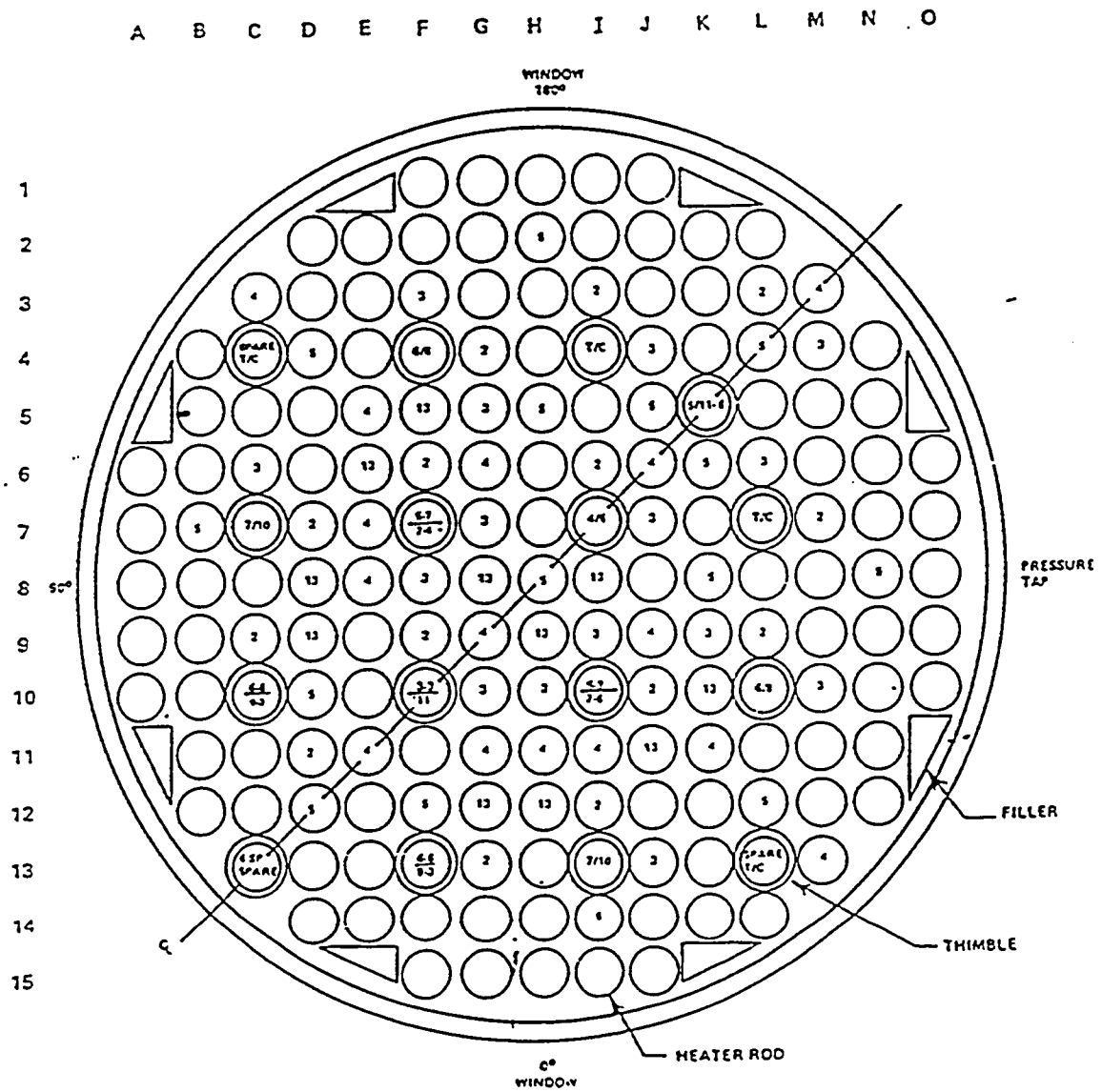

Fig. 3 Bundle Cross Section of FLECHT-SEASET Test Section

Table 1. Assessment Matrix for FLECHT SEASET 161 Rod Test

Test Run Number	Pressure (Mpa)	Maximum Clad Temperature (K)	Flooding Rate (cm/sec)	Injected Liquid Temperature (K)
31504	0.28	1136	2.4	324
31805	0.28	1144	2.1	324
31302	0.28	1142	7.65	325
31701	0.28	1145	15.5	326
33338	0.28	1144	Gravity	325

Table 2 Test Matrix for Assessment

Group	Run	System Pressure (MPa)	Rod Initial temperature (°C)	Rod peak power (kW/m)	Flooding Rate (mm/sec)	Coolant temperature (°C)	Radial power distribution	Remark
1.Flooding rate	31203	0.28	872	2.3	38.4	52	Uniform	(1)
	31302	0.28	869	2.3	76.5	52	Uniform	(2)
	31504	0.28	863	2.3	24.6	51	Uniform	
	31702	0.28	872	2.3	155.0	53	Uniform	
	31805	0.28	871	2.3	21.0	51	Uniform	
2.System pressure	31504	same as (2)						
	32013	0.41	887	2.3	26.4	66	Uniform	
	34209	0.14	889	2.4	27.2	32	Uniform	
3. Initial clad temp.	30518	0.28	256	2.3	38.9	52	Uniform	
	30817	0.27	531	2.3	38.9	53	Uniform	
	31203	same as (1)						
	34420	0.27	1119	2.4	38.9	51	Uniform	
4. Rod bundle power	31021	0.28	879	1.3	38.6	52	Uniform	
	31203	same as (1)						
	34524	0.28	878	3.0	39.9	52	Uniform	
5. Others	31108	0.28	871	2.3	79.0	33	Uniform	variable flooding rate
	32235	0.14	888	2.3	165.8 (5sec) 24.9 (20 sec) 15.7 onward	31	Uniform	variable flooding rate
	32333	0.28	889	2.3	162 (5 sec) 21 onward	53	Uniform	gravity feed test
	33338	0.28	871	2.3 (hot) 1.3 (cold)	5.9 kg/s (15 sec) 0.807 kg/s onward	52	Hot/cold channels	
	34006	0.27	882	1.3	15	51	Uniform	
	35026	0.28	900	2.42 2.31 2.19	25	51	FLECHT	distributed radial power

3.1 Simulation Model

The test section was modeled using 20 uniform cells, as shown in Figure 4. Measured fluid conditions were used to define the thermal- hydraulic conditions in the upper and lower time-dependent volumes, which represented the upper and lower plena, respectively. The measured flow injection velocity was used to define the flow conditions at the time-dependent junction that connects the lower plena and the test section. The measured power, which decreased during the test period, was used as input for heat structures representing the rods. If a modeled cell has a grid spacer, the head loss of spacer grid was considered by subtracting the spacer grid blockage from the normal junction. The spacer grid was also considered in the CHF calculation for heat structures. The heatup and reflood phases of tests were simulated in a single transient calculation using the measured heatup and decay power. The measured cladding temperatures before the heatup phase were used as the input for the initial temperatures required for each heat structures. The start time of water injection was also used as the input value.

The nodalization diagram for Gravity Feed Test is shown in Figure 5. As shown in the Figure, the test section and heater rod model are the same as the forced feed simulation except the addition of downcomer and associated pipes. The downcomer was modeled as a pipe with 10 cells to predict the correct water level. The experimental reflood injection flow rate is applied to the time-dependent junction connected to the bottom of the downcomer and the connecting pipes and valves are also modeled. The measured flow rate injected to the bottom of downcomer was used to define the conditions at the time dependent junction connected to the bottom of downcomer.

Calculation is performed in the same way as in the forced reflood cases : one-through calculation of heat-up and reflood phase, initial condition using the experimental data at early heat-up phase. reflood feed trip at starting time of power decay, division of heater rod bundle according to the power distribution.

Assessments for base case and case for using modified version (RELAP5/MOD3/KAERI) were performed using same nodalization and same sequence of events. Also, there were no diviations from the user guidelines in assessment. The one difference between base and modified case is that the input deck of modified case have "Group 1 Options" which activate the modified model. See the Appendix A for the details of option used in modified version.

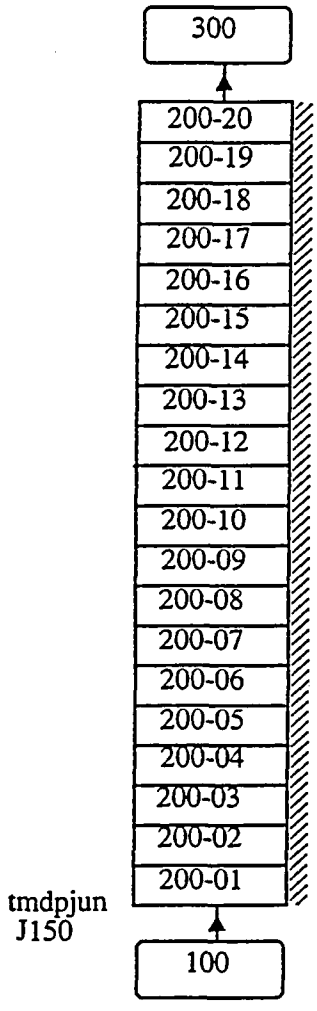

Fig.4 Nodalization for forced reflood test

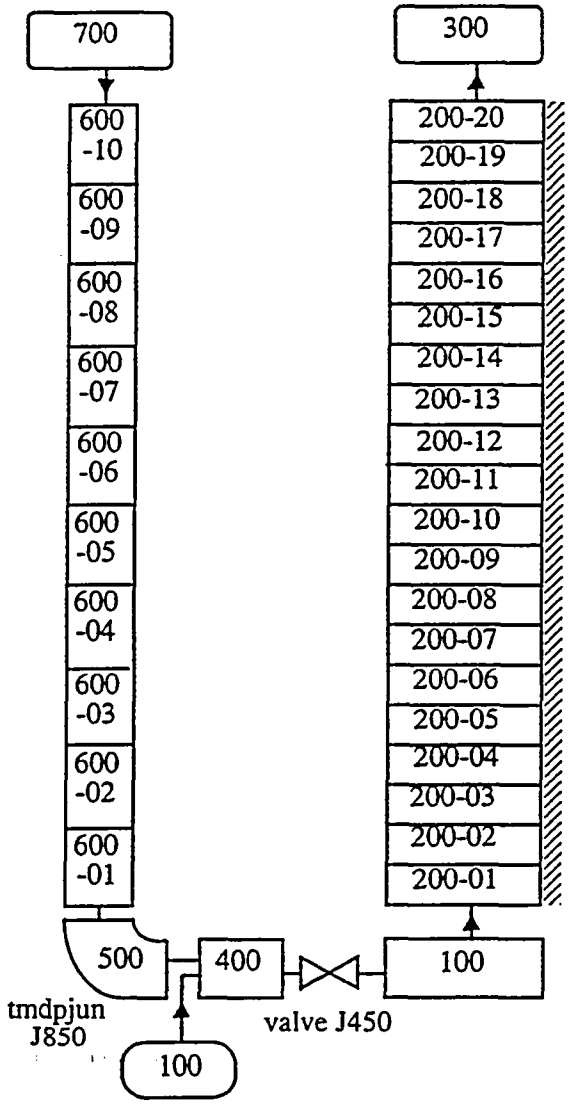

Fig.5 Nodalization for gravity feed reflood test

3.2 Assessment Results

The experimental data for 161-rod FLECHT SEASET were obtained from the ENCOUNTER Data Bank of USNRC [34]. The raw experimental data contain information's from the 256 channels of the data acquisition system. The data channels consist of 177 heater rod surface temperatures, system temperatures, bundle power, flows and absolute and differential pressures. However, some of the raw data from the measurement channels contained failed or spurious data which were rejected after inspection and in some cases by engineering decision.

The data for each test were sorted according to the measurement location and measurement type, and then used for the comparison of calculation results and uncertainty quantification of reflood PCT (Peak Clad Temperature).

As shown in Figure 4, the test section was nodalized into 20 equal size nodes using the 'PIPE' component. However, the axial measurement points are not spaced at regular intervals but concentrated in the mid-elevation region. This meant that for most axial measurement locations, a computational cell which accurately matches the given measurement location was not available. Thus an interpolation scheme for calculation results was necessary for the valid comparison between the calculation and the experimental data. In the present assessment, the assessment of forced feed and gravity feed test were performed based on a simple linear interpolation of the calculated results.

3.2.1 Forced Feed Test

In addition to the reference run (Test 31504), three forced feed cases were simulated to investigate the capability of the code with respect to varying injection rates while keeping other parameters constant.

a) Test Run 31504 - Reference Test Run

On the reference test run 31504, with an injection velocity of 2.46 cm/s (0.97 in./s), the original RELAP5/MOD3.1 code exhibited a number of weaknesses. In the comparison, all the experimental data at the same elevation excluding the failed channel data were averaged whereas the calculation results were linearly interpolated between the hydraulic cells that

fence the measurement location.

Comparisons of averaged experiment data and calculated rod surface temperature histories are presented in Figure 6 (48 in. : low elevation) . 7 (72 in. : midplane), and 8 (96 in. : high elevation). The measured steam temperature at midplane (72 in.) is shown in Figure 9. The predicted initial slope of the heatup rod temperature increase is accurate, but the calculated temperature turnaround occurs too early. As a consequence, the peak temperature at the midplane is underpredicted by about 50 K. This trend becomes more severe as the elevation increases. In the comparison of the steam temperature at midplane, the calculated steam temperature is much lower than the experimental data and this will contribute to the underprediction of PCT. The unsatisfactory prediction of the steam temperature may be caused by the inaccurate energy partition in the dispersed flow regime and the inaccurate interfacial heat transfer. In the modified version, an enhancement model of single phase heat transfer in dispersed flow regime is incorporated and this model contributed to the slight increase in the vapor temperature seen in Fig. 9. However, the improvement in the PCT prediction is less than 10 K.

The calculated quenching behavior using the original version well illustrates the shortcomings of the reflood model. In the calculated results obtained with the original mod 3.1 code, there is an unrealistic 200 second quenching tail at the midplane. This is suspected to be caused by the Chen transition boiling model which yields values that are too small. In the modified version, a quenching temperature model (Modified Henry correlation) and a CHF temperature are used for determining the transition boiling heat transfer derived by interpolating between these two temperatures. These schemes resulted in great improvements in the prediction of the quenching behavior as shown in the Figures.

Comparison of inlet absolute pressure is presented in Figure 10. Unrealistic large pressure spikes were calculated to occur with the original version at the time of quenching for each heat structure. The wall vaporization smoothing model and level tracking model for the developing flow were incorporated in the modified version which rectified these deficiencies and consequently the pressure trends were well predicted. These improvements were also found in exit steam and liquid flow as shown in Figures 11 and 12.

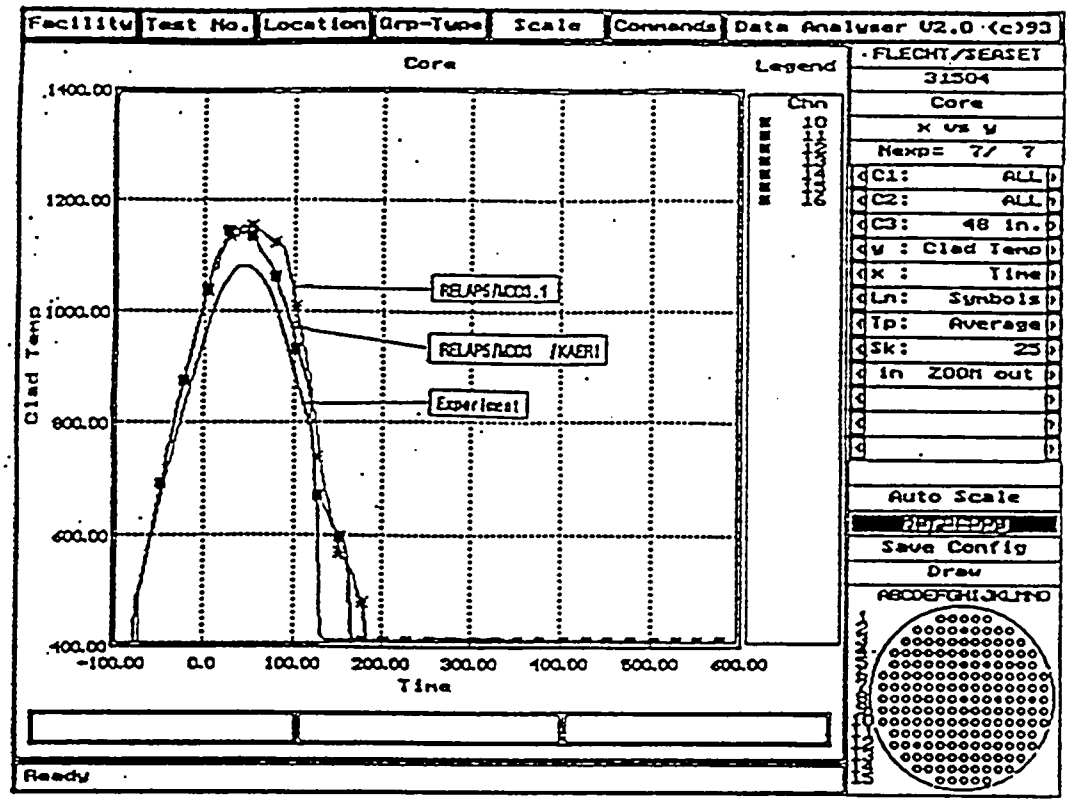

Figure 6. Cladding Temperature at 48 in. elevation, Test 31504

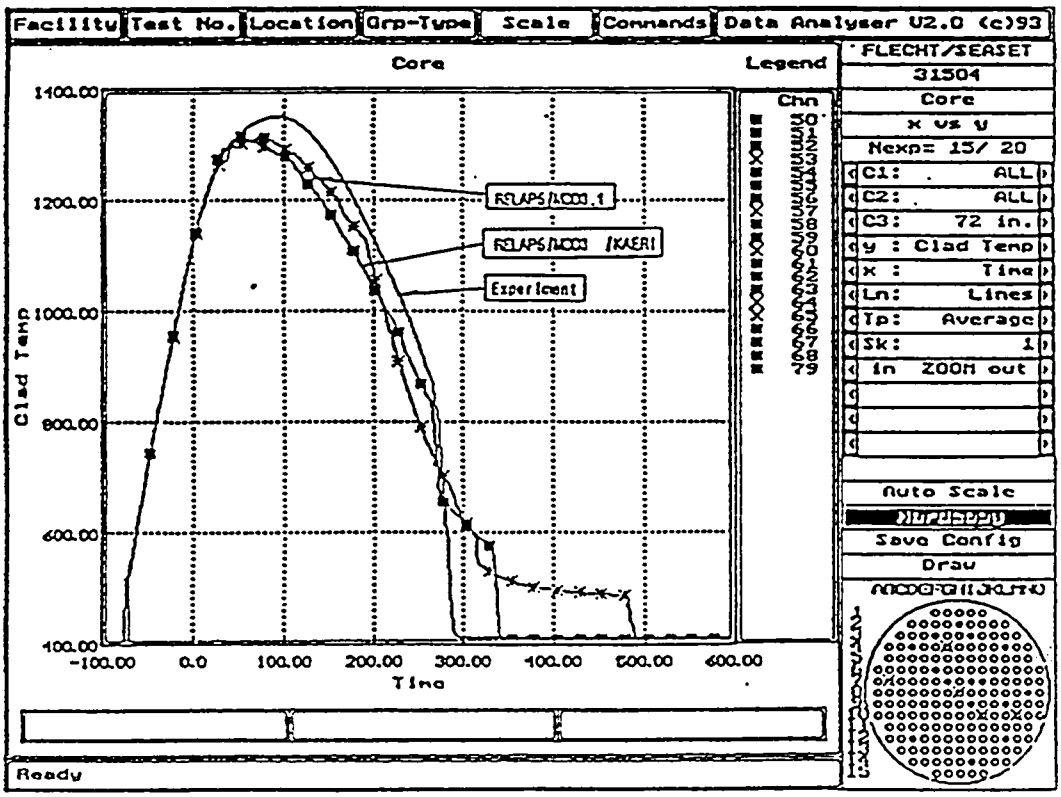

Figure 7. Cladding Temperature at 72 in. elevation, Test 31504

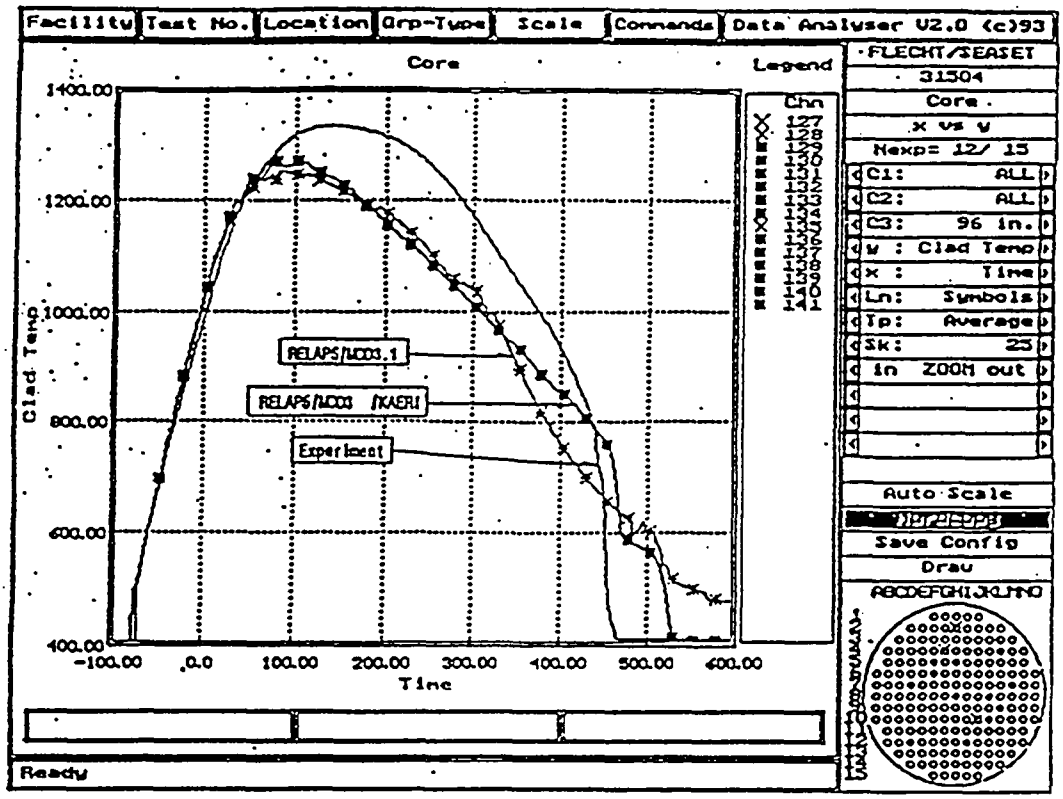

Figure 8. Cladding Temperature at 96 in. elevation, Test 31504

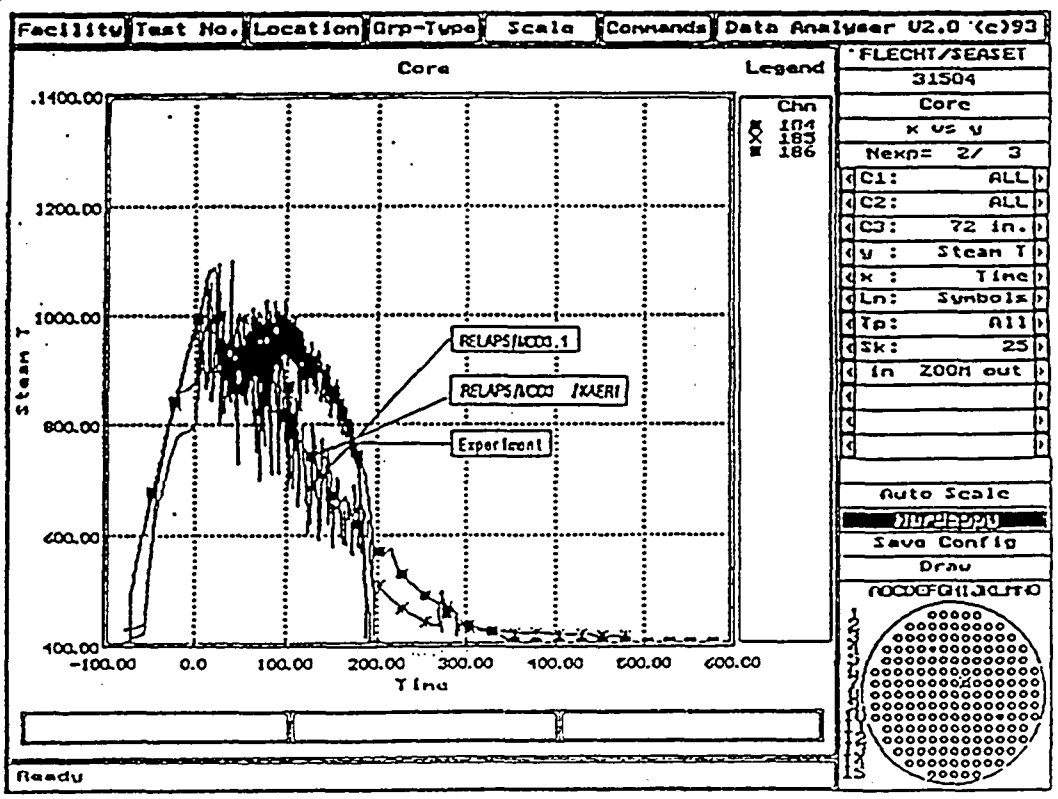

Figure 9. Steam Temperature at 72 in. elevation, Test 31504

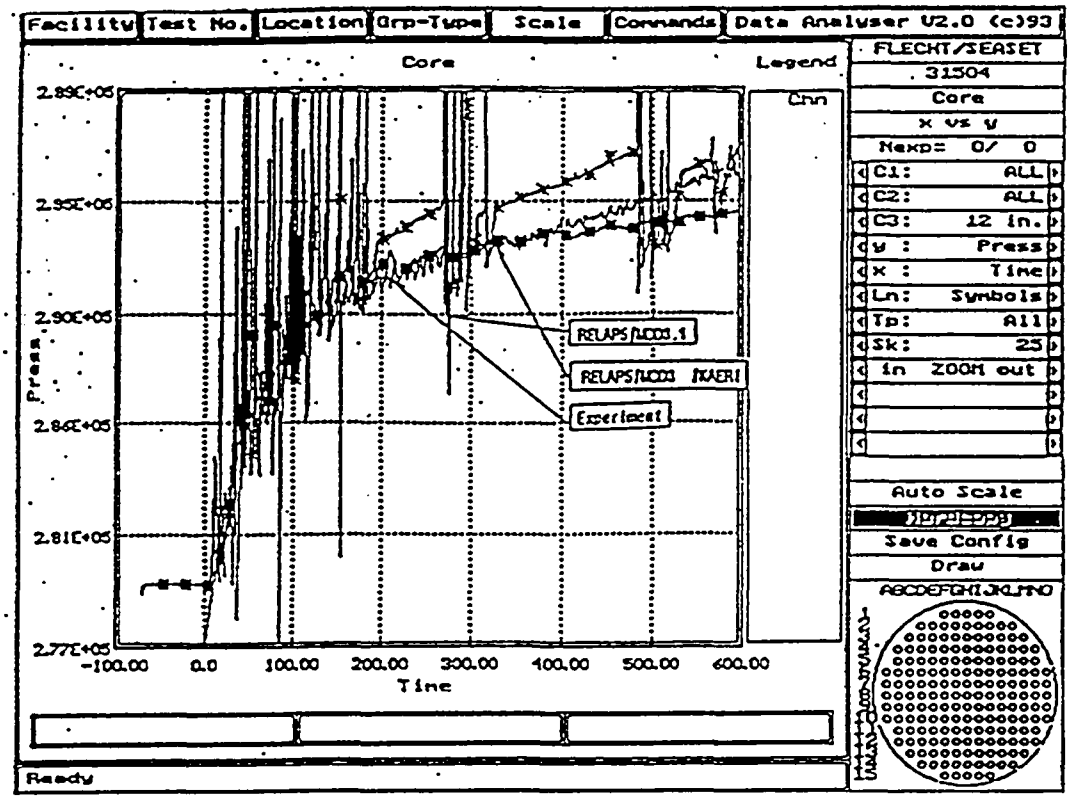

Figure 10. Pressure at 12 in. elevation, Test 31504

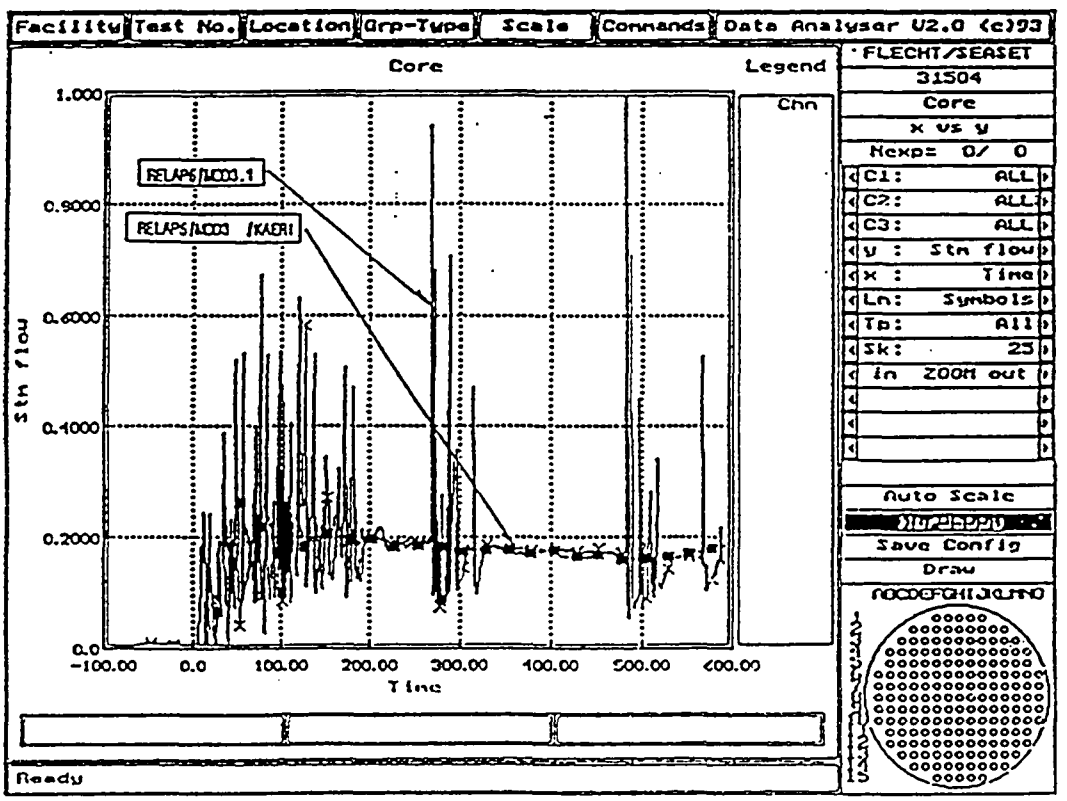

Figure 11. Exit Steam Flow, Test 31504

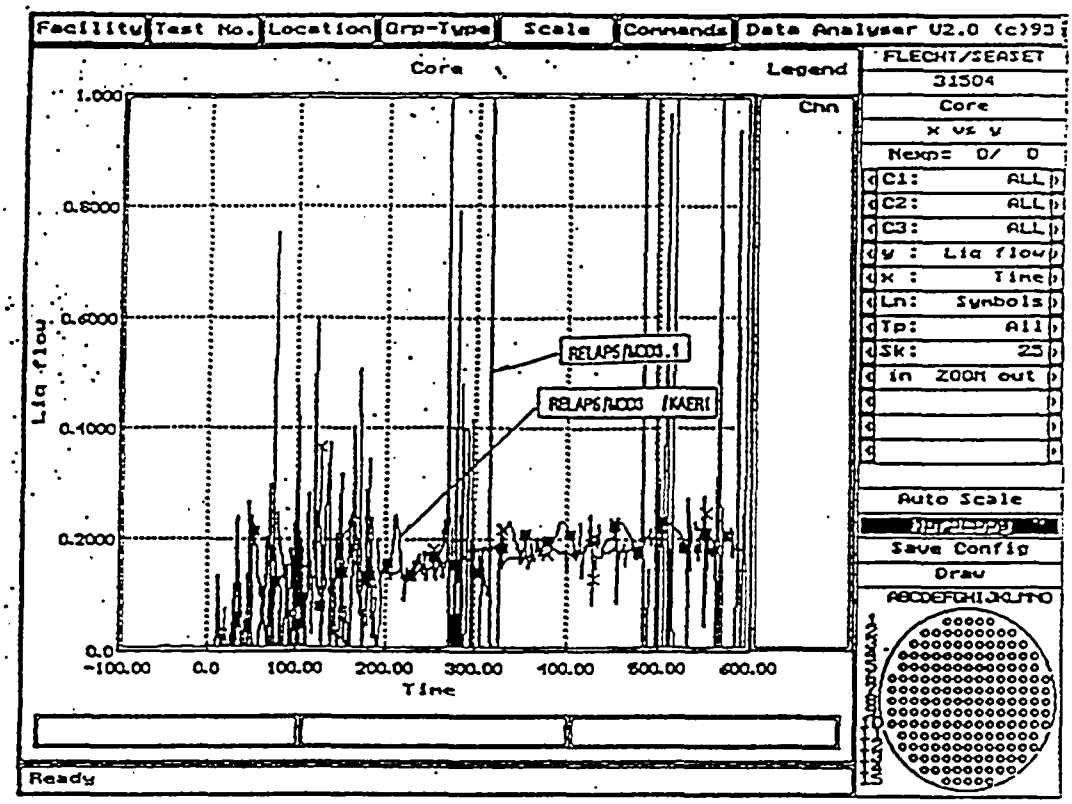

Figure 12. Exit Liquid Flow, Test 31504

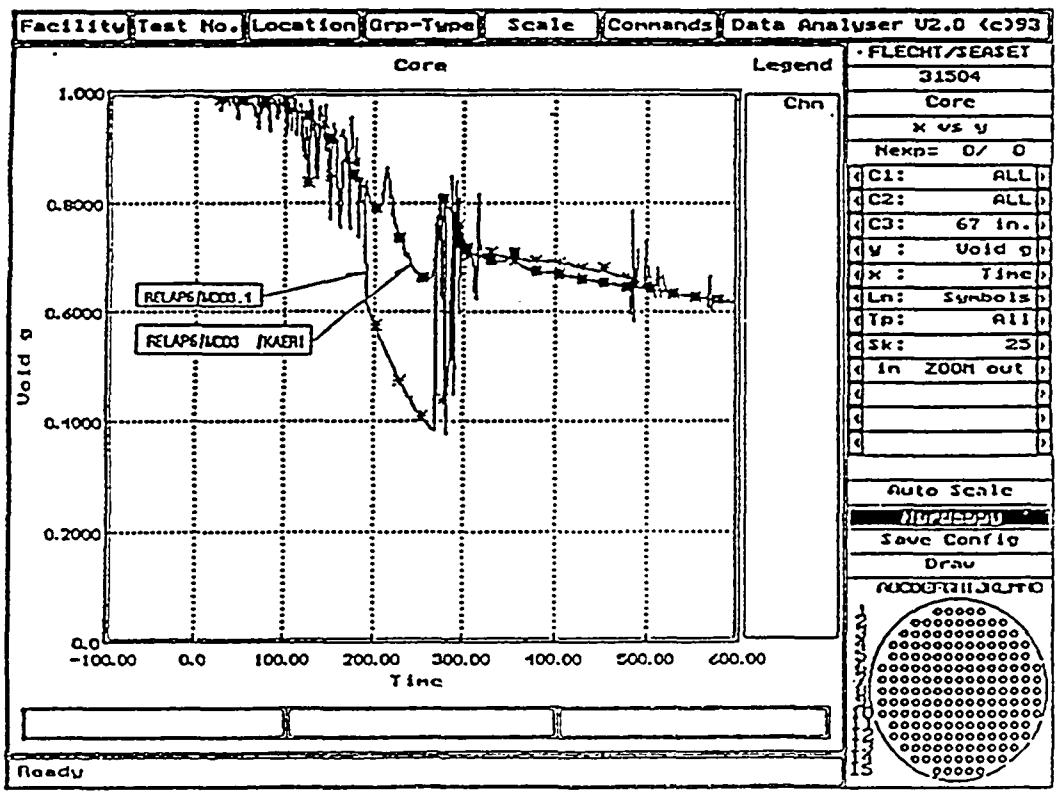

Figure 13. Void Fraction at 67 in. elevation, Test 31504

The calculated void fractions near the midplane (67 in.) is presented in Figure 13. It shows that there is excessive liquid accumulation downstream of quenching front. This may be caused by the low predicted interfacial friction for the dispersed flow regime. Based on the FLECHT experimental observations, modified version the maximum diameter of droplet size was set at the value of 2.0 mm. This restriction contributed to increasing the interfacial drag in dispersed flow regime and improving the axial void profile. Figure 14 shows that the trend of collapsed liquid level of the test section is also much improved with the modified version.

b) Test Run 31701 - High Injection Velocity

The calculated rod surface temperatures for run 31701 are presented in Figures 15 through 17 and the Figures show that the calculated results in the lower-to-middle elevation region agree well with the data. However, the results of the calculation with the original version for the upper elevation (Fig. 17) show that the quenching of this section is calculated to occur too quickly. This is probably the result of high liquid fraction and high oscillatory steam velocity caused by the pressure spikes. Figure 16 shows this pressure spikes at the inlet of test section during high reflood injection. With the modified version, the pressure spikes are very much reduced and the void fraction and steam velocity are well predicted. As a result, the surface temperatures are predicted well with the modified version.

c) Test Run 31302 - Medium Injection Velocity

In the medium reflood injection test, the main characteristics are similar to the high injection test (run 31701). As shown in Figure 19 through 22, the rod surface temperature and hydraulic behaviors are well predicted with the modified version.

d) Test Run 31805 - Very Low Injection Velocity

The main characteristics of the test run 31805 with a liquid injection velocity of 2.1 cm/sec are similar to reference test run (run 31504) which was conducted with the injection

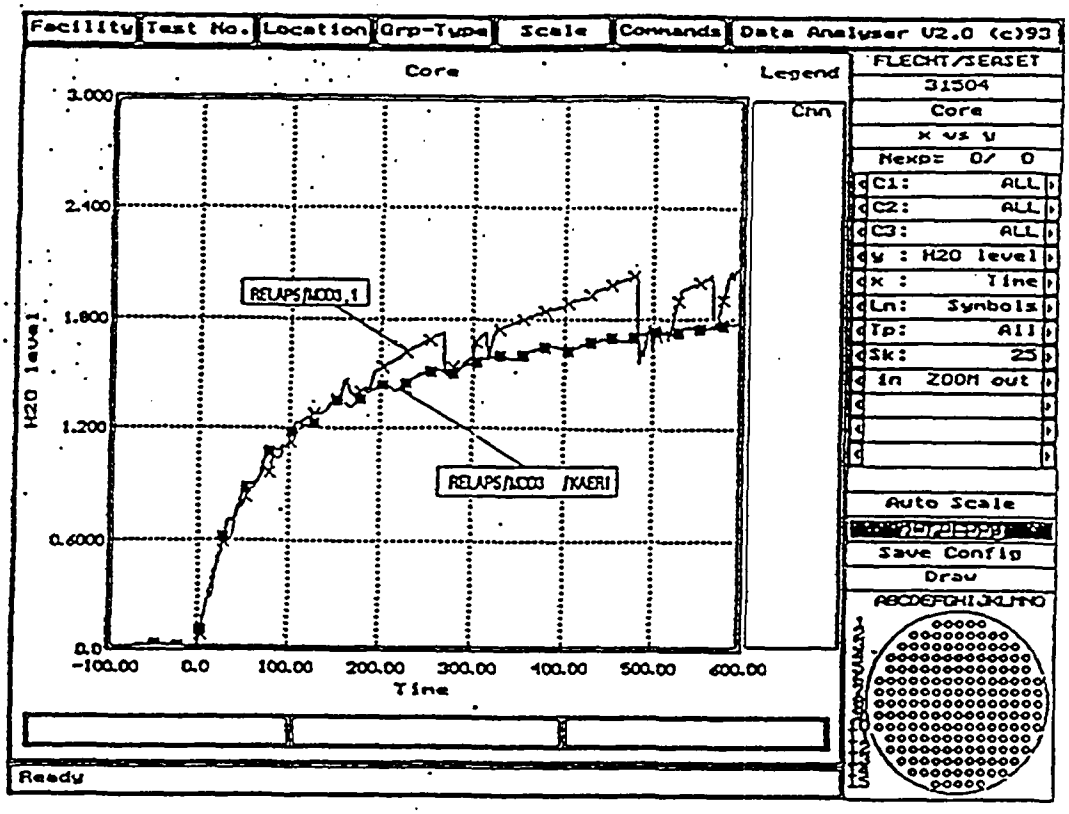

Figure 14. Water Level, Test 31504

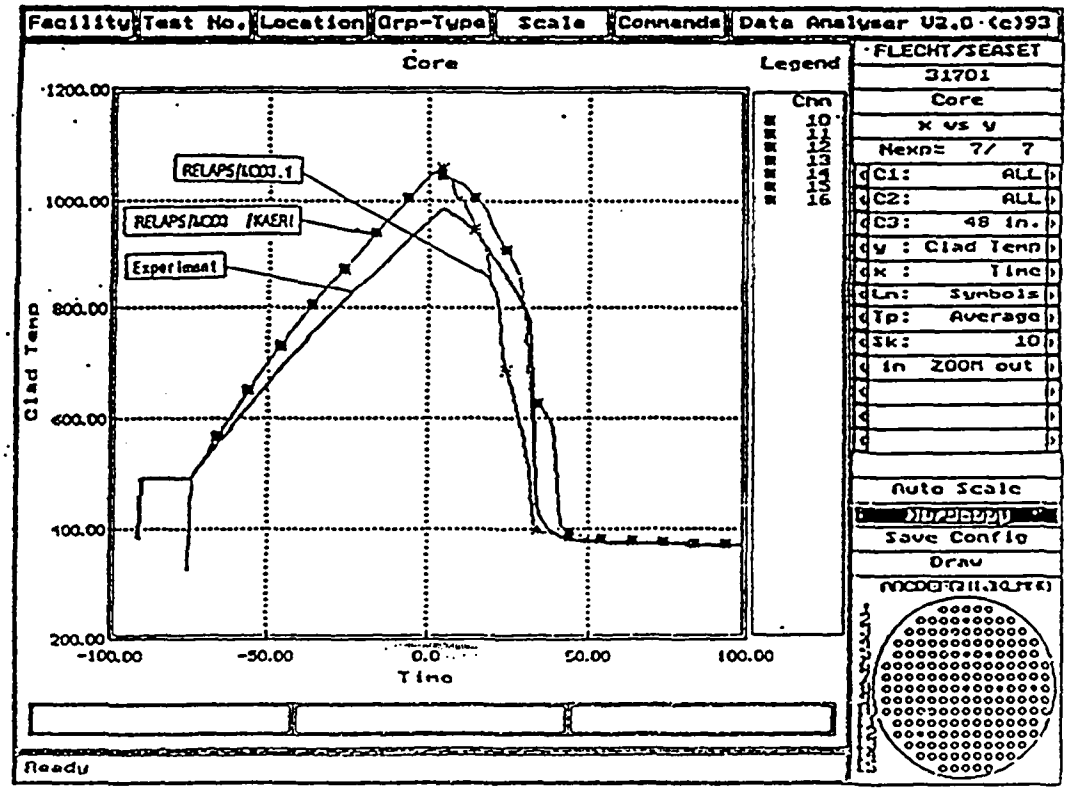

Figure 15. Cladding Temperature at 48 in. elevation, Test 31701

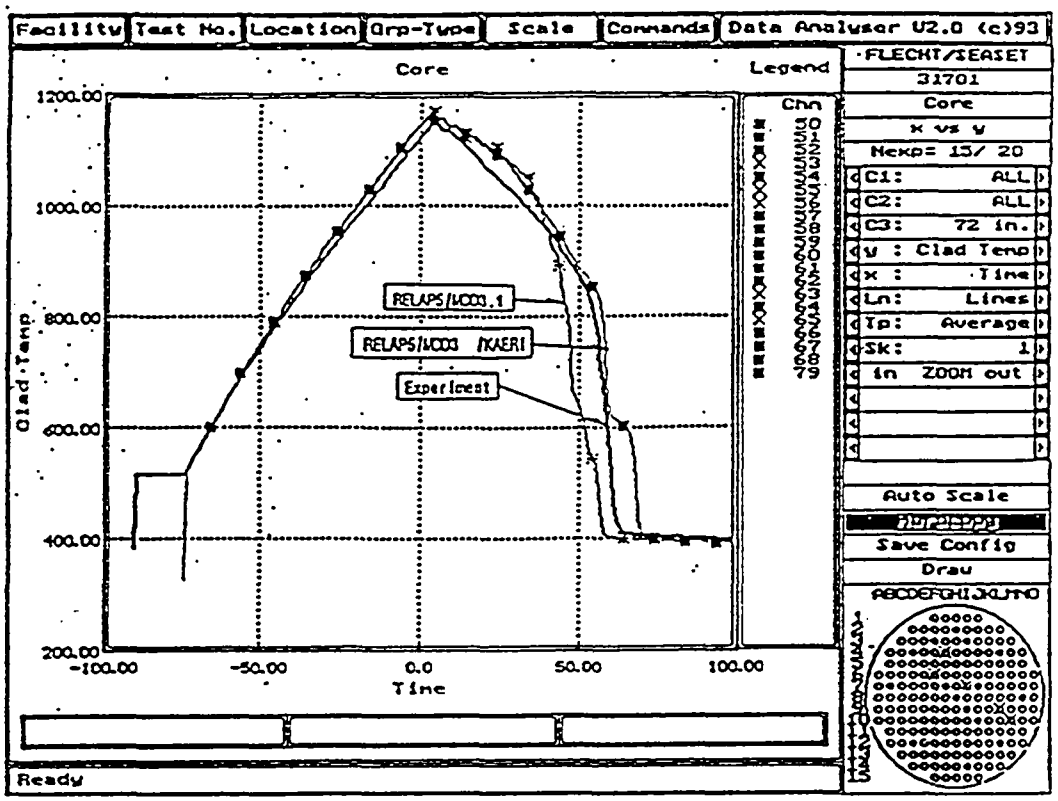

Figure 16. Cladding Temperature at 72 in. elevation, Test 31701

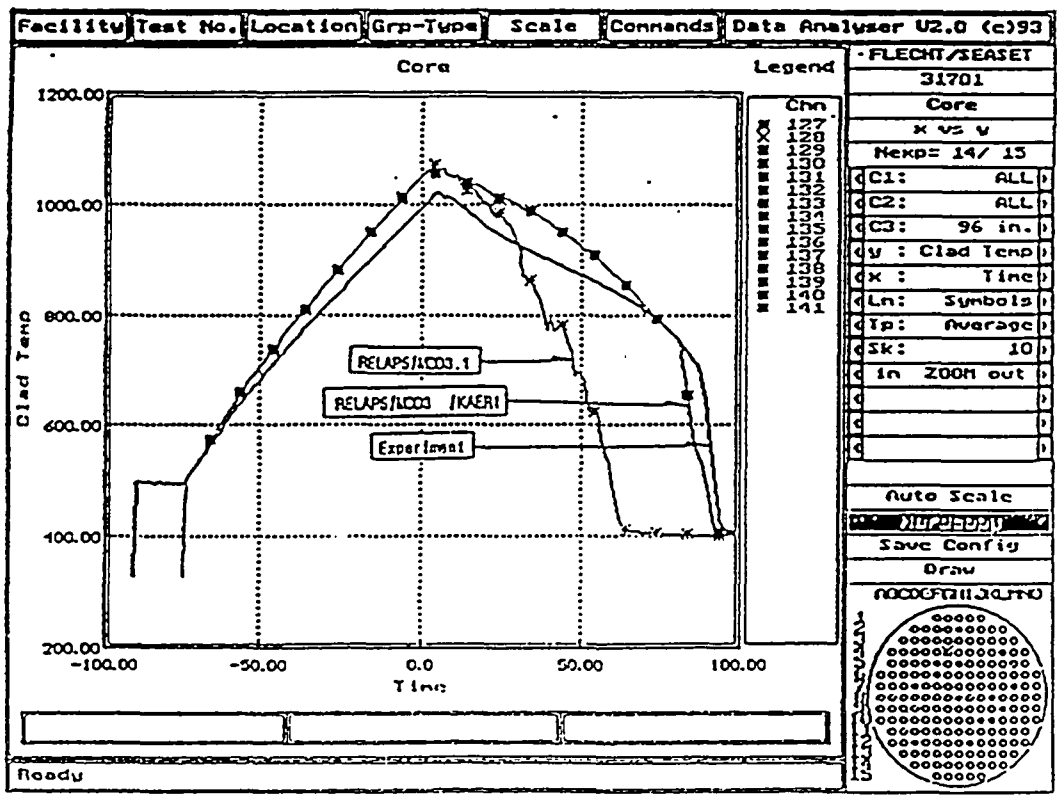

Figure 17. Cladding Temperature at 96 in. elevation, Test 31701

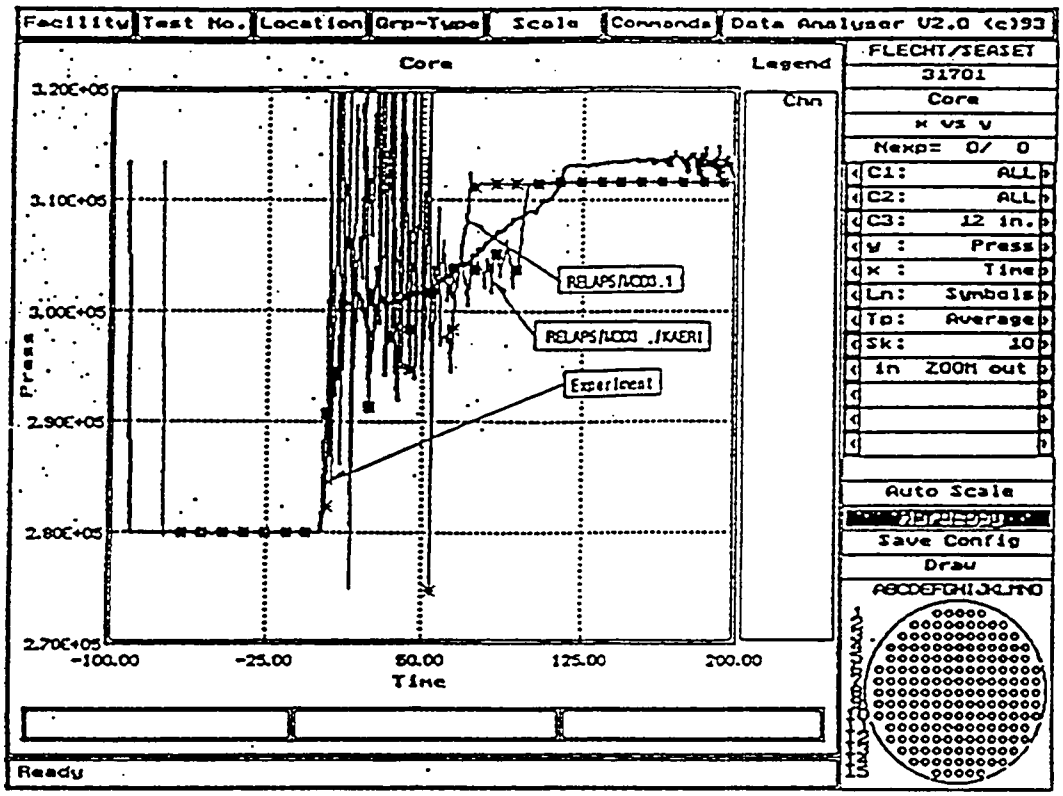

Figure 18. Inlet Pressure, Test 31701

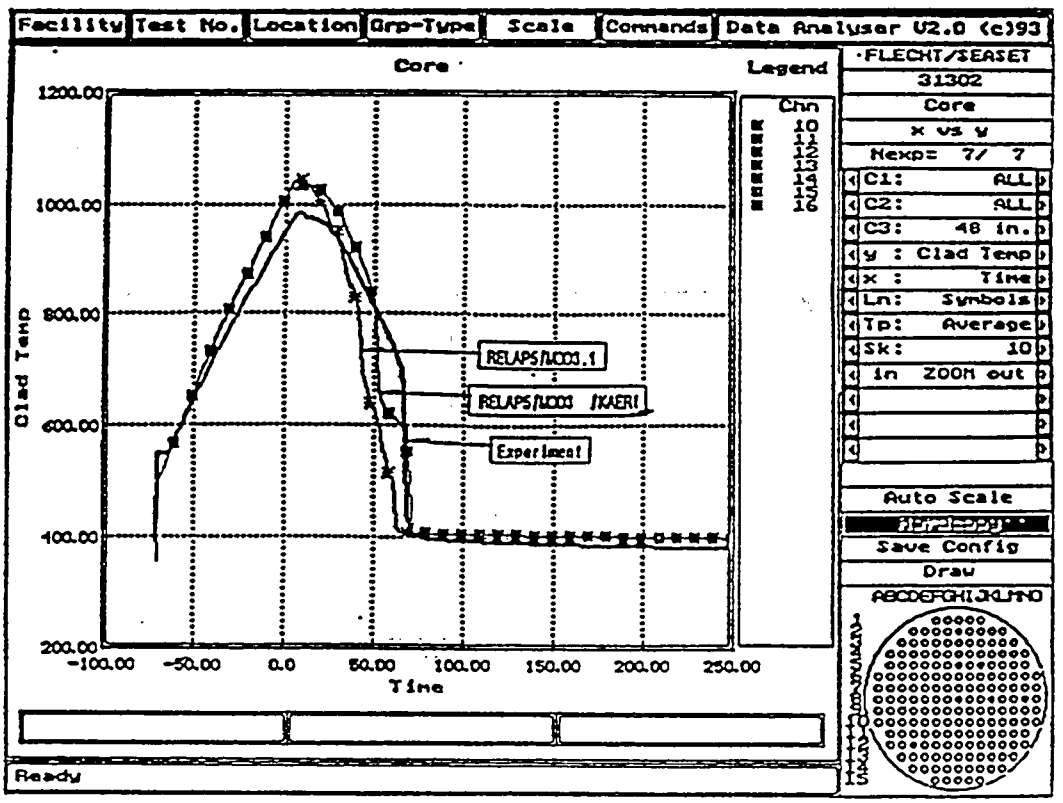

Figure 19 Cladding Temperature at 48 in. elevation, Test 31302

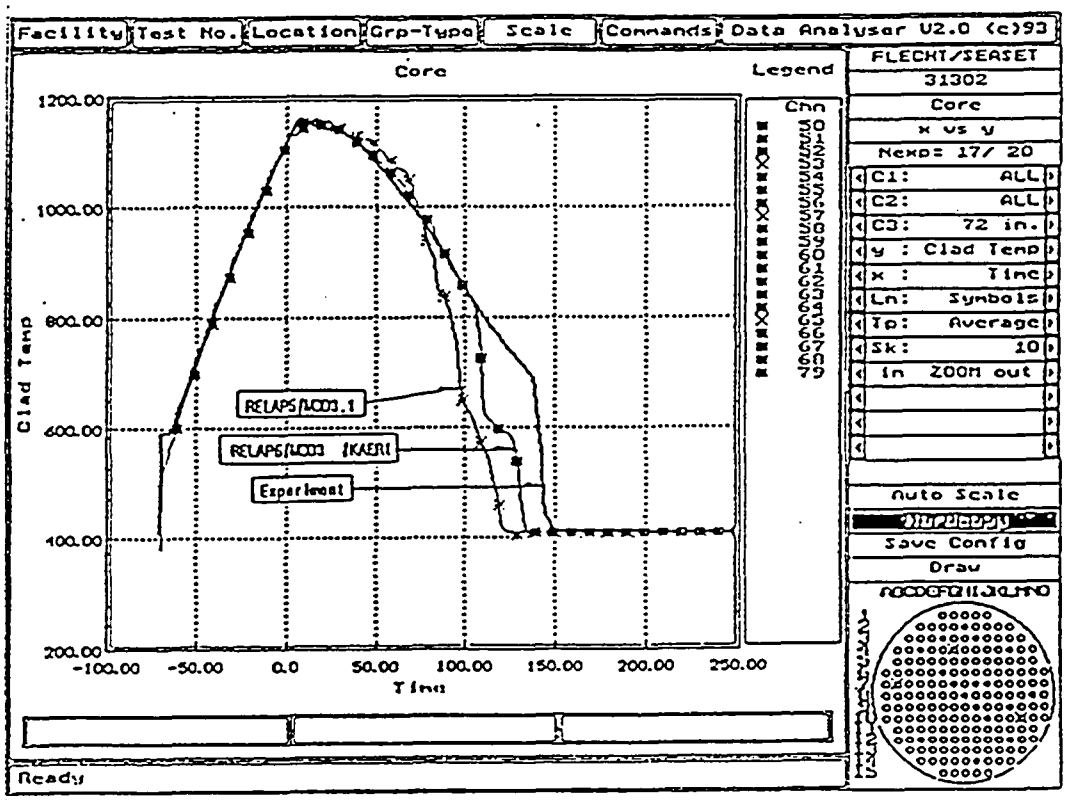

Figure 20 Cladding Temperature at 72 in. elevation, Test 31302

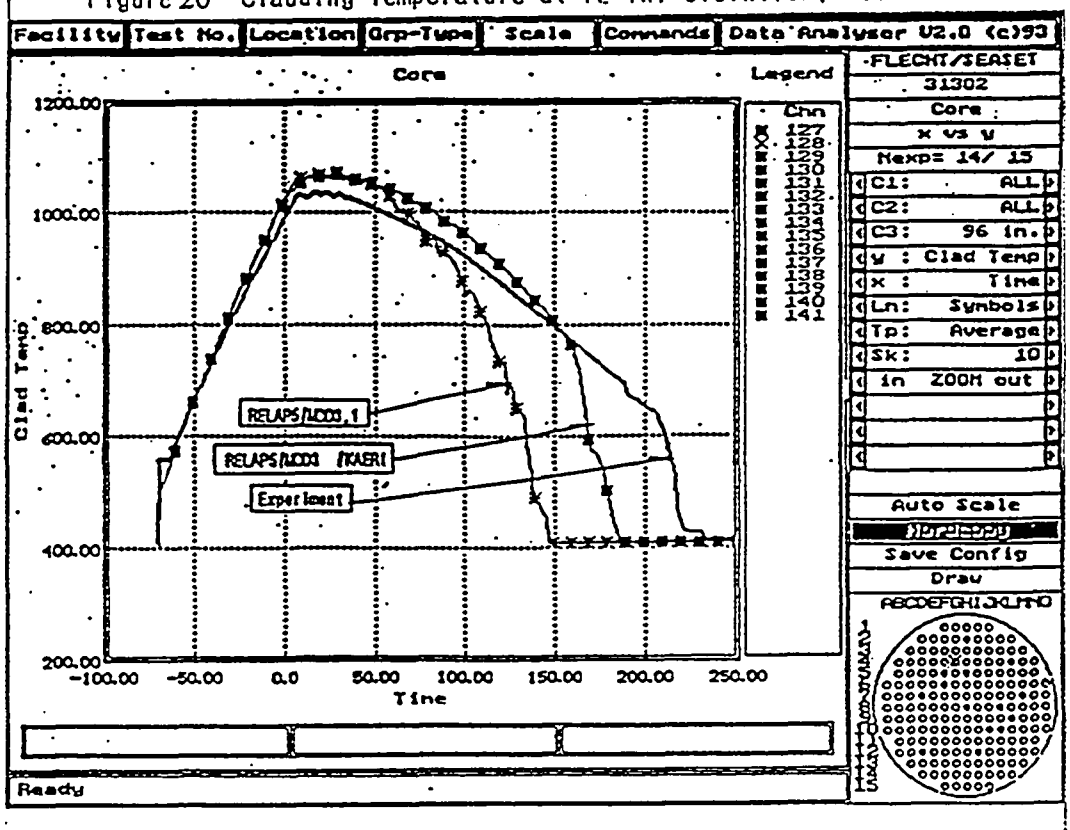

Figure 21 Cladding Temperature at 96 in. elevation, Test 31302

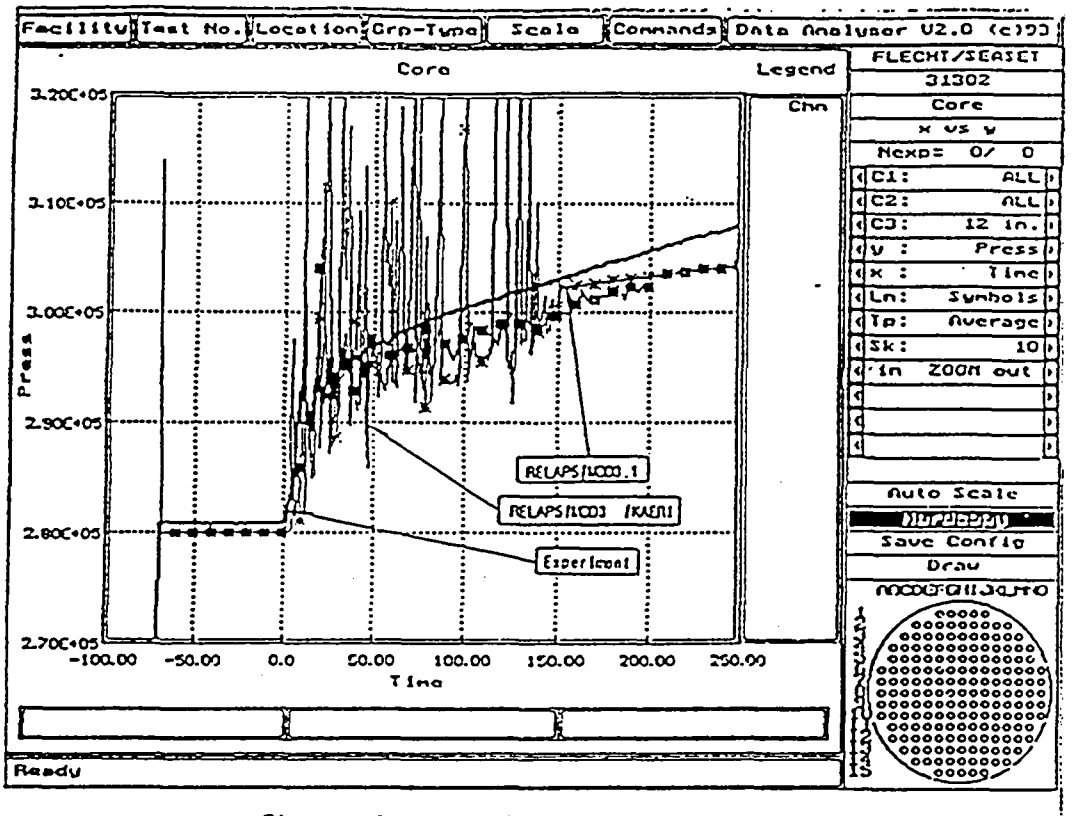

Figure 22. Inlet Pressure, Test 31302

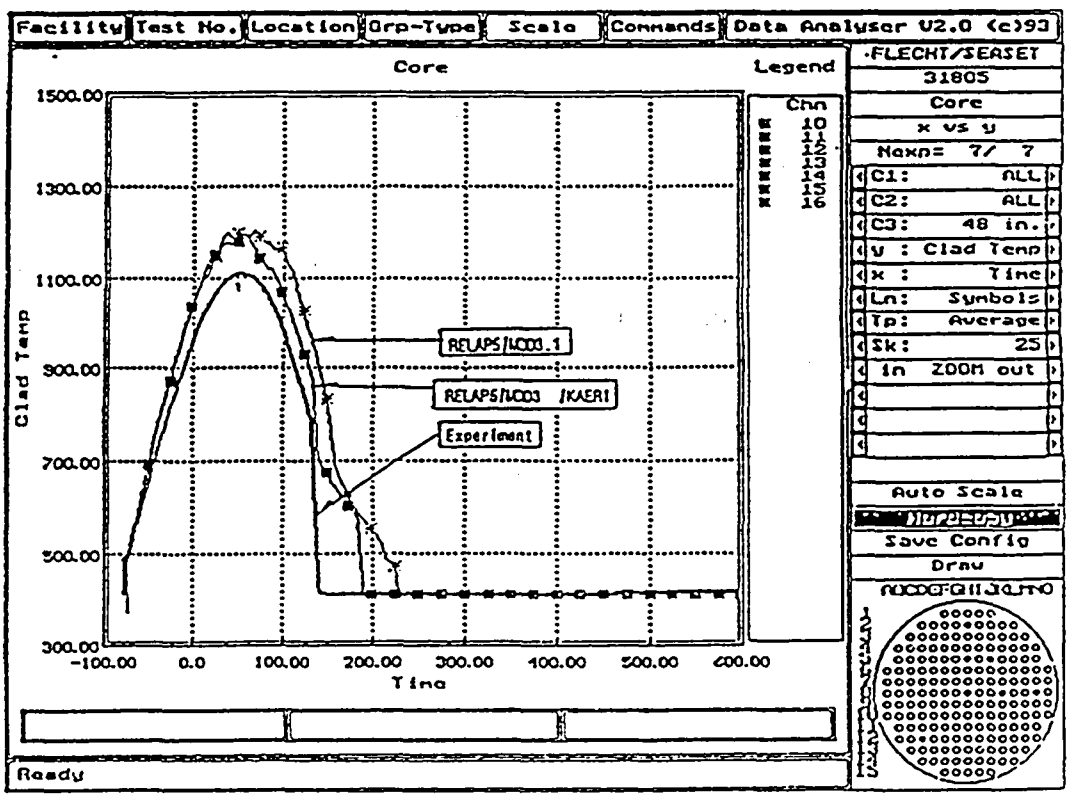

Figure 23. Cladding Temperature at 48 in. elevation, Test 31805

velocity of 2.46 cm/sec. All thermal-hydraulic behaviors were delayed compared to the reference test due to the slightly lower injection velocity. The Figures 23 - 26 show that the quenching tail and pressure trends are improved with the modified version, although the rod surface temperature turnaround occurs too early due to the same reasons as in the reference test (31504) case.

3.2.2 Gravity Feed Test

Test run 33338 of gravity feed was selected for developmental assessment because it is a more realistic reflood situation. The radial power distribution was accounted for in the calculation and the rod surface temperature results from hot channel were presented in Figures 27 through 29.

The surface temperature is reasonably predicted during the initial high reflood injection (~ 15 second). After the reduction of reflood rate, the test data show a slight increase in temperature while the original code predicted the continuous decrease and early quenching. The deviations became greater in the middle-to-upper elevation. This weakness of original version is probably due to the incorrect void fraction and steam velocity in test section. Unlike the forced reflood case, the liquid flow entering in the test section depends on the small pressure difference between the downcomer and the test section. If pressure spikes are predicted to occur in calculation, these may greatly affect the liquid injection velocity. Figure 30 shows the pressure variation at the test section inlet and shows the severe pressure spikes calculated to occur with the original code. With the help of wall vaporization smoothing in the modified version, these pressure spikes were diminished after the deduction of reflood rate. This reduced the flow oscillation in test section (Figure 31) and resulted in the correct prediction of rod surface temperature.

The quenching behavior of surface temperature were also predicted well in the modified version due to the quenching temperature model.

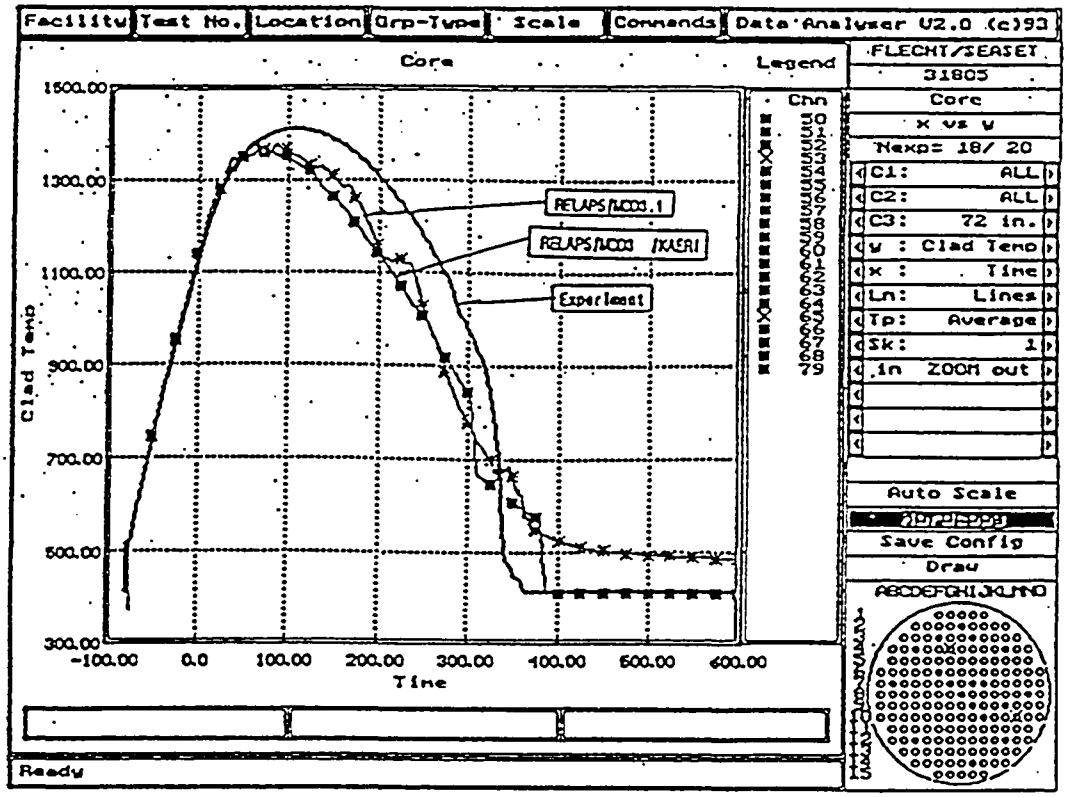

Figure 24. Cladding Temperature at 72 in. elevation, Test 31805

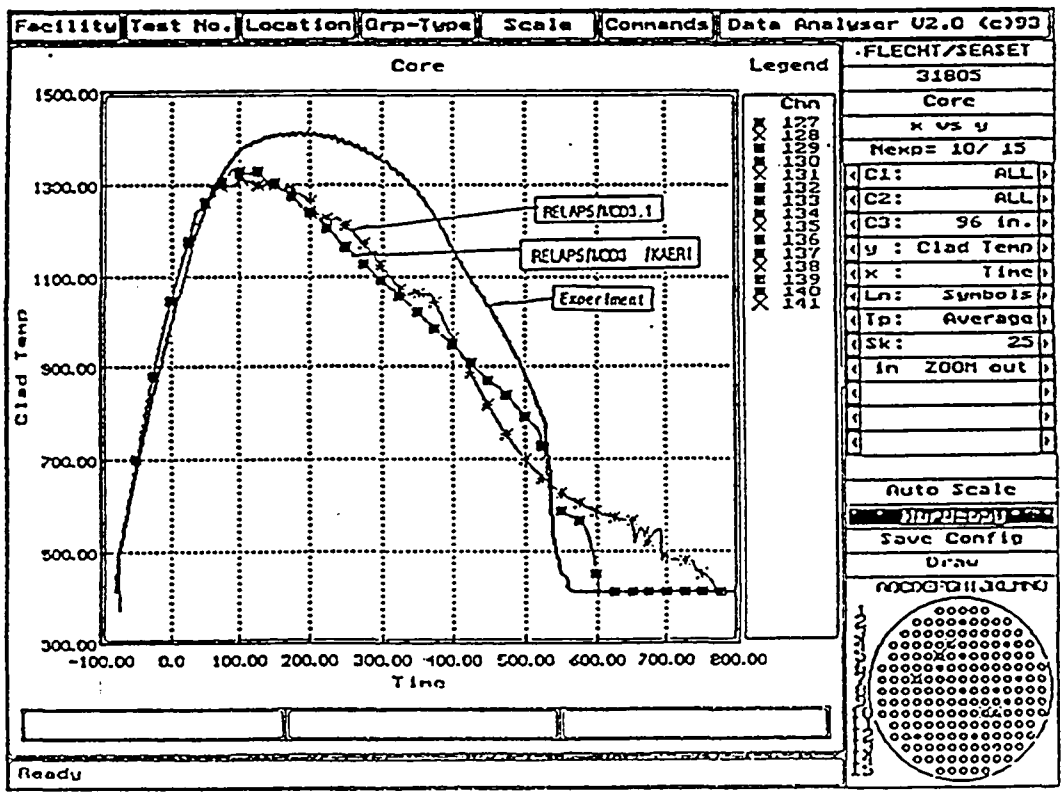

Figure 25. Cladding Temperature at 96 in. elevation, Test 31805

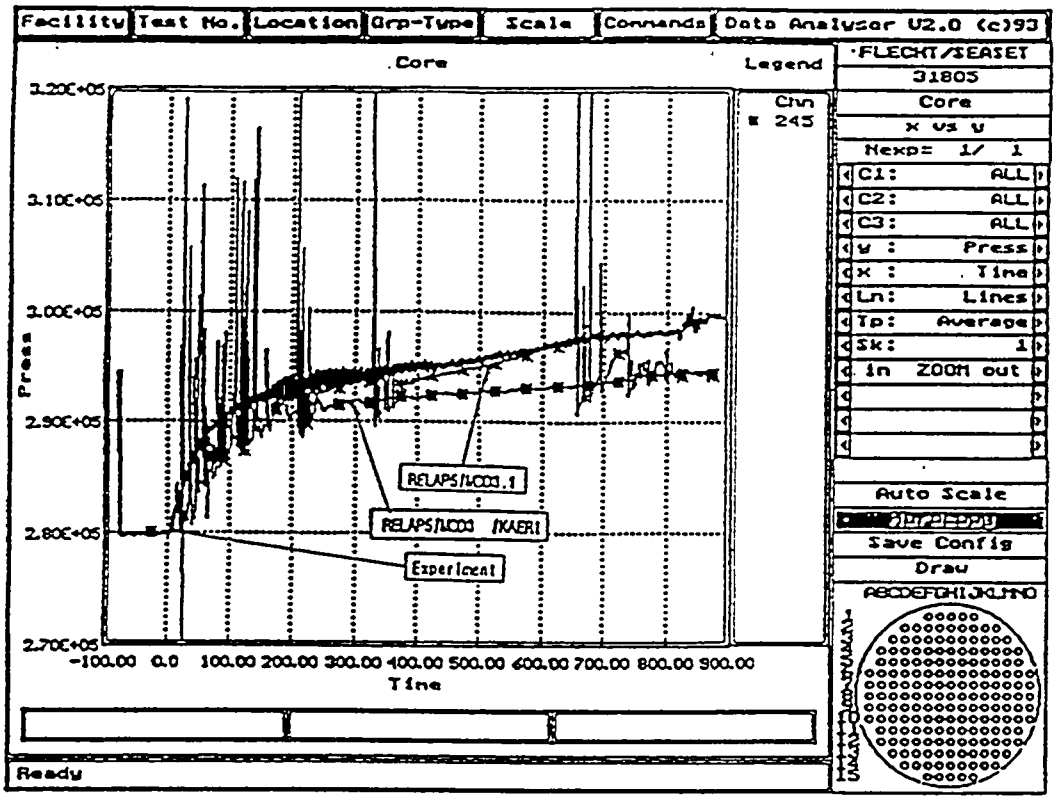

Figure 26. Pressure, Test 31805

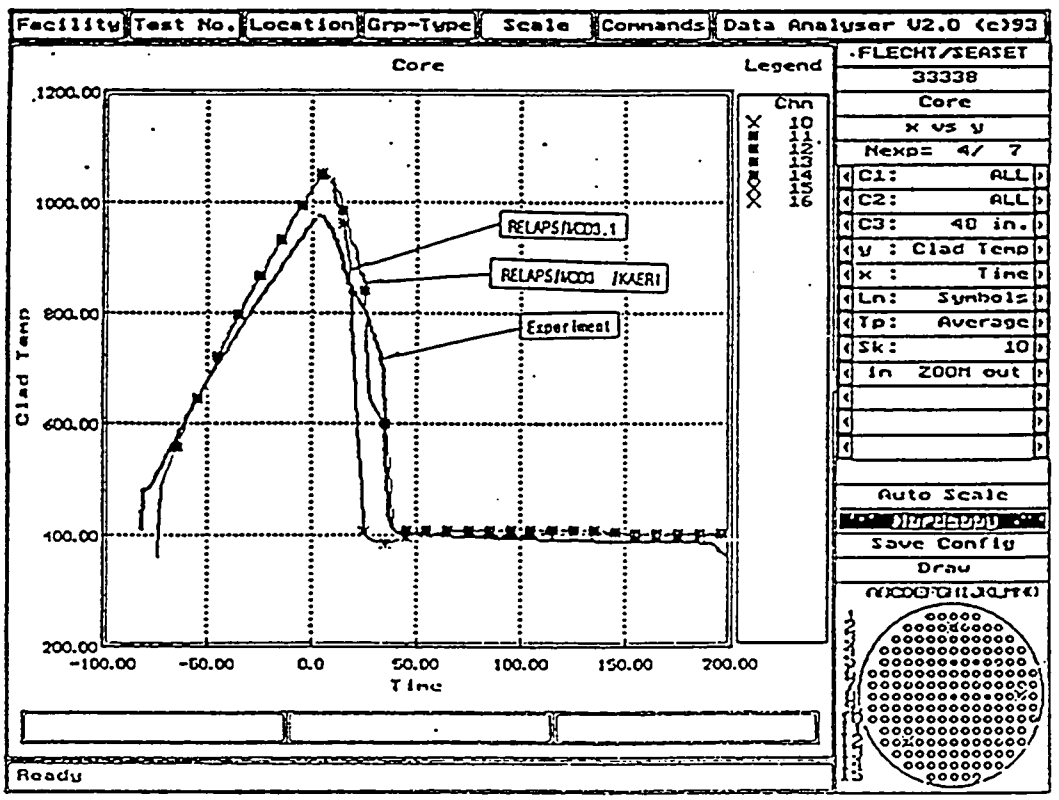

Figure 27. Cladding Temperature at 48 in. elevation, Test 33338

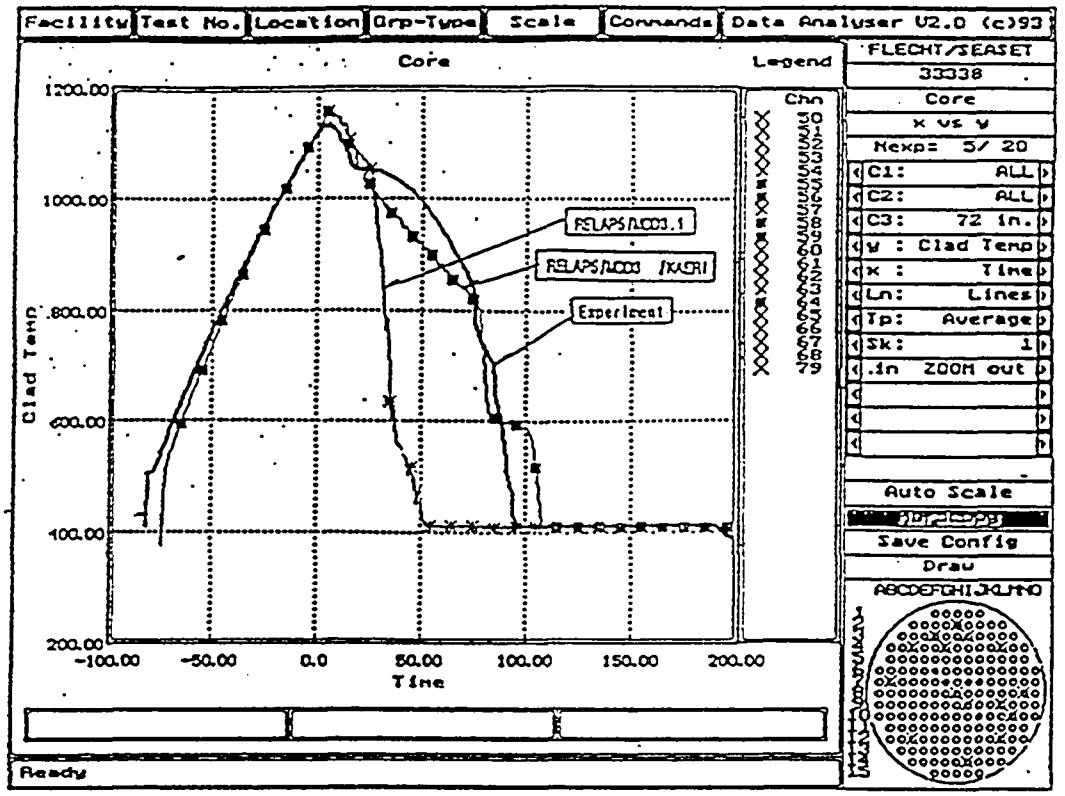

Figure 28. Cladding Temperature at 72 in. elevation, Test 33338

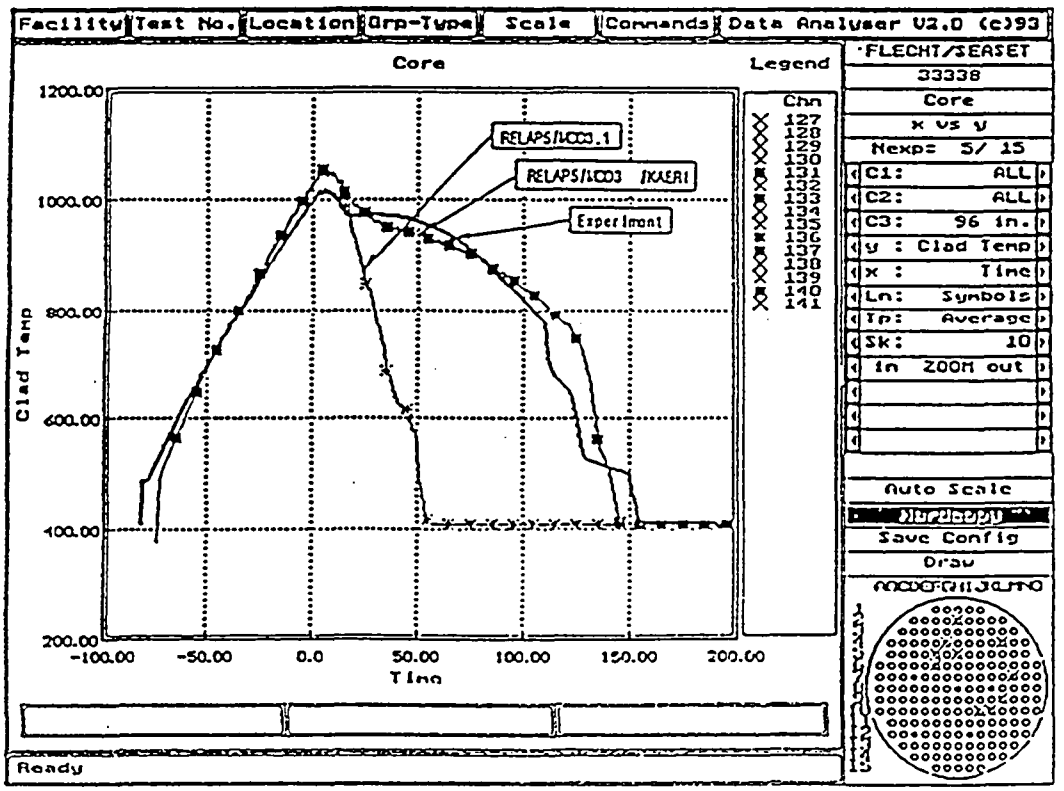

Figure 29. Cladding Temperature at 96 in. elevation, Test 33338

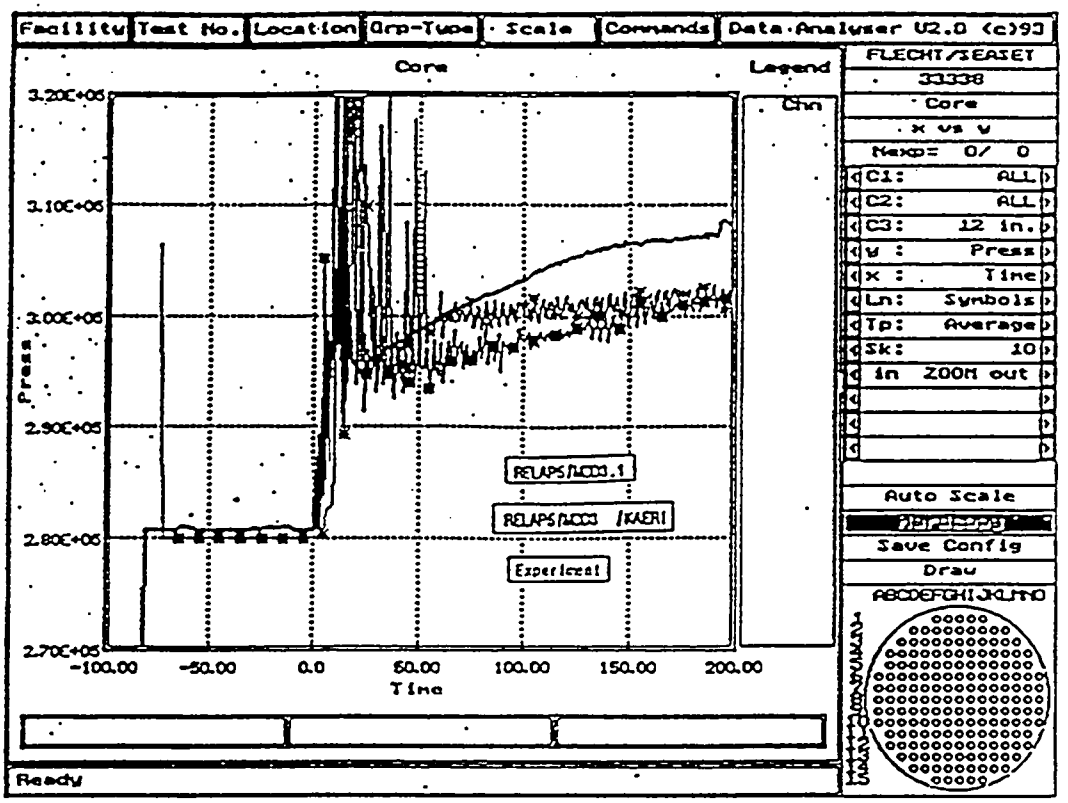

Figure 30. Inlet Pressure, Test 33338

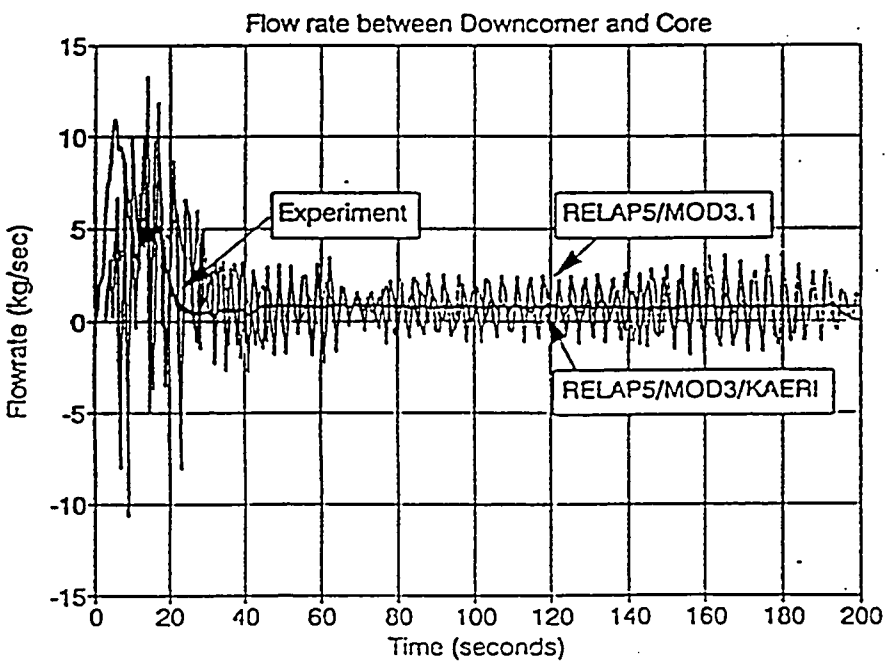

Figure 31. Flow-rate between Downcomer and Core, Test 33338

3.3 Turn-around Temperature

In FLECHT experiment there are many radial measurement locations in same elevation. The test data are scattered due to many reasons; e.g., non-uniform manufactures of electric heaters, 2D/3D effect of flow, and errors in the measuring calibration. To account for these measurement and hydraulic uncertainties the calculated turn-around temperature (i.e. peak clad temperature) at each measurement elevation was compared with all of the radial measurement channels available for that elevation. The scatter-graph of the calculated PCT of original version versus measured PCT is presented in Figure 32. In this figure, the gravity reflood case was excluded in order to identify the effect of liquid injection rate on PCT. As shown in the Figure, the scattering band of test data is about 100 K. There is a general trend in PCT of a slight overprediction at low temperatures and an underprediction at high temperatures. It shows that the RELAP5/MOD3.1 underpredicts the clad temperature when the injection flow rate is low. With the modified version, although there is a slight improvement in low temperature region, nearly the same results were obtained. The Figure 33 shows the graph of calculation results versus test data the and uncertainty band.

3.4 Quenching Time

The determination of quenching time depends on the definition of quenching. In this report the quenching time was defined as the latest time that the clad temperature reaches 500 K (50 K above the CHF temperature). Such a simple definition enabled an easy comparison between the calculation result with the test data.

Figure 34 shows that the original code predicts early quenching in the case of high liquid injection and delayed quenching in low liquid injection case. The scattering of predicted results is too broad and it highlights the shortcomings in the transition boiling model and the problem of the flow oscillation due to pressure spikes during reflood. These weaknesses of the code were addressed and improved in the modified version and much better results were obtained as can be seen in Figure 35.

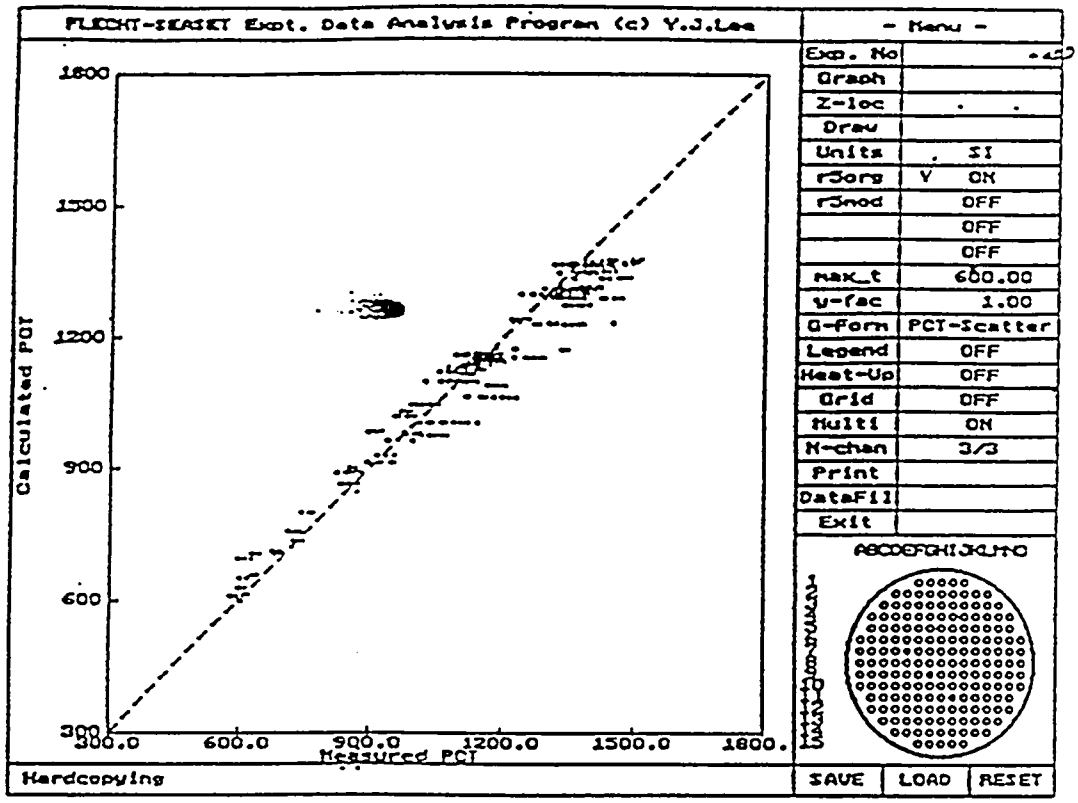

Figure 32. Measured vs. Calculated PCT scatter-diagram for RELAP5/MOD3.1, Tests 31302, 31701, 31805 and 33338

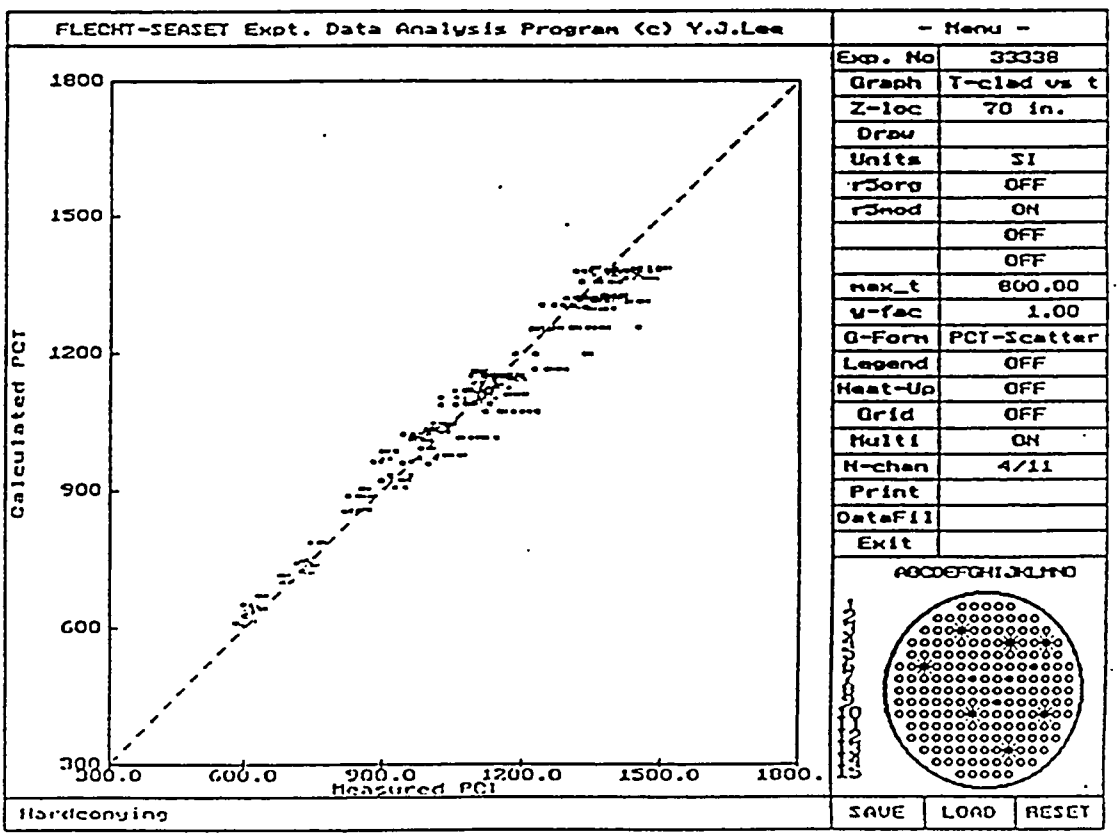

Figure 33. Measured vs. Calculated PCT scatter-diagram for RELAP5/MOD3/KAERI, Tests 31302, 31701, 31805 and 33338

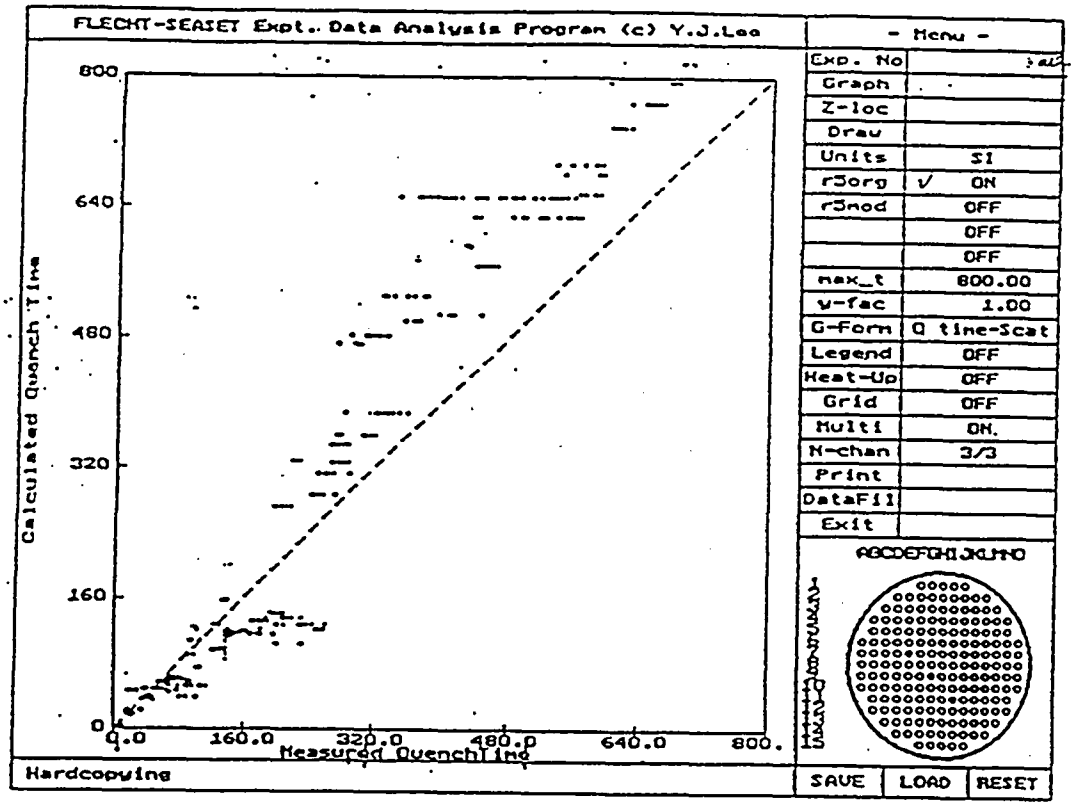

Figure 34. Measured vs. Calculated Quench-Time for RELAP5/MOD3.1, Tests 31302, 31701, 31805 and 33338

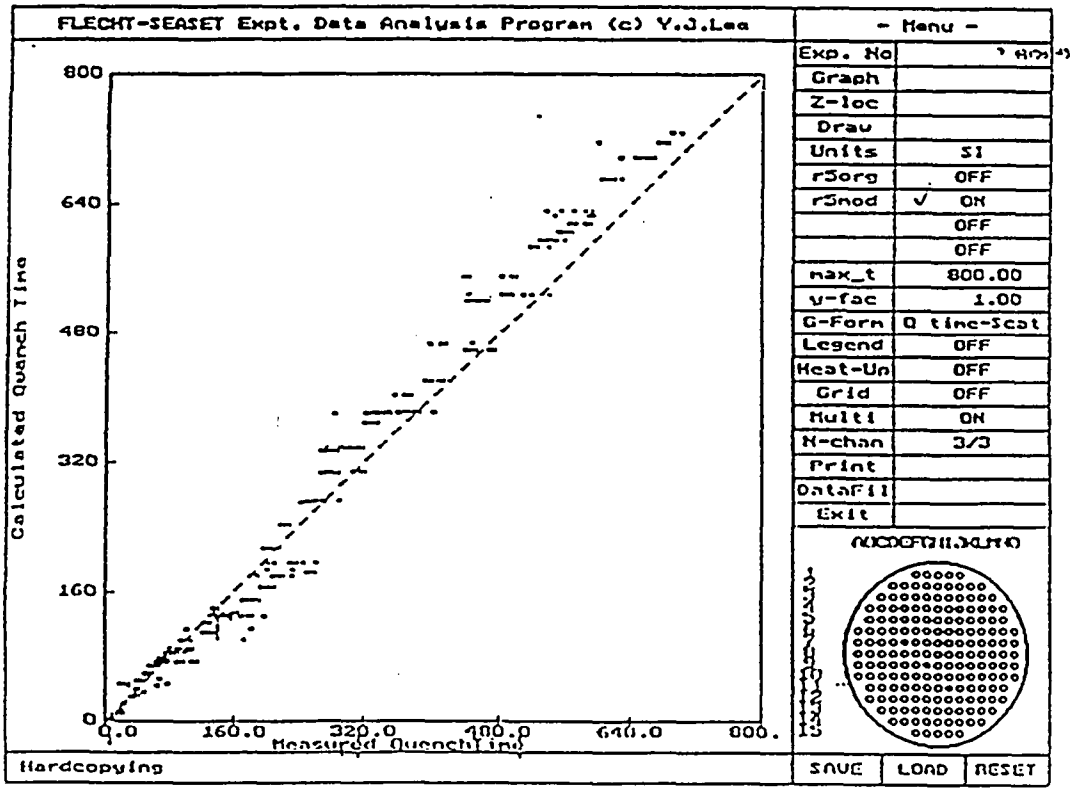

Figure 35. Measured vs. Calculated Quench-time scatter-diagram for RELAP5/MOD3/KAERI, Tests 31302, 31701, 31805 and 33338

4. Model Assessment and Uncertainty Quantification

We focus our concern on assessing the reflood PCT predictability of RELAP5/MOD3/KAERI during LBLOCA and quantifying the associated uncertainty applicable to an LBLOCA realistic evaluation model(REM). For uncertainty quantification there should be a sufficiently large number of available test data so that a statistical treatment may be possible, and the pool of data should cover the conditions expected to occur during LBLOCA. FLECHT SEASET test is chosen because the test facility is full sized with respect to axial height and experiments were performed on wide ranges of test conditions. We compare the experimental and calculational PCTs for the forced and gravity feed reflooding of 161 rod unblocked bundle tests with variations of the parameters such as flooding rate, initial clad temperature, rod peak power, and system pressure. The code uncertainty evaluated from data comparison with the relevant experimental data could be an estimate of the uncertainty attributable to the combined effect of the reflood models and correlation's in the code, RELAP5/MOD3/KAERI.

4.1 Assessment

The experimental data for the assessment are selected from the 161-rod FLECHT SEASET reflood test data in the data bank of USNRC, ENCOUNTER[34]. The raw data consist of 177 heater rod surface temperatures, steam probe temperatures, rod bundle powers, flow rates, and absolute and differential pressures. The failed data in the total 256 channels are determined and rejected in the assessment. Linear interpolation of calculation results is necessary to correctly compare calculational and experimental data at the same elevation. (Fig. 36)

The 18 selected test runs with wide range of several parameters including flooding rate, system pressure, initial clad temperature, rod bundle power, and others, are divided into 5 groups designed to investigate the effect of each parameters as shown in table 1, and described below.

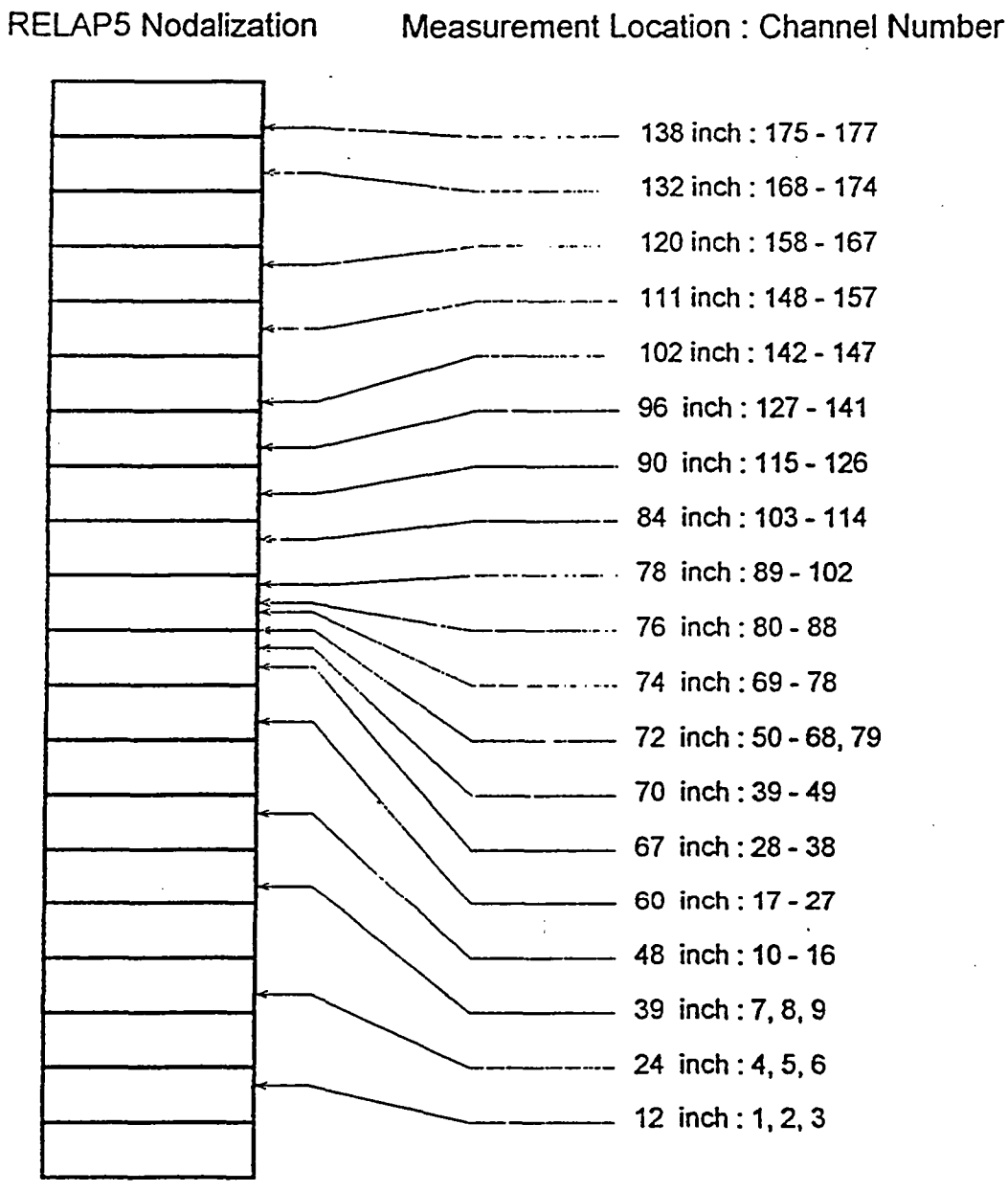

Fig. 36 RELAP5 Nodalization versus Location of Measurement

Group 1 - effect of flooding rate

Three planes of test section are chosen for the comparison of calculated and experimental cladding temperatures in the test run 31701: low plane(at 48 inch elevation), mid plane(at 72 inch elevation), and high plane(94 inch elevation). Fig. 37 shows the clad temperature comparisons at low, mid, and high planes. The experimental data at the same elevation except the failed channel data are averaged to be compared with the corresponding calculational value. The thicker line represents the averaged experimental cladding temperatures at the elevation, and the thinner line represents the corresponding calculational values. Calculation shows very good agreement with the experiment at mid plane, but tends to over-predicts the cladding temperatures at low and high planes. However it is noted here that the experimental data show a broad spread especially in the low and high region of test section. Fig. 38 compares the non-averaged experimental and calculational cladding temperatures at high plane. The line marked with solid square shows calculational value and the others represent experimental data. It can be seen that the predicted clad surface temperatures are within the scattered band of the experimental data. Therefore we can conclude that slight over-prediction of peak cladding temperature(PCT) shown from the curves for low and high planes in Fig. 37 is acceptable, and that RELAP5/MOD3/KAERI code well predicts the cladding temperature in the entire core for the high flooding rate experiment, 31701. Fig. 39 shows the comparison of calculational and averaged experimental cladding temperatures at mid plane for various flooding rate. Calculation agrees well with the experiment in medium flooding rate(test runs, 31302 and 31203), but slightly under- estimate the PCT in low flooding rate(test runs, 31504 and 31805). And the under- prediction of PCTs in low flooding rate results from the early turn-around as shown in that figure.

Group 2 - effect of system pressure

The test run, 31504 has been discussed in group 1, but the results of the test runs, 32013 and 34209 are represented in Fig. 40. The calculational PCTs agree well with the experimental values both in the low and in the high pressures, but quenching is delayed in low pressure test, 34209. Then the delayed quenching may result in the over-prediction of

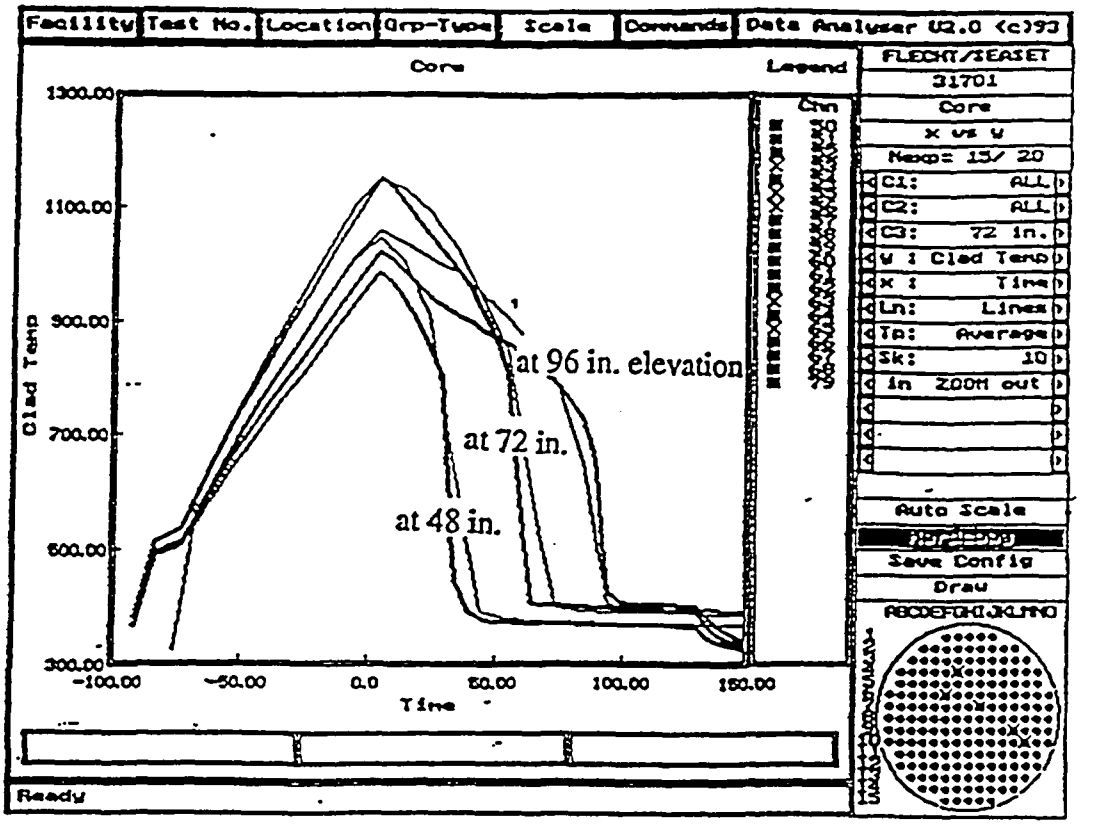

Fig. 37 Comparison of calculational and experimental cladding temperatures at selected elevations for test run, 31701

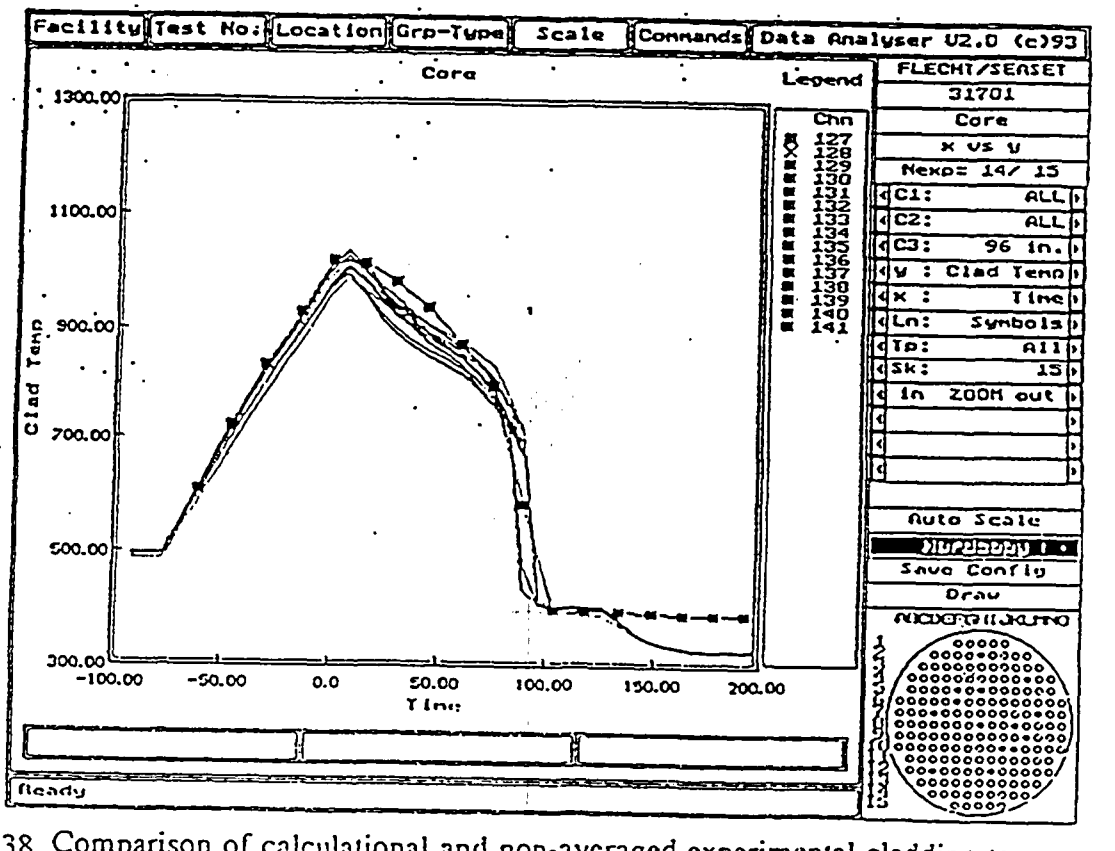

Fig. 38 Comparison of calculational and non-averaged experimental cladding temperatures at 96 inch elevation for test run, 31701

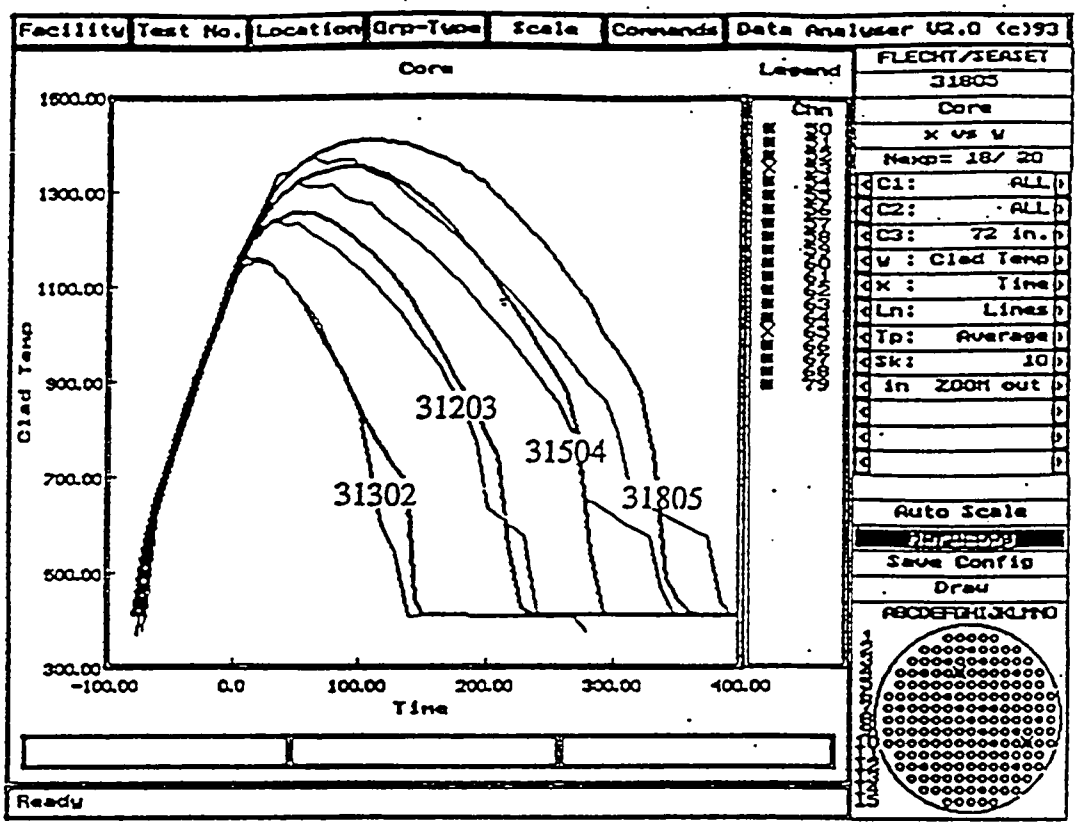

Fig. 39 Comparison of calculational and experimental cladding temperatures at 72 inch elevation for test runs, 31302, 31203, 31504, and 31805

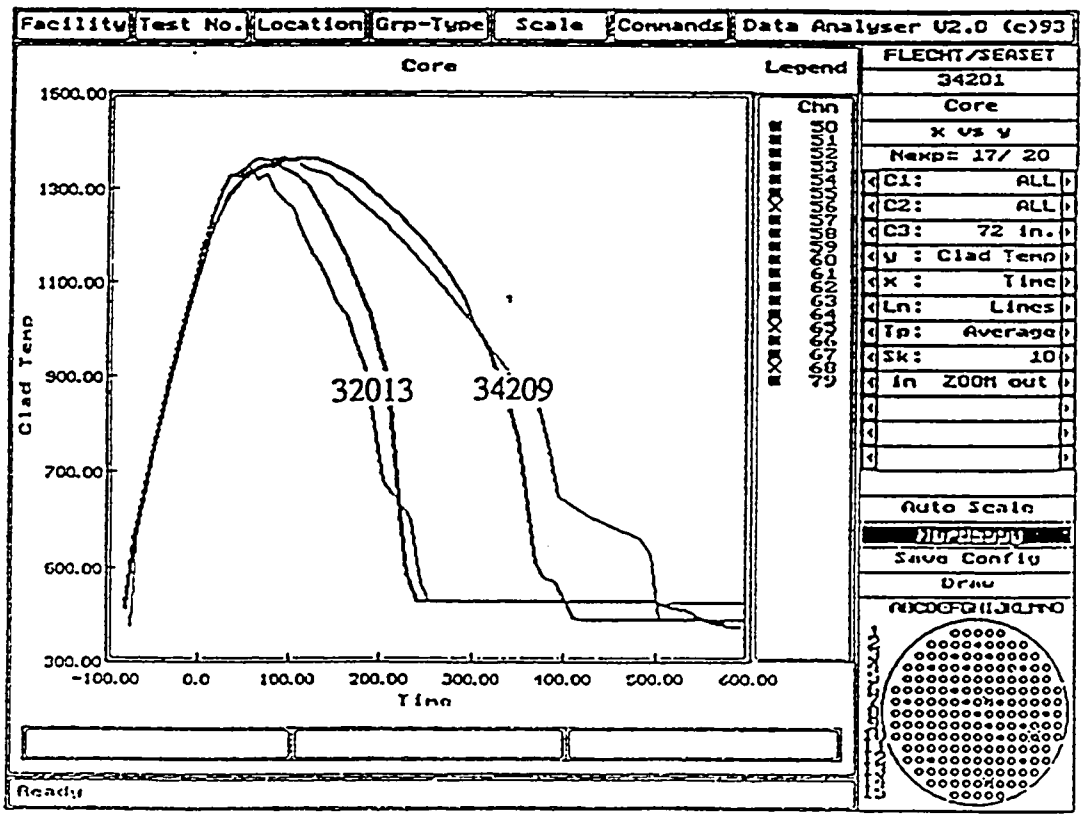

Fig. 40 Comparison of calculational and experimental cladding temperatures at 72 inch elevation for test runs, 32013 and 34209

PCT in the down stream of core.

Group 3 - effect of initial clad temperature

Experimental and calculational clad surface temperatures are compared in Fig. 41 for the test runs, 34420, 30817, and 30518. The test run 31203 was already discussed in group 1. Somewhat early quenching appears in low initial clad temperature as shown in the curves for the test run, 30518, but PCTs are little impacted by the early quenching. Therefore PCTs are well predicted even with the variation of initial clad temperature.

Group 4 - effect of rod bundle power

The test runs, 31021 and 34524 are presented in Fig. 42. The test run 31203, which belongs to group 1 as well, is omitted here. The tests in the group 4 commonly show early turn-around behavior because of the low flooding rate. Quenching is delayed in high power as shown in the curves of test run, 34524, and it may result in over-prediction of PCT in the top region of core.

Group 5 - The other effect

The test run, 36026 is selected to analyze the effect of radial power distribution. It can be seen from the comparison of computational and experimental data in the radial high power region that the radial power distribution has no significant impact on PCT prediction. However, probably because the flooding rate is low, the code under-predicts the turn-around time. In the test runs, 32333 and 32235, the flooding rate is varied during the transient. The RELAP5/MOD3/KAERI predicts well the PCTs even for the variable flooding rates. The delayed quenching in test run, 32235, does not seem to be due to variable flooding rate, but due to the low system pressure. The test run, 31108, is performed in low pressure and at medium flooding rate. The calculation shows good agreement with the experimental data. The low pressure does not delay the quenching in this test in contrast to the low flooding rate cases. The test run 34006 is characterized by low rod bundle power and low flooding rate. Early turn-around of clad surface temperature

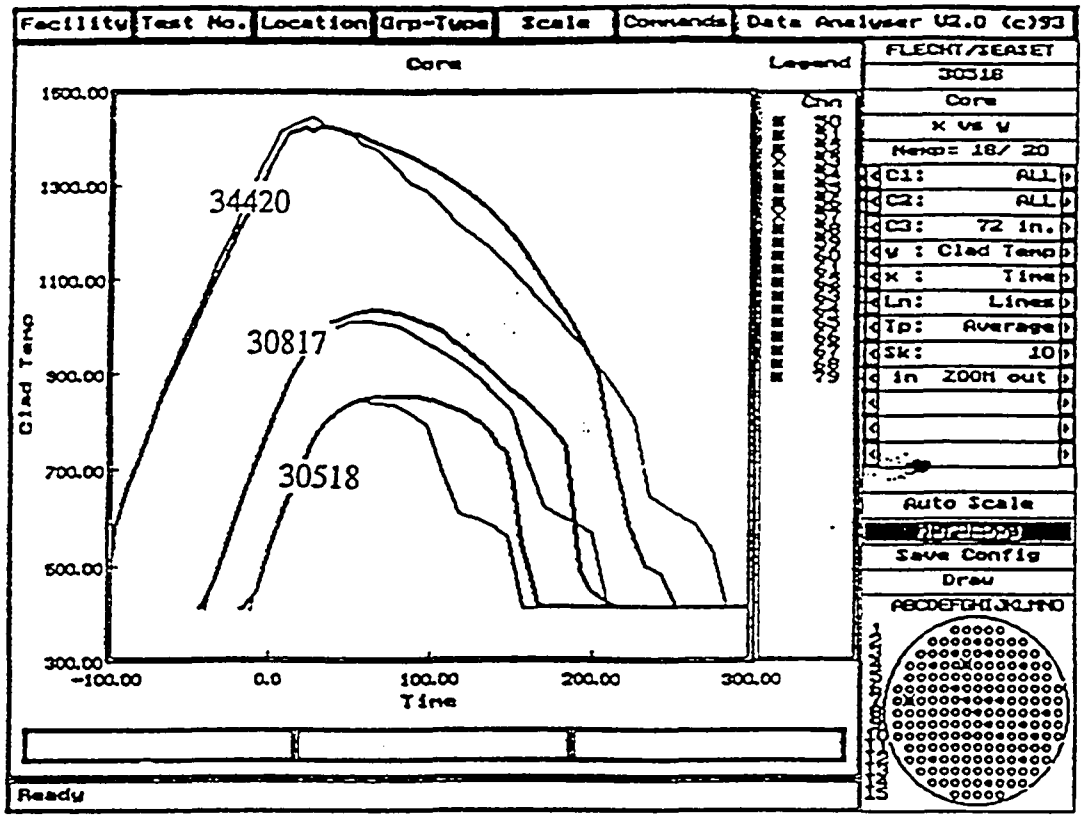

Fig. 41 Comparison of calculational and experimental cladding temperatures at 72 inch elevation for test runs, 30518, 30817, and 34420

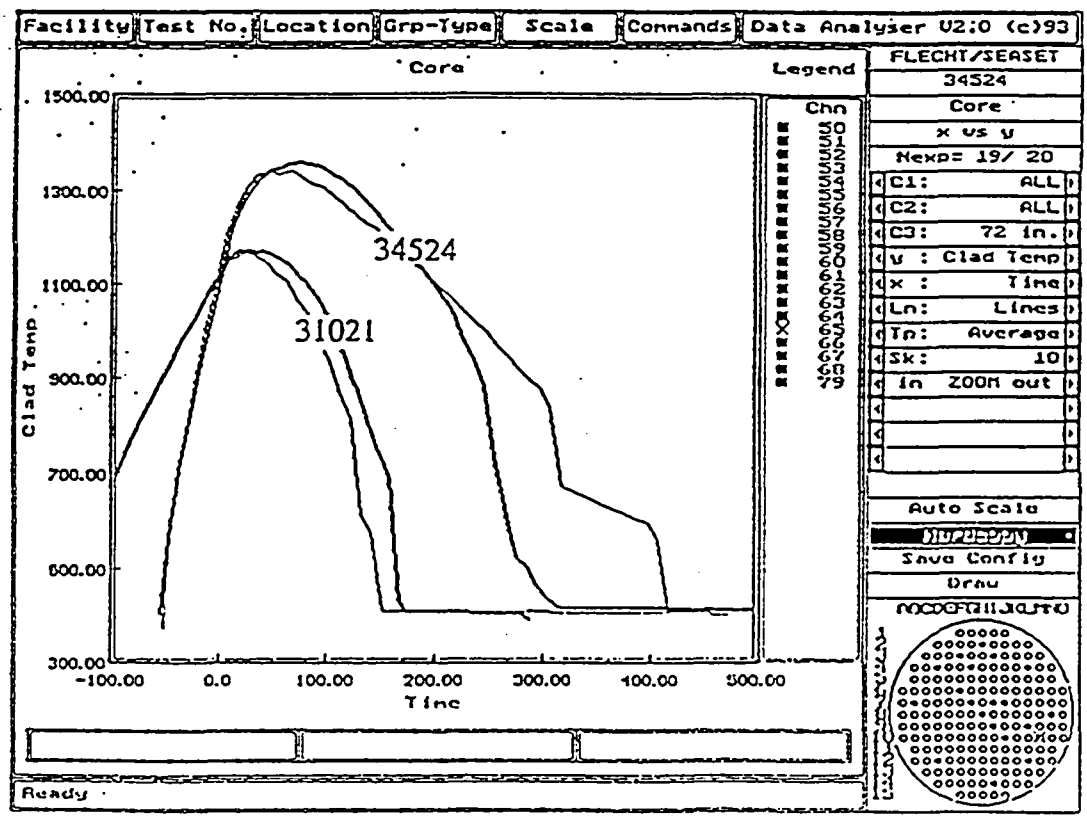

Fig. 42 Comparison of calculational and experimental cladding temperatures at 72 inch elevation for test runs, 31021 and 34524

and early quenching appear in that test. These trends become more severe and result in large under-prediction of PCT in top region of core. The comparison plots for the test runs, 36026, 32333, 32235, 31108, and 34006, which were discussed above, are omitted here for brevity. The gravity feed test, which is closer to the reflood conditions, is conducted in test run, 33338. Radial power distribution is also allowed in this test. The predicted clad surface temperatures in the radially hot region are compared with the corresponding experimental values in Fig. 43. The behavior of cladding temperature including turn-around time, quenching time, and PCT, agree well with experiment in entire test section.

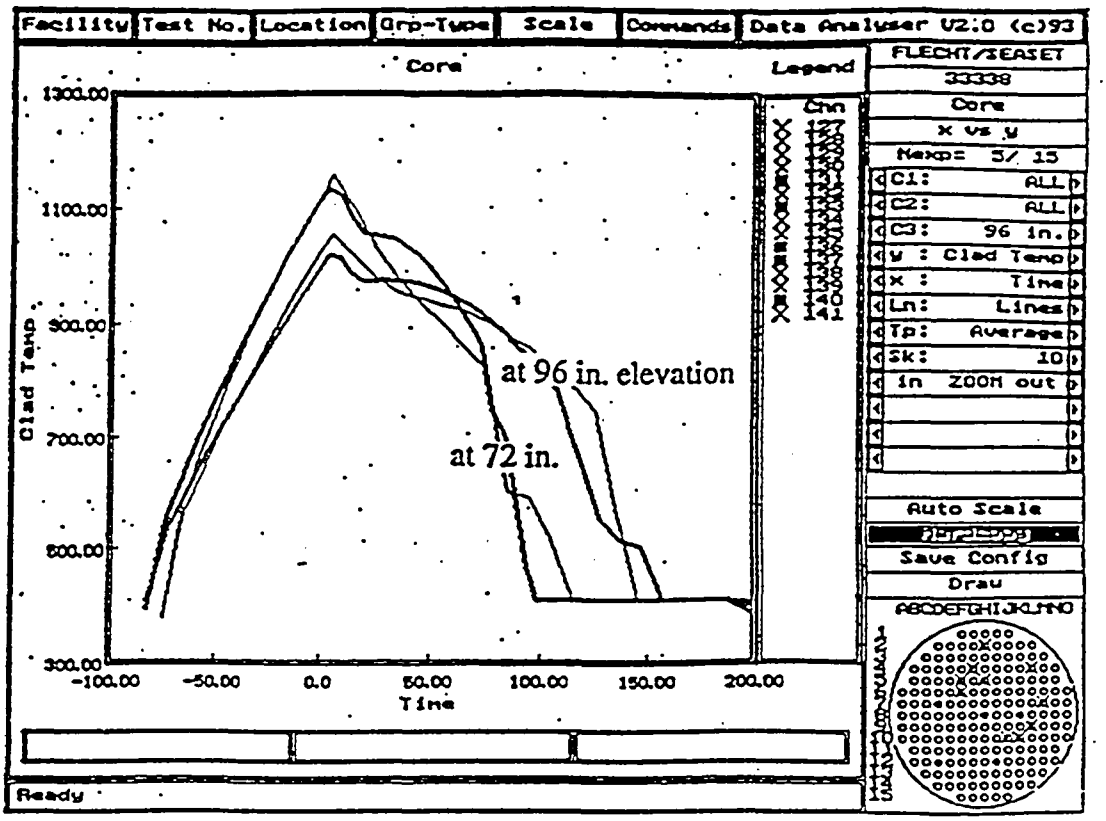

Fig. 43 Comparison of calculational and experimental cladding temperatures at selected elevations for the gravity feed test, 33338

4.2 Uncertainty quantification of Reflood PCT

For the application to the best estimate methodology, the uncertainty associated reflood model should be quantified. The selected FLECHT reflood test runs include a gravity feed test and several forced feed tests with wide range of the parameters such as flooding rate, system pressure, initial clad temperature, rod bundle power.

PCT is generally defined as the maximum of clad surface temperatures in the entire core region during the whole transient history. However this definition would require too many simulations in order to carry out statistically meaningful quantification of the uncertainty of PCT, because it produce only one value in a test run. We notice here that the clad surface temperature at PCT location is not the only important temperature, but those at other locations are also important to assess the code predictability of PCT. For practical purpose, PCT is then defined in this study as the local maximum value at a location of probe during the transient. Deviation between calculational and experimental PCTs is defined as follows.

$$\Delta PCT_{Zi} = PCT_{Zi,\exp} - PCT_{Z,cal} \tag{11}$$

where subscripts, z means a elevation and subscript, zi means each measuring probe at the same elevation. In other word the highest temperature calculated by RELAP5 for a computational cell is paired with the highest temperature measured by a probe in that cell. Many thermo-couples share each computational cell, and the center of cell do not always coincide with the measurement location. Thus the linear interpolated calculational results at certain elevation are compared with the experimental data at that elevation. PCT bias is calculated by averaging all the available PCTs for assessment test matrix, and the upper limit of uncertainty of PCTs at 95 % confidence level is calculated by addition of the PCT bias to 1.645 times of standard deviation of all the ΔPCTs, σ, under the assumption of normal distribution.

$$\Delta PCT = Bias + 1.645\,\sigma \tag{12}$$

Figs. 44 to 48 show respectively the scatter diagram of PCTs for each test group. The x-axis represents PCT predicted by the code, and the y-axis does the experimental PCT. In these figures the solid line is the line of PCT bias, and the dashed line the upper limit of

PCT at 95% confidence level. For the group 1, which is constructed to investigate the effect of flooding rate, the code under-predicts PCT by 18.65 K when compared with the averaged experimental PCT. The under-prediction of PCT is mainly due to the early turn-around in the tests with low flooding rate(test runs, 31504 and 31805). The uncertainty of PCT for the group 1 is about 100 K, containing the 18.16 K bias. Since all the tests in group 2 have low flooding rates, they commonly show PCT under-prediction owing to early turn-around behavior. The run, 34209, which is a low pressure test, shows the delayed quenching and associated PCT over-prediction. As a result the bias in test group 2 is about the same as in test group 1, but the uncertainty of PCT increases to about 130 K because of the combined effect of PCT under-prediction in low flooding rate and PCT over-prediction in low system pressure. In the test group 3 the code predicts well the PCT for a wide range of initial clad temperature in spite of a little early or delayed quenching. The PCT bias is 3.64 K and uncertainty at 95 % confidence level is about 74 K, which are very low compared with the test group 1 and group 2. The code predicts well PCTs in test group 4 except the high power test run 34524. In this case the calculation shows delayed quenching and the consequent PCT over-prediction. The PCT bias of group 4 is -1.49 K and uncertainty of PCT is about 80 K. As discussed above, the radial power distribution, variable flooding rate, and gravity feed do not have significant effect on PCT predictability. Under-predicted in the low flooding rate tests, 36026 and 34006, and the over-predicted in the low pressure test, 32235, and the well predicted PCTs in the other tests of group 5 are all combined and shown in Fig. 48. The PCT bias is 6.78 K and the corresponding uncertainty is about 108 K.

We collected the data from groups 1 to 5, and constructed the scatter diagram of PCTs for all the test runs as shown in Fig. 49. The RELAP5/MOD3/KAERI code is shown to under-predict the PCTs by 7.56 K and the associated uncertainty including the bias are quantified to be 99.2 K. The validity of the assumption of normal distribution of PCTs is also checked by using the following ratio.

$$R = |p - P| / \{p(1-p)N\}^{1/2} \tag{13}$$

where P and P respectively means the number of occurrence and its expected value from normal distribution, and N is the total number. The ratios are evaluated to be 0.12, 0.06, and 0.16 in the outside of the bands, ($\mu + \sigma$), (μ +2σ), and (μ+3σ), respectively, where μ

denotes mean value and σ denotes standard deviation. Thus the assumption of normal distribution is valid because all the above ratios satisfy the general criteria, $R<3$ [35].

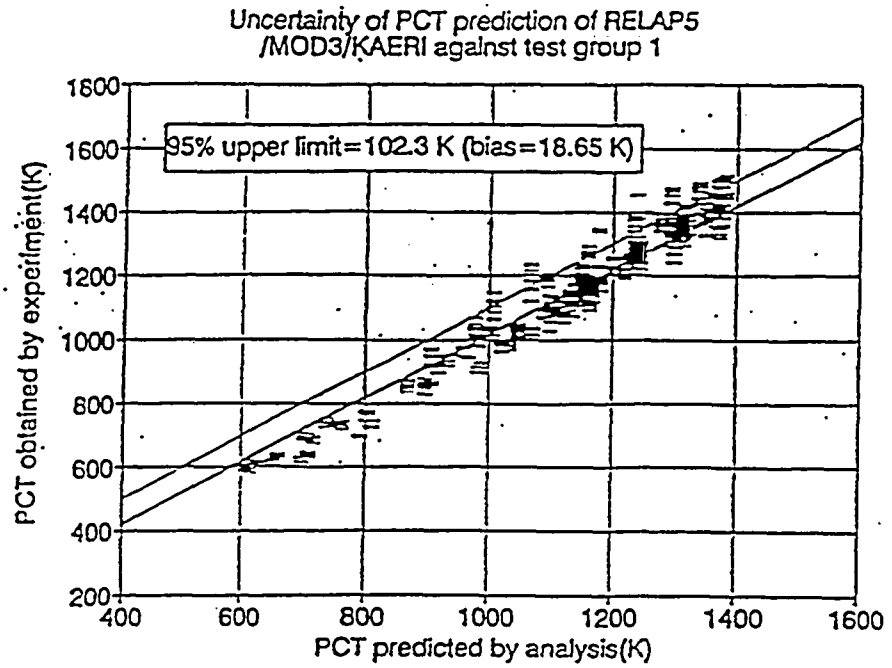

Fig. 44 Scatter diagram of calculational vs. experimental PCTs for test group 1: effect of flooding rate

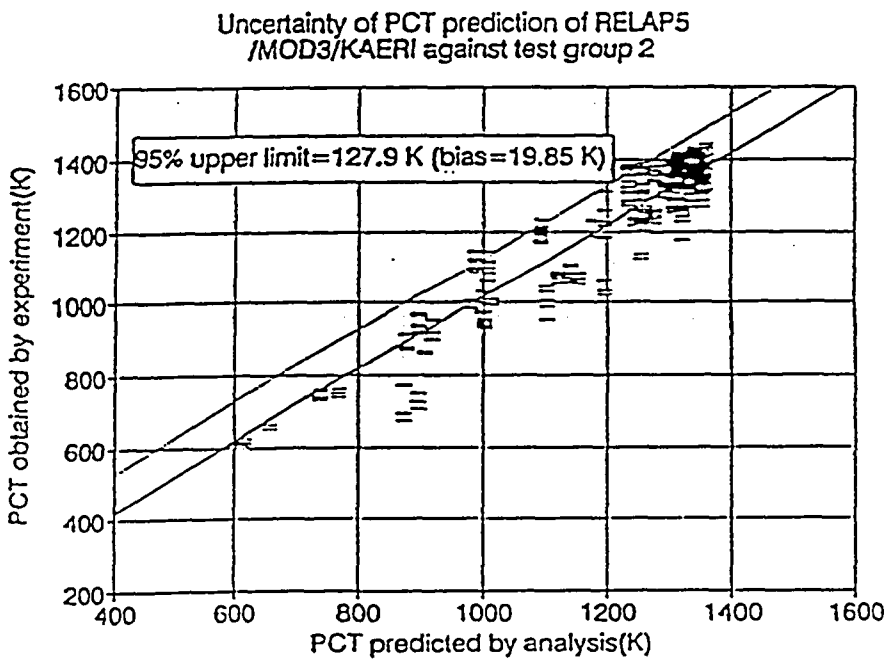

Fig. 45 Scatter diagram of calculational vs. experimental PCTs for test group 2: effect of system pressure

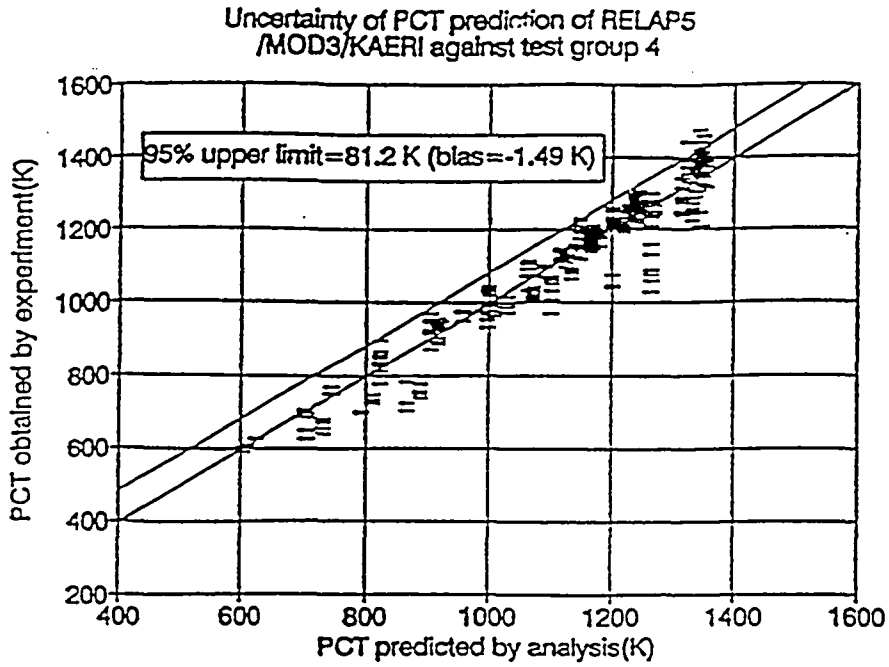

Fig. 46 Scatter diagram of calculational vs. experimental PCTs for test group 3: effect of initial clad temperature

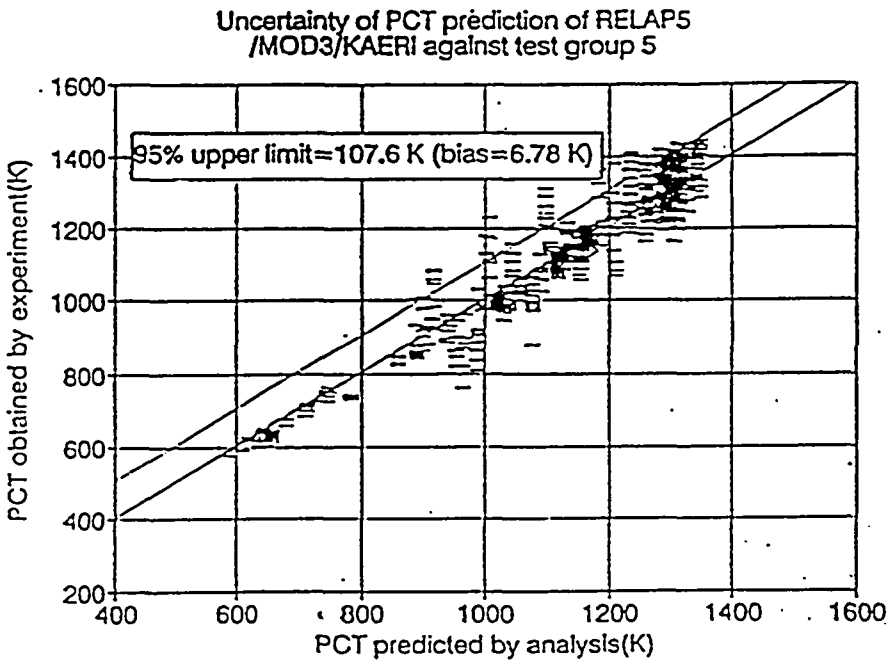

Fig. 47 Scatter diagram of calculational vs. experimental PCTs for test group 4: effect of rod bundle power

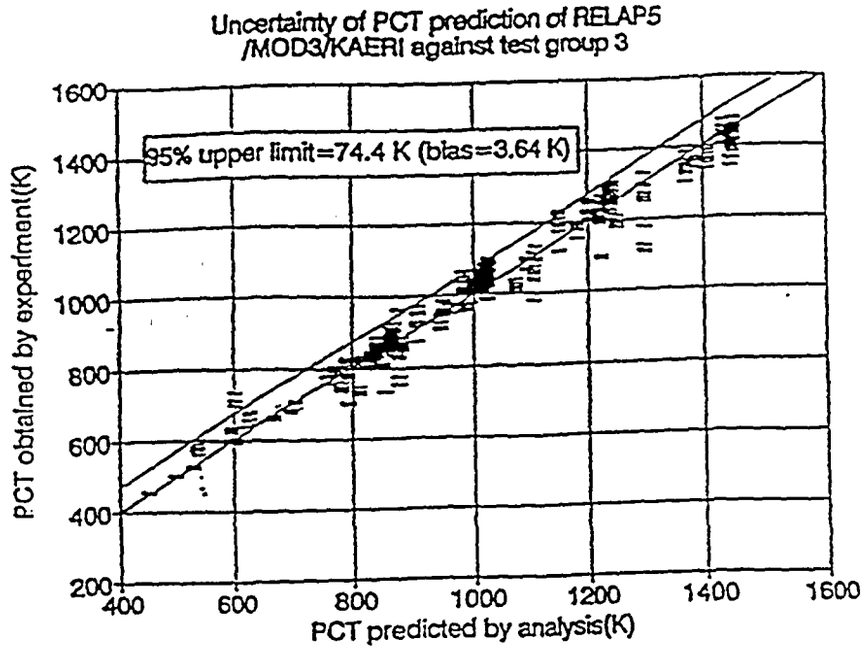

Fig. 48 Scatter diagram of calculational vs. experimental PCTs for test group 5

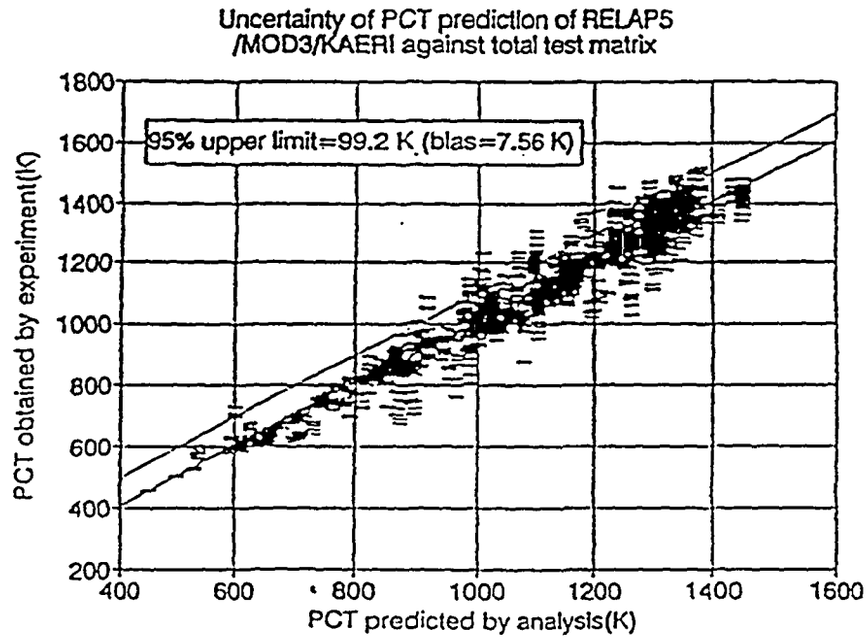

Fig. 49 Scatter diagram of calculational vs. experimental PCTs for total test matrix

5. Run Statistics

All calculation against the FLECHT SEASET series of experiments had been performed using HP-735 Workstation. For the reference run, 31504, the run statistics are summarized in Table 3. The time step sizes and total CPU time is shown in Fig. 50 and 51 as a function of transient time.

Table 3 Run Statistics for FLECHT Test Run 31504

	Standard RELAP5/MOD3	Modified RELAP5/MOD3
Total Simulation Time (sec)	900	900
Total CPU Time (sec)	4,247	5,030
Number of Time Steps	78,046	79,238
Number of Volumes	22	22
Grind Time (msec)	2.473	2.885

In modified version, the grind time was increased by 17% comparing the original version because the modified version require more calculations in the implementation of new heat transfer logic, wall vaporization smoothing and level tracking model.

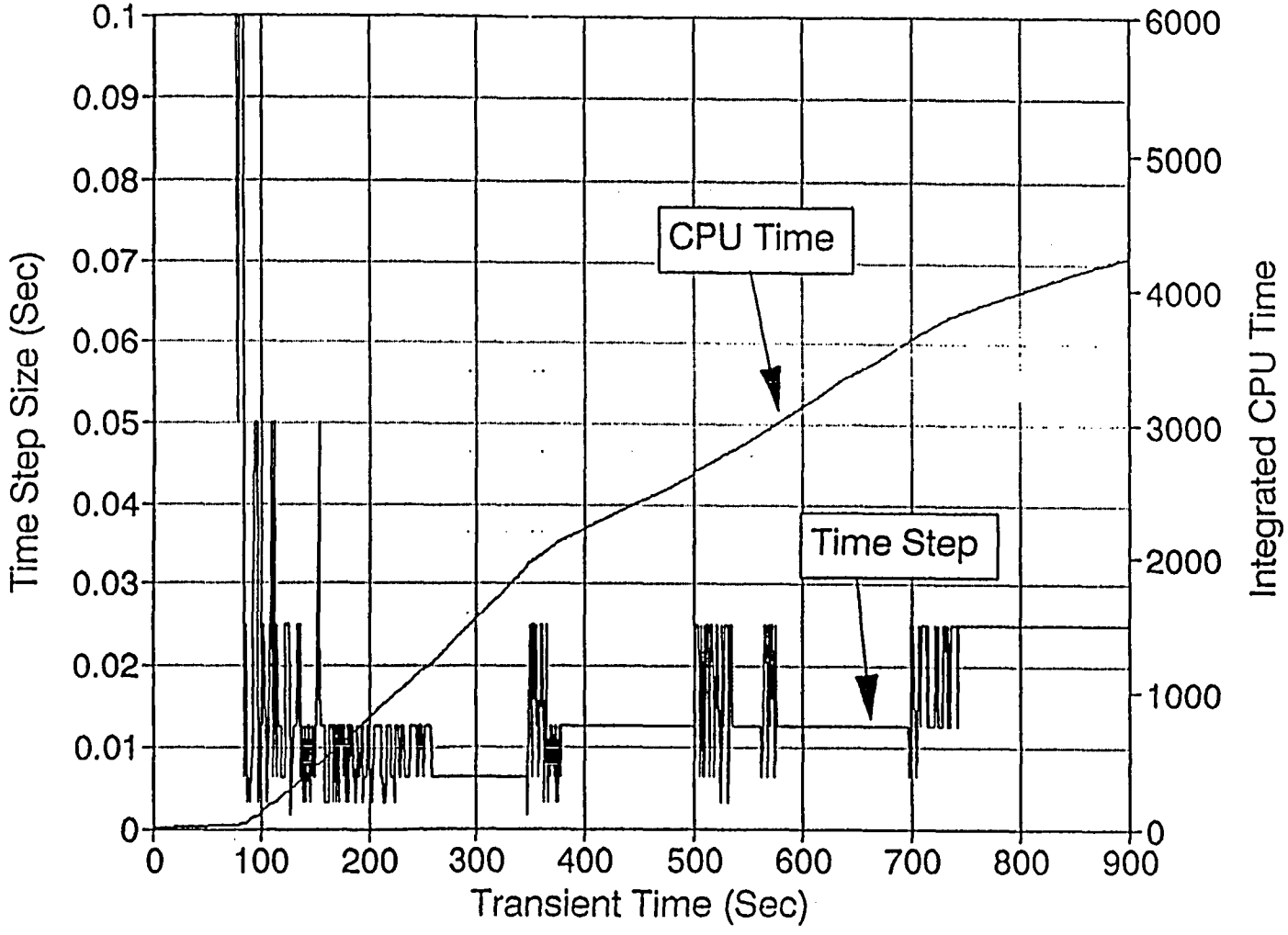

Figure 50 Time Step Size and CPU Time Required for Original RELAP5

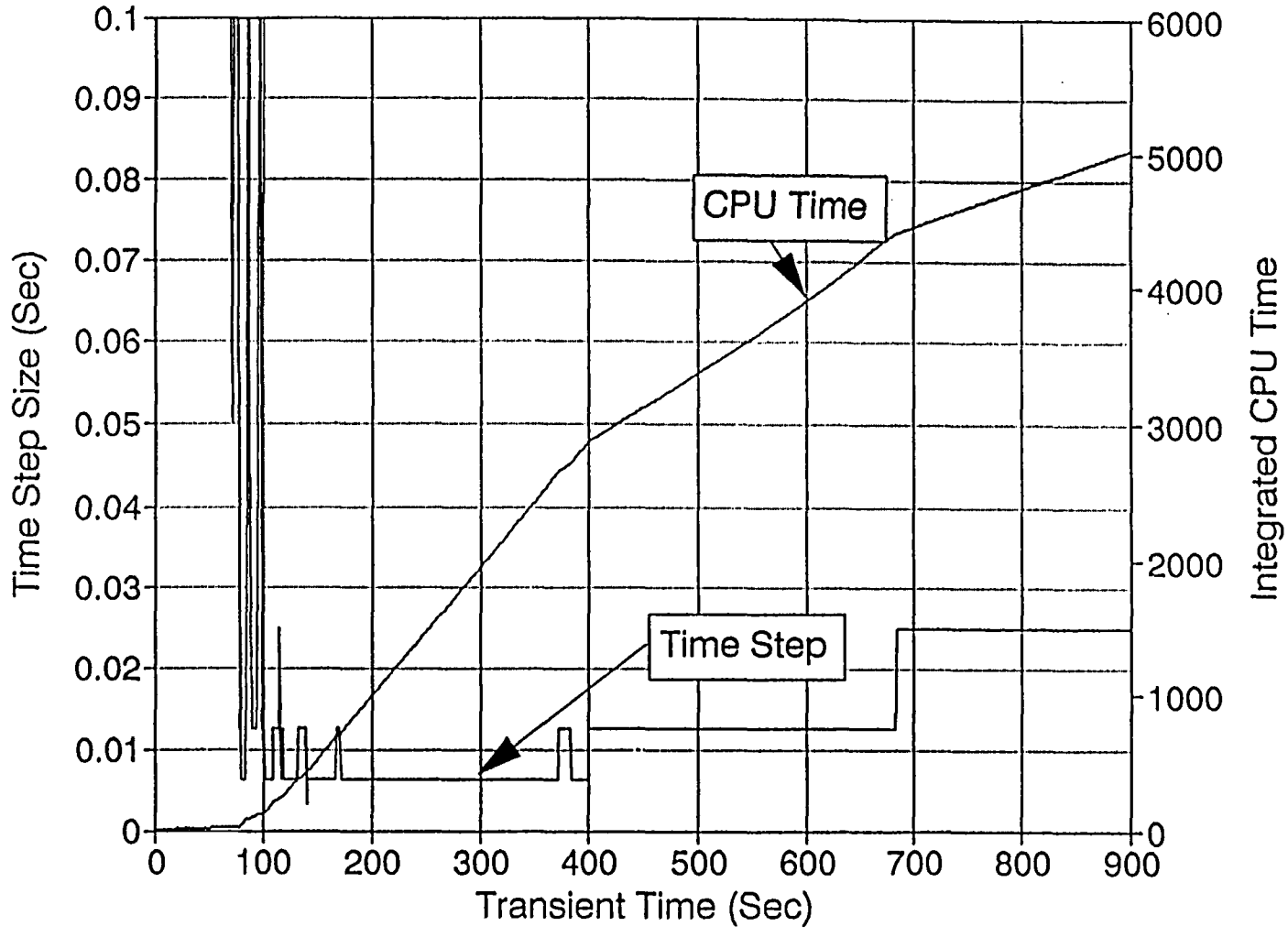

Figure 51 Time Step Size and CPU Time Required for Modified RELAP5

6. Conclusions

Assessment of original RELAP5/MOD3.1 code against the FLECHT SEASET series of experiments has identified some weakness of reflood model. The quenching of low reflood rate cases was delayed due to the lack of quenching temperature model and the shortcoming of Chen transition boiling model. Incorrect prediction of axial void profile and vapor cooling in dispersed flow resulted in increased cooling at the upper elevation. This was investigated to be caused by the incorrect prediction of droplet size and interfacial heat transfer. High pressure spikes during the reflood calculation resulted in the high steam flow oscillation and liquid carryover.

An effort had been made to improve the code with respect to the above weakness, and the necessary model for wall heat transfer package and numerical scheme had been modified. The weaknesses of RELAP5/MOD3.1 were much improved in modified version. The prediction of void profile and cladding temperature agreed better with test data. These improvements are more dramatic for gravity feed test. In the application of plant LBLOCA analysis, it can be concluded that the predictability of modified version for whole thermal hydraulic behavior was reasonable and suitable for use as best estimate code for LBLOCA.

The scatter diagram of PCTs is made from the comparison of all the calculational PCTs and the corresponding experimental values. 2793 data in form of deviation between experimental and calculational PCTs are shown to be normally distributed, and used to quantify statistically the PCT uncertainty of code. The upper limit of PCT uncertainty at 95 % confidence level is evaluated to be about 99 K. The PCT uncertainty might be attributable to reflood models and correlation's in the code and experimental data spread. As mentioned above, the used data encompass so wide ranges of parameters that they cover the conditions expected to occur at reflood phase of LBLOCA. Therefore the evaluated uncertainty of reflood PCT could be applied to realistic evaluation model of LBLOCA.

References

1. K.V. Moore and W.H. Rettig, "RELAP2 -- A Digital Program for Reactor Blowdown and Power Excursion Analysis," IDO-17263 (1968)
2. W.H. Rettig, et al., "RELAP3 - A Computer Program for Reactor Blowdown Analysis", IN-1445 (1971)
3. K.V. Moore and W.H. Rettig, "RELAP4 - A Computer Program for Transient Thermal-Hydraulic Analysis", ANCR-1127 (1975)
4. V.H. Ransom, et al., "RELAP5/MOD1 Code Manual, Volume 1 and 2", NUREG/CR-1826, EGG-2070 (1982)
5. V.H. Ransom, et al., "RELAP5/MOD2 Code Manual, Volume 1 and 2", NUREG/CR-4312, EGG-2396 (1985)
6. K.E. Calson, et al., "RELAP5/MOD3 Code Manual, Volume 1,2,3,4, and 5", NUREG/CR-5535, EGG-2596 (1990)
7. M.J. Loftus, et al., "PWR FLECHT SEASET Unblocked Bundle, Forced and Gravity Reflood Task Data Report",EPRI NP-1459, NUREG/CR-1532, WCAP-9699 (1981)
8. United States Code of Federal Regulations, Title 10, Section 50.46, " Acceptance Criteria for Emergency Core Cooling Systems for Light Water Reactors" (1988)
9. B.E. Boyack, et al., " Quantifying Reactor Safety Margins - Part 1 : An Overview of the Code Scaling, Applicability and Uncertainty Evaluation Methodology," Nucl. Engrg. Des. 119, 1 (1990)
10. G.E. Wilson, et al., " Quantifying Reactor Safety Margins - Part 2 : Characterization of Important Contributors to Uncertainty," Nucl. Engrg. Des. 119, 17 (1990)
11. W. Wulff, et al., " Quantifying Reactor Safety Margins - Part 3 : Assessment and Ranging of Parameters," Nucl. Engrg. Des. 119, 33 (1990)
12. G.S. Lellouche, et al., " Quantifying Reactor Safety Margins - Part 4 : Uncertainty Evaluation of LBLOCA Analysis based on TRAC-PF1/MOD1 ," Nucl. Engrg. Des. 119, 67 (1990)
13. N. Zuber, et al., " Quantifying Reactor Safety Margins - Part 5 : Evaluation of Scale-up Capabilities," Nucl. Engrg. Des. 119, 97 (1990)
14. I. Catton, et al., " Quantifying Reactor Safety Margins - Part 6 : A Physically

Based Method of estimating PWR Large Break Loss of Coolant Accident PCT ," Nucl. Engrg. Des. 119, 109 (1990)

15. B.E. Boyack, et al., " Quantifying Reactor Safety Margins, Application of Code Scaling, Applicability and Uncertainty Evaluation Methodology to a Large-Break Loss of Coolant Accident," NUREG/CR-5249 (1989)
16. J.C. Chen, et al., "A Phenomenological Correlation for post-CHF Heat Transfer," NUREG-0237 (1977)
17. D.C. Groenveld, et al., "1986 AECL-UO Critical Heat Flux Lookup Table," Heat Transfer Engineering, 7, 1-2, 46 (1986)
18. G.Th. Analytis, "A Comparative Study of the Post-CHF Wall Heat Transfer Package of the RELAP5 Codes and Preliminary Assessment of Model Changes in RELAP5/MOD3/v7j," Presented at the 1st CAMP Meeting at PSI, Villigen, Switzerland, June (1992)
19. N. Zuber, "The Hydraulics Crisis in Pool Boiling of Saturated and Subcooled Liquids, " Part II, No. 27 in International Developments in Heat Transfer, International Heat Transfer Conference, Boulder, CO (1961)
20. G.E. Dix and G.M. Anderson, "Spray Cooling Heat Transfer in a BWR Fuel Bundle," ASME National Heat Transfer Conference (1976)
21. Y. Murao, "Correlation of Quench Phenomena for Bottom Flooding During Loss-of Coolant Accident," J. Nucl. Sci. Technol. 15, 12 (1978)
22. P.J. Berenson, "Film Boiling Heat Transfer from a Horizontal Surface," Trans. ASME, J. Heat Transfer, 83 (1961)
23. R.E. Henry, "A correlation for the Minimum Film Boiling Temperature," AIChE Symp. Ser., 7D (1974)
24. M.J. Loftus, et al., "PWR FLECHT SEASET : 161 Rod Bundle Flow Blockage Task Data Report,",EPRI NP-3268, NUREG/CR-3314, WCAP-10307 (1984)
25. Y.A.Hassan, "Modification and Assessment of Rewetting Correlation's for Light Water Reactor System Analysis", ANS Transaction Vol.53, pp 537, 1986 ANS Winter Meeting (1986)
26. Y.A.Hassan, "Dispersed Flow Heat Transfer During Reflood in a Pressurized Water Reactor After a Large Break Loss of Coolant Accident", ANS Transaction Vol.53, pp 326, 1986 ANS Winter Meeting (1986)
27. M. Drucker, and V.K. Dhir, "Studies of Single- and Two-Phase Heat Transfer in a

Blocked Four-Rod Bundle," EPRI-NP 3485. Electric Power Research Institute (1984)

28. M.J. Thurgood et al., "COBRA/TRAC - A Thermal Hydraulic Code for Transient Analysis of Nuclear Vessels and Primary Coolant Systems", NUREG/CR-3046 (1983)
29. A.C. Spencer and M.Y. Young, "Mechanistic Model for the Best-Estimate Analysis of Reflood Transients (the BART Code)," HTD Volume 7, 19 th National Heat Transfer Conference, Orlando, FL (1980)
30. G.B. Wallis, One Dimensional Two Phase Flow, New York, McGraw-Hill Book Company (1969)
31. C.Y. Paik, et al., "Analysis of FLECHT SEASET 163-Rod Blocked Bundle Data Using COBRA-TF", EPRI-NP-4111, NUREG/CR-4166, WCAP-10375 (1985)
32. M.Sencar and N.Aksan, "Evaluation of Reflooding Models in RELAP5/MOD2.5, RELAP5/MOD3/5m5 and RELAP5/MOD3/v7j Codes by Leheigh University and PSI-NEPTUN Bundle Reflooding Experiment Data", Presented at the 2nd CAMP Meeting, Brussels, Belgium, May (1993)
33. G.Th.Analytis, N.Aksan, et al., "PSI Comment on Reflood Modelling", Reflood Specialist Meeting, Idaho Falls, Idaho, USA Oct. (1991)
34. NRC/DRPS Reactor Safety Data Bank, ENCOUNTER, EGG-RTH-7285
35. Woo Chul Kim et al. ."Modern Statistics", Seoul, Young-Zi Publ. Co. (1980)

Appendix A.

Coding Change for RELAP5/MOD3/KAERI

A.1 Changes to Code Input

Reflood models described in Section 3 were implemented in the RELAP5/MOD3.1. In the modified version, the input in the user Group 1 input card is used to actuate a specific mode, and following are the added Group 1 card options.

GROUP 1 CARD OPTION

Option 70 ;	Activate Reflood Heat Transfer Package, Level Tracking Model, and Modification for Droplet Size
Option 73 ;	Activate the Correction of Typing Error in CHF Lookup Table
Option 75 ;	Activate Wall Vaporization Time Smoothing
None ;	Same as RELAP5/MOD3.1 with no Option

A.2. Subroutines Changed

The following subroutines are modified or added by the improvement. Listing of the each modified subroutine is available from the attached diskette. The whole content of the code modification is a part of KAERI's property and restricted to be used for the purpose of review at NRC and INEL only. The attached diskette also should be used only for the purpose of review on the code assessment report.

Subroutine Name	Contents of Changed Models or Items
aatl:	change the code title
chfcal:	correct CHF table
dittus:	enhancement of convective heat transfer to single phase vapor due to droplet applicable to all of heat structures
dtstep:	NPA related modifications (pass variables for a time-step)
fidis:	restrict average droplet size for reflood case between 0.2 mm and 2.0 mm
fidis2:	restrict average droplet size for reflood case between 0.2 mm and 2.0 mm
mdata3:	newly added subroutine to find material properties such as thermal conductivity and volumetric heat capacity at outer surface of heat structure, which properties are used to Henry modified Berenson correlation of quenching temperature, a modification of the subroutine, madata
ht2tdp:	correct the representative heat transfer coefficient of each reflood heat structure from average value of fine meshes to local value at center
htadv:	under-relaxation of wall vaporization for reflood case

Subroutine Name	Contents of Changed Models or Items
htrcrfl:	newly added subroutine to apply reflood specific heat transfer selection logic
hydro:	call phantv/phantj with system index
phantj:	apply KAERI Post-CHF flow regime selection logic, call phmod2 with system index and flow regime
phantv:	call phmod with system index and flow regime enhance interfacial heat transfer coefficients considering effect of small drop shattered by grid
phmod:	newly added subroutine to solve droplet interfacial transport equation with grid effect
phmod2:	newly added subroutine to calculate interfacial drag coefficient based on the drop diameter predicted by droplet transport model
pstdrfl:	newly added subroutine to calculate reflood specific post-DNB forced convection heat transfer coefficients and wall vaporization
qfhtrc:	calculate quenching temperature, critical heat flux, and CHF temperature apply liquid level tracking scheme, call reflood specific post-DNB heat transfer package ,pstdrfl
qfsrch:	modify the fine mesh reduction scheme for reflood heat structure
rchng:	describe the additional options for user Group 1 input
relap5:	add a common block related to droplet transport model
tran:	initialize old values of direct wall flashing, gammawo

Subroutine Name	Contents of Changed Models or Items
trnset:	add droplet related variables for NPA, initialize droplet related variables for all volumes find the volumes and junctions connected to each volume, read grid data given by user
wrplid:	NPA related modification

A.3 New Variables Added

The following are new variables added to the volume common block, voldat

gammawo:	old time value of direct wall flashing
tchfvl:	representative value of CHF temperature in a hydro volume
tqfvol:	representative value of quenching temperature in a hydro volume
twvol:	representative value of wall temperature in a hydro volume

a common block, vol2 is newly added due to droplet transport model. The variables in vol2 are as follow.

curs(i,j):	volumetric droplet area concentration
olds(i,j):	volumetric droplet area concentration, old time value
volidx(i,j):	volume index in ftb
volnum(i,j):	volume number
oldreg(i,j):	volume flow regime number
njun(i,j):	number of junction connections
conjun(i,j,k):	index of k-th junction
convol(i,j):	index of k-th connected volume
grdlen(i,j):	distance from volume inlet to grid
grdeta(i,j):	grid efficiency

i:	system ordinal number
j:	volume ordinal number

Appendix B.

Estimation of FLECHT SEASET Experimental Data Error

The instrumentation error associated with the data from FLECHT SEASET unblocked bundle test series were derived either from equipment manufacturers' specifications or system calibration data. The data channel number and it's brief descriptions are shown in Table B.1. Table B.2 is a detailed listing of errors by data channel and run number. The standard deviation of best estimate of error is presented in Table B.2. The maximum possible error is also presented in Table. This is the sum of all possible component errors and is the outer bound of error. Detail explanation of the error analysis is presented in Appendix D of FLECHT Data Report (Ref. 7).

TABLE B.1

INITIAL DATA ACQUISITION SYSTEM CHANNEL ASSIGNMENTS

Channel No.	Description	Location	Elevation [m (in.)]	Fluke Channel[a]	Strip Chart Recorder[b]
1	Heater rod T/C	7E	0.30 (12)		
2	Heater rod T/C	9G	0.30 (12)		
3	Heater rod T/C	11I	0.30 (12)		
4	Heater rod T/C	5H	0.61 (24)		
5	Heater rod T/C	8N	0.61 (24)		
6	Heater rod T/C	12F	0.61 (24)		
7	Heater rod T/C	7E	0.99 (39)		
8	Heater rod T/C	9G	0.99 (39)		
9	Heater rod T/C	11I	0.99 (39)		
10	Heater rod T/C	2H	1.22 (48)		
11	Heater rod T/C	5H	1.22 (48)		
12	Heater rod T/C	5J	1.22 (48)		
13	Heater rod T/C	8H	1.22 (48)		F - red pen
14	Heater rod T/C	8K	1.22 (48)		
15	Heater rod T/C	8N	1.22 (48)		
16	Heater rod T/C	12D	1.22 (48)		
17	Heater rod T/C	3C	1.52 (60)		
18	Heater rod T/C	3M	1.52 (60)		
19	Heater rod T/C	4J	1.52 (60)		
20	Heater rod T/C	5E	1.52 (60)		
21	Heater rod T/C	6L	1.52 (60)		
22	Heater rod T/C	7E	1.52 (60)		
23	Heater rod T/C	7G	1.52 (60)		
24	Heater rod T/C	9I	1.52 (60)		
25	Heater rod T/C	11I	1.52 (60)		

a. See paragraph 3-16
b. See paragraph 3-17

TABLE B.1 (cont)

INITIAL DATA ACQUISITION SYSTEM CHANNEL ASSIGNMENTS

Channel No.	Description	Location	Elevation [m (in.)]	Fluke Channel[a]	Strip Chart Recorder[b]
26	Heater rod T/C	11K	1.52 (60)		
27	Heater rod T/C	13M	1.52 (60)		
28	Heater rod T/C	3C	1.70 (67)		
29	Heater rod T/C	3M	1.70 (67)		
30	Heater rod T/C	4J	1.70 (67)		
31	Heater rod T/C	6J	1.70 (67)		
32	Heater rod T/C	6L	1.70 (67)		
33	Heater rod T/C	8E	1.70 (67)		
34	Heater rod T/C	7G	1.70 (67)		
35	Heater rod T/C	9I	1.70 (67)		
36	Heater rod T/C	11I	1.70 (67)		
37	Heater rod T/C	11K	1.70 (67)		
38	Heater rod T/C	13M	1.70 (67)		
39	Heater rod T/C	3F	1.78 (70)		
40	Heater rod T/C	4J	1.78 (70)		
41	Heater rod T/C	4M	1.78 (70)		
42	Heater rod T/C	6C	1.78 (70)		
43	Heater rod T/C	6L	1.78 (70)		
44	Heater rod T/C	7G	1.78 (70)		
45	Heater rod T/C	7J	1.78 (70)		
46	Heater rod T/C	9I	1.78 (70)		
47	Heater rod T/C	10G	1.78 (70)		
48	Heater rod T/C	10M	1.78 (70)		
49	Heater rod T/C	13J	1.78 (70)		
50	Heater rod T/C	2H	1.83 (72)		
51	Heater rod T/C	3F	1.83 (72)		
52	Heater rod T/C	4D	1.83 (72)		

TABLE B.1 (cont)

INITIAL DATA ACQUISITION SYSTEM CHANNEL ASSIGNMENTS

Channel No.	Description	Location	Elevation [m (in.)]	Fluke Channel[a]	Strip Chart Recorder[b]
53	Heater rod T/C	4G	1.83 (72)		
54	Heater rod T/C	4L	1.83 (72)		
55	Heater rod T/C	6F	1.83 (72)		
56	Heater rod T/C	6I	1.83 (72)		
57	Heater rod T/C	7B	1.83 (72)		
58	Heater rod T/C	7G	1.83 (72)		
59	Heater rod T/C	7J	1.83 (72)		
60	Heater rod T/C	8H	1.83 (72)		F - blue pen
61	Heater rod T/C	8N	1.83 (72)		
62	Heater rod T/C	9I	1.83 (72)		
63	Heater rod T/C	9L	1.83 (72)		
64	Heater rod T/C	10J	1.83 (72)		
65	Heater rod T/C	10M	1.83 (72)		
66	Heater rod T/C	12D	1.83 (72)		
67	Heater rod T/C	12L	1.83 (72)		
68	Heater rod T/C	14I	1.83 (72)		
69	Heater rod T/C	3I	1.88 (74)		
70	Heater rod T/C	3L	1.88 (74)		
71	Heater rod T/C	4G	1.88 (74)		
72	Heater rod T/C	6F	1.88 (74)		
73	Heater rod T/C	6I	1.88 (74)		
74	Heater rod T/C	7D	1.88 (74)		
75	Heater rod T/C	7M	1.88 (74)		
76	Heater rod T/C	9L	1.88 (74)		
77	Heater rod T/C	10J	1.88 (74)		
78	Heater rod T/C	12I	1.88 (74)		
79	Heater rod T/C	3I	1.83 (72)		

TABLE B.1 (cont)

INITIAL DATA ACQUISITION SYSTEM CHANNEL ASSIGNMENTS

Channel No.	Description	Location	Elevation [m (in.)]	Fluke Channel[a]	Strip Chart Recorder[b]
80	Heater rod T/C	3L	1.93 (76)		
81	Heater rod T/C	4G	1.93 (76)		
82	Heater rod T/C	6F	1.93 (76)		
83	Heater rod T/C	6I	1.93 (76)		
84	Heater rod T/C	7D	1.93 (76)		
85	Heater rod T/C	7M	1.93 (76)		
86	Heater rod T/C	9L	1.93 (76)		
87	Heater rod T/C	10J	1.93 (76)		
88	Heater rod T/C	12I	1.93 (76)		
89	Heater rod T/C	2H	1.98 (78)		
90	Heater rod T/C	7B	1.98 (78)		
91	Heater rod T/C	4G	1.98 (78)		
92	Heater rod T/C	6F	1.98 (78)		
93	Heater rod T/C	10D	1.98 (78)		
94	Heater rod T/C	7D	1.98 (78)		
95	Heater rod T/C	14I	1.98 (78)		
96	Heater rod T/C	8H	1.98 (78)		
97	Heater rod T/C	8N	1.98 (78)		
98	Heater rod T/C	5H	1.98 (78)		
99	Heater rod T/C	8K	1.98 (78)		
100	Heater rod T/C	10J	1.98 (78)		
101	Heater rod T/C	12I	1.98 (78)		
102	Heater rod T/C	13G	1.98 (78)		
103	Heater rod T/C	3I	2.13 (84)		
104	Heater rod T/C	4G	2.13 (84)		
105	Heater rod T/C	6F	2.13 (84)		
106	Heater rod T/C	6I	2.13 (84)		

TABLE B.1 (cont)

INITIAL DATA ACQUISITION SYSTEM CHANNEL ASSIGNMENTS

Channel No.	Description	Location	Elevation [m (in.)]	Fluke Channel[a]	Strip Chart Recorder[b]
107	Heater rod T/C	7D	2.13 (84)		
108	Heater rod T/C	7M	2.13 (84)		
109	Heater rod T/C	9C	2.13 (84)		
110	Heater rod T/C	9L	2.13 (84)		
111	Heater rod T/C	10J	2.13 (84)		
112	Heater rod T/C	11E	2.13 (84)		
113	Heater rod T/C	12I	2.13 (84)		
114	Heater rod T/C	13G	2.13 (84)		
115	Heater rod T/C	3I	2.29 (90)		
116	Heater rod T/C	4G	2.29 (90)		
117	Heater rod T/C	6F	2.29 (90)		
118	Heater rod T/C	6I	2.29 (90)		
119	Heater rod T/C	7D	2.29 (90)		
120	Heater rod T/C	7M	2.29 (90)		
121	Heater rod T/C	9C	2.29 (90)		
122	Heater rod T/C	9L	2.29 (90)		
123	Heater rod T/C	10J	2.29 (90)		
124	Heater rod T/C	11E	2.29 (90)		
125	Heater rod T/C	12I	2.29 (90)		
126	Heater rod T/C	6J	2.29 (90)		
127	Heater rod T/C	2H	2.44 (96)		
128	Heater rod T/C	4G	2.44 (96)		
129	Heater rod T/C	4L	2.44 (96)		
130	Heater rod T/C	6F	2.44 (96)		
131	Heater rod T/C	7D	2.44 (96)		
132	Heater rod T/C	7M	2.44 (96)		
133	Heater rod T/C	8H	2.44 (96)		F - black pen

TABLE B.1 (cont)

INITIAL DATA ACQUISITION SYSTEM CHANNEL ASSIGNMENTS

Channel No.	Description	Location	Elevation [m (in.)]	Fluke Channel[a]	Strip Chart Recorder[b]
134	Heater rod T/C	9L	2.44 (96)		
135	Heater rod T/C	10J	2.44 (96)		
136	Heater rod T/C	12D	2.44 (96)		
137	Heater rod T/C	12I	2.44 (96)		
138	Heater rod T/C	5F	2.44 (96)		
139	Heater rod T/C	5H	2.44 (96)		
140	Heater rod T/C	8K	2.44 (96)		
141	Heater rod T/C	10K	2.44 (96)		
142	Heater rod T/C	7B	2.59 (102)		
143	Heater rod T/C	8H	2.59 (102)		
144	Heater rod T/C	8K	2.59 (102)		
145	Heater rod T/C	2H	2.59 (102)		
146	Heater rod T/C	5J	2.59 (102)		
147	Heater rod T/C	4L	2.59 (102)		
148	Heater rod T/C	3I	2.82 (111)		
149	Heater rod T/C	6F	2.82 (111)		
150	Heater rod T/C	6I	2.82 (111)		
151	Heater rod T/C	7D	2.82 (111)		
152	Heater rod T/C	7M	2.82 (111)		
153	Heater rod T/C	9C	2.82 (111)		
154	Heater rod T/C	10J	2.82 (111)		
155	Heater rod T/C	11E	2.82 (111)		
156	Heater rod T/C	12I	2.82 (111)		
157	Heater rod T/C	13G	2.82 (111)		
158	Heater rod T/C	2H	3.05 (120)		
159	Heater rod T/C	4D	3.05 (120)		
160	Heater rod T/C	5H	3.05 (120)		

TABLE B.1 (cont)

INITIAL DATA ACQUISITION SYSTEM CHANNEL ASSIGNMENTS

Channel No.	Description	Location	Elevation [m (in.)]	Fluke Channel[a]	Strip Chart Recorder[b]
161	Heater rod T/C	5J	3.05 (120)		
162	Heater rod T/C	7B	3.05 (120)		
163	Heater rod T/C	8H	3.05 (120)		F - green pen
164	Heater rod T/C	8K	3.05 (120)		
165	Heater rod T/C	8N	3.05 (120)		
166	Heater rod T/C	12L	3.05 (120)		
167	Heater rod T/C	14I	3.05 (120)		
168	Heater rod T/C	5E	3.35 (132)		
169	Heater rod T/C	6J	3.35 (132)		
170	Heater rod T/C	7E	3.35 (132)		
171	Heater rod T/C	9G	3.35 (132)		
172	Heater rod T/C	11E	3.35 (132)		
173	Heater rod T/C	11I	3.35 (132)		
174	Heater rod T/C	11K	3.35 (132)		
175	Heater rod T/C	5I	3.51 (138)		
176	Heater rod T/C	7B	3.51 (138)		
177	Heater rod T/C	8H	3.51 (138)		
178	Thimble T/C	4I	2.13 (84)		C - blue pen
179	Steam probe T/C	10F	0.99 (39)		
180	Steam probe T/C	7I	1.22 (48)		
181	Steam probe T/C	5K	1.52 (60)		
182	Steam probe T/C	7F	1.70 (67)		
183	Steam probe T/C	10I	1.70 (67)		C - green pen
184	Steam probe T/C	4F	1.83 (72)		
185	Steam probe T/C	7I	1.83 (72)		
186	Steam probe T/C	10L	1.83 (72)		
187	Steam probe T/C	10C	1.98 (78)		

TABLE B.1 (cont)

INITIAL DATA ACQUISITION SYSTEM CHANNEL ASSIGNMENTS

Channel No.	Description	Location	Elevation [m (in.)]	Fluke Channel[a]	Strip Chart Recorder[b]
188	Steam probe T/C	13F	1.98 (78)		
189	Steam probe T/C	7C	2.13 (84)		
190	Steam probe T/C	13I	2.13 (84)		C - red pen
191	Steam probe T/C	7F	2.29 (90)		
192	Steam probe T/C	10I	2.29 (90)		C - blue pen
193	Steam probe T/C	4F	2.44 (96)		
194	Steam probe T/C	10L	2.44 (96)		
195	Steam probe T/C	10C	2.82 (111)		
196	Steam probe T/C	13F	2.82 (111)		C - green pen
197	Steam probe T/C	7C	3.05 (120)		
198	Steam probe T/C	13I	3.05 (120)		
199	Steam probe T/C	10F	3.51 (138)		C - red pen
200	Steam probe T/C	5K	3.51 (138)		
201	Exhaust line steam probe T/C				
202	Thimble T/C	7L	1.22 (48)		
203	Thimble T/C	4I	1.83 (72)		
204	Out of service				
205	Thimble T/C	13L	2.44 (96)		
206	Thimble T/C	7L	2.82 (111)		
207	Thimble T/C	4I	3.05 (120)		
208	Upper plenum bundle out fluid T/C				
209	Upper plenum fluid T/C				
210	Upper plenum housing extension fluid T/C				
211	Lower plenum fluid T/C				

TABLE B.1 (cont)

INITIAL DATA ACQUISITION SYSTEM CHANNEL ASSIGNMENTS

Channel No.	Description	Location	Elevation [m (in.)]	Fluke Channel[a]	Strip Chart Recorder[b]
212	Accumulator fluid T/C		0.18 (7.25)	10	
213	Carryover tank fluid T/C		0.0064 (2.5)	8	
214	Steam separator drain tank fluid T/C		0.076 (3)	9	
215	Exhaust orifice fluid T/C				
216	Carryover tank wall T/C		0.30 (12)	1	
217	Steam separator middle wall T/C				
218	Steam separator drain tank wall T/C		1.07 (42)	6	
219	Test section outlet pipe wall T/C			7	
220	Pipe upstream exhaust orifice wall T/C			15	
221	Lower plenum bundle in fluid T/C			11	
222	Primary power - zone A				E - red pen
223	Redundant power - zone A				
224	Primary power - zone B				E - blue pen
225	Redundant power - zone B				
226	Primary power - zone C				E - green pen
227	Redundant power - zone C				

TABLE B.1 (cont)

INITIAL DATA ACQUISITION SYSTEM CHANNEL ASSIGNMENTS

Channel No.	Description	Location	Elevation [m (in.)]	Fluke Channel[a]	Strip Chart Recorder[b]
228	0-3.8 x 10^{-3} m^{-3}/sec (0-60 gal/min) turbine/meter or 0-9.5 x 10^{-3} m^{-3}/sec (0-150 gal/min) turbine/meter			59	A - red pen
229	Low-flow rotameter				A - blue pen
230	Medium-flow rotameter				A - black pen
231	High-flow rotameter				A - green pen
232	Bidirectional turbo-probe				D - black pen
233	Bundle 0-0.30 m (0-12 in.) D/P			45	
234	Bundle 0.30-0.61 m (12-24 in.) D/P			46	
235	Bundle 0.61-0.91 m (24-36 in.) D/P			47	
236	Bundle 0.91-1.22 m (36-48 in.) D/P			48	
237	Bundle 1.22-1.52 m (48-60 in.) D/P			49	
238	Bundle 1.52-1.83 m (60-72 in.) D/P			50	
239	Bundle 1.83-2.13 m (72-84 in.) D/P			51	
240	Bundle 2.13-2.44 m (84-96 in.) D/P			52	
241	Bundle 2.44-2.74 m (96-108 in.) D/P			53	
242	Bundle 2.74-3.05 m (108-120 in.) D/P			54	
243	Bundle 3.05-3.35 m (120-132 in.) D/P			55	

TABLE B.1 (cont)

INITIAL DATA ACQUISITION SYSTEM CHANNEL ASSIGNMENTS

Channel No.	Description	Location	Elevation [m (in.)]	Fluke Channel[a]	Strip Chart Recorder[b]
244	Bundle 3.35-3.66 m (132-144 in.) D/P			56	
245	Bundle overall D/P			57	
246	Upper plenum level D/P			58	
247	Carryover tank level D/P				B - green pen
248	Steam separator tank level D/P				
249	Steam separator drain tank level D/P				D - blue pen
250	Accumulator level D/P				D - red pen
251	Exhaust orifice D/P				B - black pen
252	Upper plenum pressure PT				D - green pen
253	Exhaust orifice pressure PT				
254	Upper plenum to steam separator D/P				
255	Downcomer to steam separator D/P				
256	Downcomer level D/P				B - blue pen

TABLE B.2
INSTRUMENTATION ERRORS

Channel[a]	Run No.[b]	Sensor		Conditioner	Readout	Data Path Error		Equipment Response		Calibration Data		System Results	
		Type	Error	Error	Error	Most Probable	Maximum	Most Probable	Maximum	Most Probable	Maximum	Most Probable	Maximum
1-201	30123-37170	Heater rod and steam probe thermocouples	±1°C (±2°F) at -17.8°C-277°C (0°F-530°F) ±0.375% at 277°C-1316°C (530°F-2400°F)	±1.01°C(±1.82°F)	±2.03°C(±3.66°F)	±1.46°C(±2.63°F)	±4.16°C(±7.48°F)						
202-207	30123-37170	Thimble thermocouples	±1°C(±2°F) at -17.8°C-277°C (0°F-530°F) ±0.375% at 277°C-1316°C (530°F-2400°F)	±1.01°C(±1.82°F)	±2.03°C(±3.66°F)	±1.46°C(±2.63°F)	±4.16°C(±7.48°F)						
204	Out of service												
208-221	30123-37170	Loop thermocouple	±2°C(±4°F) at -17.8°C-277°C (0°F-530°F) 0.75% at 277°C-1316°C (530°F-2400°F) Use ±10°C(±18°F) maximum	±0.3°C(±0.5°F)	±2.03°C(±3.66°F)	±1.74°C(±3.14°F) ±5.89°C(±10.61°F)	4.53°C(8.16°F) ±12.3°C (±22.2°F)						

a. Refer to table 3-1 for identification of channels and functions.

b. All of these run numbers were applicable to these sensors, even though certain tests did not require certain transducers.

TABLE B.2 (cont)

INSTRUMENTATION ERRORS

Channel[a]	Run No.[b]	Sensor		Conditioner	Readout	Data Path Error		Equipment Response		Calibration Data		System Results	
		Type	Error	Error	Error	Most Probable	Maximum	Most Probable	Maximum	Most Probable	Maximum	Most Probable	Maximum
222	30123-37170	Power measurement						±1.12 kw	±2.43 kw	±2.13 kw	±3.9 kw	±2.41 kw	±6.30 kw
223	30123-37170	Power measurement						±0.15 kw	±0.25 kw	±2.13 kw	±3.9 kw	±2.14 kw	±4.15 kw
224	30123-37170	Power measurement						±2.48 kw	±4.58 kw	±2.13 kw	±3.9 kw	±3.27 kw	±8.57 kw
225	30123-37170	Power measurement						±0.29 kw	±1.11 kw	±2.13 kw	±3.9 kw	±2.15 kw	±5.10 kw
226	30123-37170	Power measurement						±2.19 kw	±3.96 kw	±2.13 kw	±3.9 kw	±3.05 kw	±7.92 kw
227	30123-37170	Power measurement						±0.7 kw	±3.7 kw	±2.13 kw	±3.9 kw	±2.24 kw	±7.66 kw
228	30123-32333	Turbine meter	±0.515x10^{-6} m^3/sec (±0.0817 gal/min)	±5.5x10^{-5} m^3/sec (±0.87 gal/min)	±5.4x10^{-6} m^3/sec (±0.086 gal/min)	±5.54x10^{-5} m^3/sec (±0.878 gal/min)	±6.549x10^{-5} m^3/sec (±1.038 gal/min)						
229	33544-36026	Low-flow rotameter						±5.2x10^{-6} m^3/sec (±0.082 gal/min)	±1.38x10^{-5} m^3/sec (±0.218 gal/min)	±2.0x10^{-6} m^3/sec (±0.031 gal/min)	±3.3x10^{-6} m^3/sec (0.053 gal/min)		
230	33338-33436	Medium-flow rotameter						±1.07x10^{-4} m^3/sec (±1.69 gal/min)	±1.23x10^{-4} m^3/sec (±1.95 gal/min)	3.05x10^{-5} m^3/sec (±0.484 gal/min)	±5.29x10^{-5} m^3/sec (0.838 gal/min)		
231		High-flow rotameter						±1.86x10^{-5} m^3/sec (±0.295 gal/min)	5.05x10^{-5} m^3/sec (±0.800 gal/min)	±4.0x10^{-6} m^3/sec (±0.063 gal/min)	±6.88x10^{-6} m^3/sec (±0.109 gal/min)		
232	33338-33436	Turbo-probe	±7.70x10^{-5} m^3/sec (±1.22 gal/min)	±1.63x10^{-4} m^3/sec (±2.58 gal/min)	±1.53x10^{-5} m^3/sec (±0.242 gal/min)	±1.34x10^{-4} m^3/sec (±2.12 gal/min)	±2.87x10^{-4} m^3/sec (±4.55 gal/min)						

TABLE B.2 (cont)

INSTRUMENTATION ERRORS

Channel[a]	Run No.[b]	Sensor		Conditioner	Readout	Data Path Error		Equipment Response		Calibration Data		System Results	
		Type	Error	Error	Error	Most Probable	Maximum	Most Probable	Maximum	Most Probable	Maximum	Most Probable	Maximum
233-244	30123-37170	D/P cell	±6.9 kPa (±1.0 psid)	±0.03 kPa (±0.005 psid)	±0.026 kPa (±0.0038 psid)	±0.047 kPa (±0.0068 psid)	±0.130 kPa (±0.0188 psid)						
245	30123-37170	D/P cell	±69.0 kPa (±10.0 psid)	±0.34 kPa (±0.05 psid)	±0.36 kPa (±0.053 psid)	±0.66 kPa (±0.096 psid)	±1.74 kPa (±0.253 psid)						
246	30123-37170	D/P cell	±6.9 kPa (±1.0 psid)	±0.03 kPa (±0.005 psid)	±0.026 kPa (±0.0068 psid)	±0.047 kPa (±0.0068 psid)	±0.130 kPa (±0.0188 psid)						
248	30123-37170	D/P cell	±69.0 kPa (±10.0 psid)	±0.34 kPa (±0.05 psid)	±0.36 kPa (±0.053 psid)	±0.66 kPa (±0.096 psid)	±1.74 kPa (±0.253 psid)						
249	30123-37170	D/P cell	±17 kPa (±2.5 psid)	±0.17 kPa (±0.025 psid)	±0.19 kPa (±0.027 psid)	±0.33 kPa (0.048 psid)	±0.876 kPa (±0.127 psid)						
250	30123-37170	D/P cell	±69.0 kPa (±10.0 psid)	±0.34 kPa (±0.05 psid)	±0.36 kPa (±0.053 psid)	±0.66 kPa (±0.096 psid)	±1.74 kPa (0.253 psid)						
251	30123-37170	D/P cell	±69.0/±34.5 kPa (±10.0/±5.0 psid)	±0.34/±0.17 kPa (±0.05/±0.025 psid)	±0.36/±0.19 kPa (±0.053/±0.027 psid)	±0.66/±0.33 kPa (±0.096/0.048 psid)	±1.74/±0.876 kPa (±0.253/±0.127 psid)						
252, 253	30123-37170	D/P cell	0.101-1.14 MPa (0-150 psig)	±2.59 kPa (±0.375 psid)	±2.70 kPa (±0.391 psid)	±2.63 kPa (±0.381 psid)	±7.874 kPa (±1.142 psid)						
254, 255	30123-37170	D/P cell	±69.0 kPa (±10.0 psid)	±0.34 kPa (±0.05 psid)	±0.36 kPa ±0.053 psid)	±0.66 kPa (±0.096 psid)	±1.74 kPa (±0.253 psid)						
256	30123-37170	D/P cell	±0.172 MPa (±25.0 psid)	±5.2 kPa (±0.75 psid)	±1.00 kPa (±0.145 psid)	±6.6 kPa (±0.96 psid)	±17 kPa (±2.5 psid)						

Appendix C

RELAP5 Input Listings of Base Case and Modified Version for FLECHT-SEASET Test 31504

A single input deck except Group 1 Card (the card number is 1) was used to both the Standard RELAP5/MOD3.1 code and the KAERI-Modified code.
In the following RELAP5 Input Listing,
Group 1 Card was not used in standard RELAP5/MOD3.1 calculation,
while three words " 70, 73, 75" were added at Group 1 Card for modified code calculation

```
=flecht seaset test no. 31805 using 20 nodes & 20 heat strs.
*****************************************************************
*  Chnage Mode Input (KAERI version specific)              *
*     70 : KAERI Quench Model ON                          *
*     71 : KAERI Post-CHF Flow Regime Selection Login ON      *
*     72 : KAERI Droplet Transport Model ON                *
*     73 : KAERI Corrected CHF Table ON                    *
*     74 : Restriction for Reflood fij of core            *
*     75 : KAERI Wall Vaporization Smoothing               *
*****************************************************************
*1    70   75   73
*****************************************************************
* The Group 1 Card above is activated only at Modified Version of Code
*****************************************************************
*  input deck for non-CCFL option & calculated grid volume
*****************************************************************
100   new    transnt
101   run
102   si    si
105   10.0   20.0
*****************************************************************
*  time
*****************************************************************
201   900.0   1.e-8   0.1   3   10  5000  5000
*****************************************************************
**    mimor edits   **
*****************************************************************
*
361   cntrlvar   200        * core collapsed water level
362   cntrlvar   210        * integrated water carry-over
363   cntrlvar   220        * steam flow rate
364   cntrlvar   250        * total power
*
20800001   fij   200010000
20800002   fij   200020000
20800003   fij   200030000
20800004   fij   200040000
20800005   fij   200050000
20800006   fij   200060000
20800007   fij   200070000
20800008   fij   200080000
20800009   fij   200090000
20800010   fij   200100000
20800011   fij   200110000
20800012   fij   200120000
20800013   fij   200130000
20800014   fij   200140000
20800015   fij   200150000
20800016   fij   200160000
20800017   fij   200170000
20800018   fij   200180000
20800019   fij   200190000
20800020   fij   250000000
*
20800021   htmode   200100101
20800022   htmode   200100201
20800023   htmode   200100301
20800024   htmode   200100401
20800025   htmode   200100501
20800026   htmode   200100601
20800027   htmode   200100701
20800028   htmode   200100801
20800029   htmode   200100901
20800030   htmode   200101001
20800031   htmode   200101101
20800032   htmode   200101201
20800033   htmode   200101301
20800034   htmode   200101401
20800035   htmode   200101501
20800036   htmode   200101601
20800037   htmode   200101701
20800038   htmode   200101801
20800039   htmode   200101901
20800040   htmode   200102001
```

```
*
20800050  dt     0
*
*** contrl variables
*
** core collapsed water level
*
20520000 wt-level sum 1.0 0.0 1
20520001 0.0 0.18288 voidf 200010000
20520002     0.18288 voidf 200020000
20520003     0.18288 voidf 200030000
20520004     0.18288 voidf 200040000
20520005     0.18288 voidf 200050000
20520006     0.18288 voidf 200060000
20520007     0.18288 voidf 200070000
20520008     0.18288 voidf 200080000
20520009     0.18288 voidf 200090000
20520010     0.18288 voidf 200100000
20520011     0.18288 voidf 200110000
20520012     0.18288 voidf 200120000
20520013     0.18288 voidf 200130000
20520014     0.18288 voidf 200140000
20520015     0.18288 voidf 200150000
20520016     0.18288 voidf 200160000
20520017     0.18288 voidf 200170000
20520018     0.18288 voidf 200180000
20520019     0.18288 voidf 200190000
20520020     0.18288 voidf 200200000
*
** water carry-over
*
20523000  flowrate  mult 0.0116574  0.0  1
20523001  voidfj  250000000
20523002  rhofj  250000000
20523003  velfj  250000000
*
20521000  w-inte  integral  1.0  0.0  1
20521001  cntrlvar  230
*
** steam  flow  rate
*
20522500  stflow  mult  0.0116574  0.0  1
20522501  voidgj  250000000
20522502  rhogj  250000000
20522503  velgj  250000000

20522000  s-inte  integral  1.0  0.0  1
20522001  cntrlvar  225
**
** total power
*
20525000  power  function  1.0  0.0  1
20525001  time  0  200
*
*****************************************************************
*                                        *
*     TRIP LOGICS                              *
*                                        *
*****************************************************************
*
500  time        0  gt  null  0   71.0  1  -1.0
501  httemp  200101008  ge  null  0  1129.0  1  -1.0
*****************************************************************
*
***  lower plenum
*
*****************************************************************
1000000  lplenum  tmdpvol
1000101  1.0  1.0  0.0  0.0  0.0  0.0  0.0  0.0  00010
1000200  3   500
1000201    0.0   2.8e5  324.15
1000202  1000.0   2.8e5  324.15
*****************************************************************
*
```

```
***   inlet junction
*
*****************************************************************
1500000 inlet   tmdpjun
1500101 100000000 200000000 0.0116574
1500200 1       500
1500201   -1.0  0.0  0.0  0.0
1500202    0.0  0.378318  0.0  0.0
1500203 1000.0  0.378318  0.0  0.0
*****************************************************************
*
**    core
*
*****************************************************************
2000000 core   pipe
2000001 20
2000101 0.0       20        * vol. flow area
2000201 0.015571   2        * jun. flow area
2000202 0.0116574  3
2000203 0.015571   5
2000204 0.0116574  6
2000205 0.015571   8
2000206 0.0116574  9
2000207 0.015571  11
2000208 0.0116574 12
2000209 0.015571  14
2000210 0.0116574 15
2000211 0.015571  17
2000212 0.0116574 18
2000213 0.015571  19
2000301 0.18288   20        * vol. length
2000401 2.67366e-3   1      * vol. volume
2000402 2.84762e-3   2
2000403 2.67366e-3   3      * vol. volume - grid volume
2000404 2.84762e-3   5
2000405 2.67366e-3   6
2000406 2.84762e-3   8
2000407 2.67366e-3   9
2000408 2.84762e-3  11
2000409 2.67366e-3  12
2000410 2.84762e-3  14
2000411 2.67366e-3  15
2000412 2.84762e-3  17
2000413 2.67366e-3  18
2000414 2.84762e-3  19
2000415 2.67366e-3  20
2000601 90.0      20        * vol. vertical orientation
2000701 0.18288   20        * vol. elevation change
2000801 1.e-6 0.009731 20   * vol. friction data
2000901 1.14  1.14     1    * jun. loss coefficient
2000902 0.0   0.0      2
2000903 1.14  1.14     3
2000904 0.0   0.0      5
2000905 1.14  1.14     6
2000906 0.0   0.0      8
2000907 1.14  1.14     9
2000908 0.0   0.0     11
2000909 1.14  1.14    12
2000910 0.0   0.0     14
2000911 1.14  1.14    15
2000912 0.0   0.0     17
2000913 1.14  1.14    18
2000914 0.0   0.0     19
2001001 00100  20          * vol. control flag
2001101 000000 19          * jun. control flag
2001201 3 2.8e5  410.0  0.0 0.0 0.0  1
2001202 3 2.8e5  410.0  0.0 0.0 0.0  2
2001203 3 2.8e5  410.0  0.0 0.0 0.0  3
2001204 3 2.8e5  410.0  0.0 0.0 0.0  4
2001205 3 2.8e5  410.0  0.0 0.0 0.0  5
2001206 3 2.8e5  410.0  0.0 0.0 0.0  6
2001207 3 2.8e5  410.0  0.0 0.0 0.0  7
2001208 3 2.8e5  410.0  0.0 0.0 0.0  8
2001209 3 2.8e5  410.0  0.0 0.0 0.0  9
```

```
2001210 3 2.8e5  410.0  0.0 0.0 0.0 10
2001211 3 2.8e5  410.0  0.0 0.0 0.0 11
2001212 3 2.8e5  410.0  0.0 0.0 0.0 12
2001213 3 2.8e5  410.0  0.0 0.0 0.0 13
2001214 3 2.8e5  410.0  0.0 0.0 0.0 14
2001215 3 2.8e5  410.0  0.0 0.0 0.0 15
2001216 3 2.8e5  410.0  0.0 0.0 0.0 16
2001217 3 2.8e5  410.0  0.0 0.0 0.0 17
2001218 3 2.8e5  410.0  0.0 0.0 0.0 18
2001219 3 2.8e5  410.0  0.0 0.0 0.0 19
2001220 3 2.8e5  410.0  0.0 0.0 0.0 20
2001300 0
2001301 0.0 0.0 0.0 19    * jun. initial condition
*2001401 0.0027353  0.0  1.0  1.0  1   * junc. hyd. diameter
*2001402 0.009731   0.0  1.0  1.0  2
*2001403 0.0027353  0.0  1.0  1.0  3
*2001404 0.009731   0.0  1.0  1.0  5
*2001405 0.0027353  0.0  1.0  1.0  6
*2001406 0.009731   0.0  1.0  1.0  8
*2001407 0.0027353  0.0  1.0  1.0  9
*2001408 0.009731   0.0  1.0  1.0  11
*2001409 0.0027353  0.0  1.0  1.0  12
*2001410 0.009731   0.0  1.0  1.0  14
*2001411 0.0027353  0.0  1.0  1.0  15
*2001412 0.009731   0.0  1.0  1.0  17
*2001413 0.0027353  0.0  1.0  1.0  18
*2001414 0.009731   0.0  1.0  1.0  19
2001401 0.009731   0.0  1.0  1.0  19
*****************************************************************
*
***     outlet junction
*
*****************************************************************
2500000 outlet  sngljun
2500101 200010000 300000000 0.0116574  1.34  1.34  101000
2500102 1.0 1.0  1.0
*2500110 0.0027353  0.0  1.0  1.0
2500201 0 0.0 0.0 0.0
*****************************************************************
*
***     upper plenum
*
*****************************************************************
3000000 uplenum  tmdpvol
3000101 1.0 1.0 0.0 0.0 0.0 0.0 0.0 0.0 00010
3000200 2
3000201 0.0 2.8e5 1.0
*
*****************************************************************
*
****    heat structure input
*
*****************************************************************
**      fuel rod
*****************************************************************
*
12001000 20 8 2 0 0.0 1 1  32
12001100 0  1
12001101 2 0.00122
12001102 1 0.00222
12001103 2 0.00411
12001104 2 0.00475
12001201 1  2          * boron nitride
12001202 2  3          * kanthal
12001203 1  5          * boron nitride
12001204 4  7          * ss 347
12001301 0.0  2
12001302 1.0  3
12001303 0.0  7
12001400 -1
12001401 337.5  337.5  337.5  337.5  337.5  337.5  337.5  337.5
12001402 366.3  366.3  366.3  366.3  366.3  366.3  366.3  366.3
12001403 386.9  386.9  386.9  386.9  386.9  386.9  386.9  386.9
12001404 419.8  419.8  419.8  419.8  419.8  419.8  419.8  419.8
```

```
12001405 436.3  436.3  436.3  436.3  436.3  436.3  436.3  436.3
12001406 465.1  465.1  465.1  465.1  465.1  465.1  465.1  465.1
12001407 481.6  481.6  481.6  481.6  481.6  481.6  481.6  481.6
12001408 498.0  498.0  498.0  498.0  498.0  498.0  498.0  498.0
12001409 502.1  502.1  502.1  502.1  502.1  502.1  502.1  502.1
12001410 510.4  510.4  510.4  510.4  510.4  510.4  510.4  510.4
12001411 510.4  510.4  510.4  510.4  510.4  510.4  510.4  510.4
12001412 510.4  510.4  510.4  510.4  510.4  510.4  510.4  510.4
12001413 502.1  502.1  502.1  502.1  502.1  502.1  502.1  502.1
12001414 493.9  493.9  493.9  493.9  493.9  493.9  493.9  493.9
12001415 477.4  477.4  477.4  477.4  477.4  477.4  477.4  477.4
12001416 461.0  461.0  461.0  461.0  461.0  461.0  461.0  461.0
12001417 451.1  451.1  451.1  451.1  451.1  451.1  451.1  451.1
12001418 440.4  440.4  440.4  440.4  440.4  440.4  440.4  440.4
12001419 436.3  436.3  436.3  436.3  436.3  436.3  436.3  436.3
12001420 428.1  428.1  428.1  428.1  428.1  428.1  428.1  428.1
12001501 0 0 0 1 29.07792 20
12001601 200010000 10000  1 1 29.07792 20
12001701 200 0.02145  0.0 0.0  3
12001702 200 0.03395  0.0 0.0  4
12001703 200 0.04395  0.0 0.0  5
12001704 200 0.05545  0.0 0.0  6
12001705 200 0.06495  0.0 0.0  7
12001706 200 0.07445  0.0 0.0  8
12001707 200 0.07995  0.0 0.0  9
12001708 200 0.08295  0.0 0.0 11
12001709 200 0.07995  0.0 0.0 12
12001710 200 0.07445  0.0 0.0 13
12001711 200 0.06495  0.0 0.0 14
12001712 200 0.05545  0.0 0.0 15
12001713 200 0.04395  0.0 0.0 16
12001714 200 0.03395  0.0 0.0 17
12001715 200 0.02145  0.0 0.0 20
12001801 0.0112 20.0 20.0 0.0 0.0 0.0 0.0 1.0 20
12001901 0.0112 0.09144 3.56616 0.09144 0.44196 1.14 1.14 0.43  1
12001902 0.0112 0.27432 3.38328 0.27432 0.25908 1.14 1.14 0.43  2
12001903 0.0112 0.4572  3.2004  0.45720 0.07620 1.14 1.14 0.43  3
12001904 0.0112 0.64008 3.01752 0.10668 0.40132 1.14 1.14 0.68  4
12001905 0.0112 0.82296 2.83464 0.28956 0.21844 1.14 1.14 0.88  5
12001906 0.0112 1.00584 2.65176 0.47244 0.03556 1.14 1.14 1.11  6
12001907 0.0112 1.18872 2.46888 0.14732 0.38608 1.14 1.14 1.30  7
12001908 0.0112 1.3716  2.286   0.33020 0.20320 1.14 1.14 1.49  8
12001909 0.0112 1.55448 2.10312 0.51308 0.02032 1.14 1.14 1.60  9
12001910 0.0112 1.73736 1.92024 0.16256 0.37084 1.14 1.14 1.66 10
12001911 0.0112 1.92024 1.73734 0.34544 0.18796 1.14 1.14 1.66 11
12001912 0.0112 2.10312 1.55448 0.52832 0.00508 1.14 1.14 1.60 12
12001913 0.0112 2.286   1.3716  0.17780 0.33020 1.14 1.14 1.49 13
12001914 0.0112 2.46888 1.18872 0.36068 0.14732 1.14 1.14 1.30 14
12001915 0.0112 2.65176 1.00584 0.03556 0.49784 1.14 1.14 1.11 15
12001916 0.0112 2.83464 0.82296 0.21844 0.31496 1.14 1.14 0.88 16
12001917 0.0112 3.01752 0.64008 0.40132 0.13208 1.14 1.14 0.68 17
12001918 0.0112 3.2004  0.4572  0.05080 0.45720 1.14 1.14 0.43 18
12001919 0.0112 3.38328 0.27432 0.23368 0.27432 1.14 1.14 0.43 19
12001920 0.0112 3.56616 0.09144 0.41656 0.09144 1.14 1.14 0.43 20
**
**      housing
*
12002000 20 3 2 0 0.097  0  0
12002100 0  1
12002101 2 0.10208
12002201 3  2            * ss 304
12002301 0.  2
12002400 -1
12002401 337.5  337.5  337.5
12002402 366.3  366.3  366.3
12002403 386.9  386.9  386.9
12002404 419.8  419.8  419.8
12002405 436.3  436.3  436.3
12002406 465.1  465.1  465.1
12002407 481.6  481.6  481.6
12002408 498.0  498.0  498.0
12002409 502.1  502.1  502.1
12002410 510.4  510.4  510.4
12002411 510.4  510.4  510.4
```

```
12002412 510.4  510.4  510.4
12002413 502.1  502.1  502.1
12002414 493.9  493.9  493.9
12002415 477.4  477.4  477.4
12002416 461.0  461.0  461.0
12002417 451.1  451.1  451.1
12002418 440.4  440.4  440.4
12002419 436.3  436.3  436.3
12002420 428.1  428.1  428.1
12002501 200010000  10000  1 1 0.18288  20
12002601 0 0 0 1 0.18288  20
12002701 0 0.0 0.0 0.0 20
12002801 0.0 20.0 20.0 0.0 0.0 0.0 0.0 1.0 20
12002901 0.0 20.0 20.0 0.0 0.0 0.0 0.0 1.0 20
*
**      thimbles
*
12003000 20 3 2 0 0.005461  0  1
12003100 0  1
12003101 2 0.0060198
12003201 3  2              * ss 304
12003301 0.0  2
12003400 -1
12003401 337.5  337.5  337.5
12003402 366.3  366.3  366.3
12003403 386.9  386.9  386.9
12003404 419.8  419.8  419.8
12003405 436.3  436.3  436.3
12003406 465.1  465.1  465.1
12003407 481.6  481.6  481.6
12003408 498.0  498.0  498.0
12003409 502.1  502.1  502.1
12003410 510.4  510.4  510.4
12003411 510.4  510.4  510.4
12003412 510.4  510.4  510.4
12003413 502.1  502.1  502.1
12003414 493.9  493.9  493.9
12003415 477.4  477.4  477.4
12003416 461.0  461.0  461.0
12003417 451.1  451.1  451.1
12003418 440.4  440.4  440.4
12003419 436.3  436.3  436.3
12003420 428.1  428.1  428.1
12003501 0 0 0 1 2.92608 20
12003601 200010000  10000  1 1 2.92608  20
12003701 0 0.0 0.0 0.0 20
12003801 0.0 20.0 20.0 0.0 0.0 0.0 0.0 1.0 20
12003901 0.0 20.0 20.0 0.0 0.0 0.0 0.0 1.0 20
*
**      fillers
*
12004000 20 3 2 0 0.0  0  1
12004100 0  1
12004101 2 0.005022
12004201 3  2
12004301 0.0  2
12004400 -1
12004401 337.5  337.5  337.5
12004402 366.3  366.3  366.3
12004403 386.9  386.9  386.9
12004404 419.8  419.8  419.8
12004405 436.3  436.3  436.3
12004406 465.1  465.1  465.1
12004407 481.6  481.6  481.6
12004408 498.0  498.0  498.0
12004409 502.1  502.1  502.1
12004410 510.4  510.4  510.4
12004411 510.4  510.4  510.4
12004412 510.4  510.4  510.4
12004413 502.1  502.1  502.1
12004414 493.9  493.9  493.9
12004415 477.4  477.4  477.4
12004416 461.0  461.0  461.0
12004417 451.1  451.1  451.1
```

```
12004418 440.4  440.4  440.4
12004419 436.3  436.3  436.3
12004420 428.1  428.1  428.1
12004501 0 0 0 1 1.46304 20
12004601 200010000  10000  1 1 1.46304  20
12004701 0 0.0 0.0 0.0 20
12004801 0.0 20.0 20.0 0.0 0.0 0.0 0.0 1.0 20
12004901 0.0 20.0 20.0 0.0 0.0 0.0 0.0 1.0 20
*
**      failed rod
*
12005000 20 8 2 0 0.0  0   1
12005100 0  1
12005101 2 0.00122
12005102 1 0.00222
12005103 2 0.00411
12005104 2 0.00475
12005201 1  2          * boron nitride
12005202 2  3          * kanthal
12005203 1  5          * boron nitride
12005204 4  7          * ss 347
12005301 0.0  2
12005302 1.0  3
12005303 0.0 . 7
12005400 -1
12005401 337.5  337.5  337.5  337.5  337.5  337.5  337.5  337.5
12005402 366.3  366.3  366.3  366.3  366.3  366.3  366.3  366.3
12005403 386.9  386.9  386.9  386.9  386.9  386.9  386.9  386.9
12005404 419.8  419.8  419.8  419.8  419.8  419.8  419.8  419.8
12005405 436.3  436.3  436.3  436.3  436.3  436.3  436.3  436.3
12005406 465.1  465.1  465.1  465.1  465.1  465.1  465.1  465.1
12005407 481.6  481.6  481.6  481.6  481.6  481.6  481.6  481.6
12005408 498.0  498.0  498.0  498.0  498.0  498.0  498.0  498.0
12005409 502.1  502.1  502.1  502.1  502.1  502.1  502.1  502.1
12005410 510.4  510.4  510.4  510.4  510.4  510.4  510.4  510.4
12005411 510.4  510.4  510.4  510.4  510.4  510.4  510.4  510.4
12005412 510.4  510.4  510.4  510.4  510.4  510.4  510.4  510.4
12005413 502.1  502.1  502.1  502.1  502.1  502.1  502.1  502.1
12005414 493.9  493.9  493.9  493.9  493.9  493.9  493.9  493.9
12005415 477.4  477.4  477.4  477.4  477.4  477.4  477.4  477.4
12005416 461.0  461.0  461.0  461.0  461.0  461.0  461.0  461.0
12005417 451.1  451.1  451.1  451.1  451.1  451.1  451.1  451.1
12005418 440.4  440.4  440.4  440.4  440.4  440.4  440.4  440.4
12005419 436.3  436.3  436.3  436.3  436.3  436.3  436.3  436.3
12005420 428.1  428.1  428.1  428.1  428.1  428.1  428.1  428.1
12005501 0 0 0 1 0.36576 20
12005601 200010000 10000  1 1 0.36576 20
12005701 0   0.0  0.0  0.0  20
12005801 0.0 20.0 20.0 0.0 0.0 0.0 0.0 1.0 20
12005901 0.0 20.0 20.0 0.0 0.0 0.0 0.0 1.0 20
*
*
**      heat structure thermal property data
*
20100100 tbl/fctn 1 1  * boron nitride
20100200 tbl/fctn 1 1  * kanthal
20100300 tbl/fctn 1 1  * ss 304
20100400 tbl/fctn 2 2  * ss 347
*
***     thermal conductivity data
*
20100101 255.4  25.584  533.2  24.805   * boron nitride
20100102 810.9  24.044  922.0  23.732
20100103 1033.2  24.420  1144.3  23.126
20100104 1255.4  22.815  1366.5  22.503
20100105 1477.6  22.191  1588.7  21.880
20100201 255.4  23.202  366.5  23.381   * kanthal + boron
20100202 588.7  23.737  810.9  24.094
20100203 1033.2  24.450  1255.4  24.807
20100204 1477.6  25.164  1588.7  25.342
20100301 255.4  13.069  366.5  15.821   * ss 304
20100302 922.0  23.092  1588.7  32.093
20100401 255.4 1600. 13.064 0.0143  0. 0. 0. 0. 273.15    * ss 347
*
```

```
**      volumetric heat capacity data
*
20100151  255.4  1241374.1   533.2  2619098.6   * boron nitride
20100152  810.9  3315907.6   922.0  3486554.7
20100153 1033.2  3616213.0  1144.3  3714920.7
20100154 1255.4  3791042.7  1366.5  3847925.1
20100155 1477.6  3891423.3  1588.7  3924883.6
20100251  255.4  1880143.2   366.5  2368270.9   * kanthal + boron
20100252  588.7  3209723.7   810.9  3777314.1
20100253 1033.2  4902562.0  1255.4  4224291.5
20100254 1477.6  4336390.6  1588.7  4384635.8
20100351  255.4  3593152.8   366.5  3828218.9   * ss 304
20100352  922.0  4768483.2  1588.7  5843071.0
20100451 255.4  1600. 3541405.7 1668.0 0. 0. 0. 0. 273.15      * ss 347
*
**      power table
*
20220000  power   500   1.0   804578.3
20220001   -1.0   1.0
20220002    0.    1.0
20220003    1.    0.9962
20220004    2.5   0.9884
20220005    5.    0.9752
20220006   10.    0.9493
20220007   15.    0.9306
20220008   20.    0.9110
20220009   25.    0.8963
20220010   30.    0.8817
20220011   40.    0.8590
20220012   50.    0.8376
20220013   60.    0.8201
20220014   75.    0.7860
20220015  100.    0.7484
20220016  125.    0.7383
20220017  150.    0.7040
20220018  175.    0.6835
20220019  200.    0.6665
20220020  250.    0.6362
20220021  300.    0.6116
20220022  400.    0.5756
20220023  600.    0.5255
20220024  800.    0.4912
```

NRC FORM 335 (2-89) NRCM 1102, 3201, 3202

U.S. NUCLEAR REGULATORY COMMISSION

BIBLIOGRAPHIC DATA SHEET

(See instructions on the reverse)

1. REPORT NUMBER (Assigned by NRC, Add Vol., Supp., Rev., and Addendum Numbers, if any.)

NUREG/IA-0132
CAMP001

2. TITLE AND SUBTITLE

Improvements to the RELAP5/MOD3 Reflood Model and Uncertainty Quantification of Reflood Pak Clad Temperature

3. DATE REPORT PUBLISHED

MONTH	YEAR
October	1996

4. FIN OR GRANT NUMBER

W6238

5. AUTHOR(S)

B. D. Chung, Y.J. Lee, C.E. Park, S.Y. Lee, KAERI
Y.S. Bang, K.W. Seul, H.J. Kim, KINS

6. TYPE OF REPORT

Technical

7. PERIOD COVERED *(Inclusive Dates)*

8. PERFORMING ORGANIZATION - NAME AND ADDRESS *(If NRC, provide Division, Office or Region, U.S. Nuclear Regulatory Commission, and mailing address; if contractor, provide name and mailing address.)*

Korea Atomic Energy Research Institute
P.O. Box 105, Yusung
Taejon, 305-600 Korea

Korea Institute of Nuclear Safety
P.O. Box 16, Daeduck Danji
Taejon, 305-600 Korea

9. SPONSORING ORGANIZATION - NAME AND ADDRESS *(If NRC, type "Same as above"; if contractor, provide NRC Division, Office or Region, U.S. Nuclear Regulatory Commission, and mailing address.)*

Office of Nuclear Regulatory Research
U.S. Nuclear Regulatory Research
Washington, DC 20555-0001

10. SUPPLEMENTARY NOTES

S. Smith, NRC Project Manager

11. ABSTRACT *(200 words or less)*

Assessment of the original RELAP5/MOD 3.1 code against the FLECHT SEASET series of experiment has identified some weaknesses of the reflood model, such as the lack of quenching temperature model, the shortcoming of Chen transition boiling model, and the incorrect prediction of droplet size and interfacial heat transfer. Also high pressure spikes during the reflood calculation resulted in the high steam flow oscillation and liquid carryover. An effort has been made to improve the code with respect to the above weakness and the necessary model for wall heat transfer package and numerical scheme had been modified. Some important FLECHT-SEASET experiment were assessed using the improved version and standard version. The result from the improved version of RELAP5/MOD3.1 shows the weaknesses of RELAP5/MOD3.1 was much improved when compared to the standard MOD3.1 code. The prediction of void profile and cladding temperature agreed better with test data especially for the gravity feed test. The scatter diagram of peak cladding temperatures (PCTs) is made from the comparison of all the calculated PCTs and the corresponding experimental values. The deviation between experimental and calculated PCTs were calculated for 2793 data points. The deviations are shown to be normally distributed, and used to quantify statistically the PCT uncertainty of the code. The upper limit of PCT uncertainty at 95% confidence level is evaluated to be about 99K.

12. KEY WORDS/DESCRIPTORS *(List words or phrases that will assist researchers in locating the report.)*

CAMP, RELAP5/MOD3

13. AVAILABILITY STATEMENT

unlimited

14. SECURITY CLASSIFICATION

(This Page)

unclassified

(This Report)

unclassified

15. NUMBER OF PAGES

16. PRICE

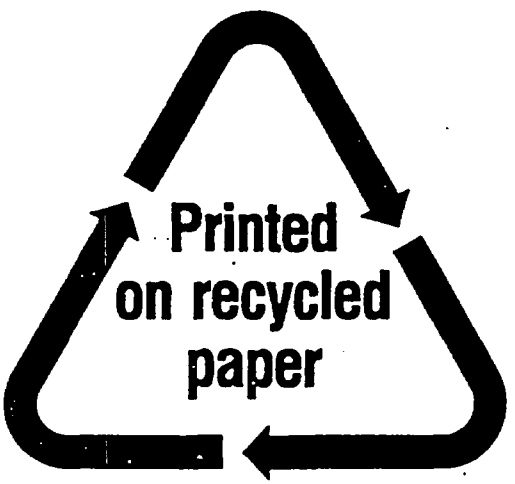

Federal Recycling Program

UNITED STATES
NUCLEAR REGULATORY COMMISSION
WASHINGTON, DC 20555-0001

OFFICIAL BUSINESS
PENALTY FOR PRIVATE USE, $300

SPECIAL STANDARD MAIL
POSTAGE AND FEES PAID
USNRC
PERMIT NO. G-67